SCHOOL OF CIVIL ENGINEERING
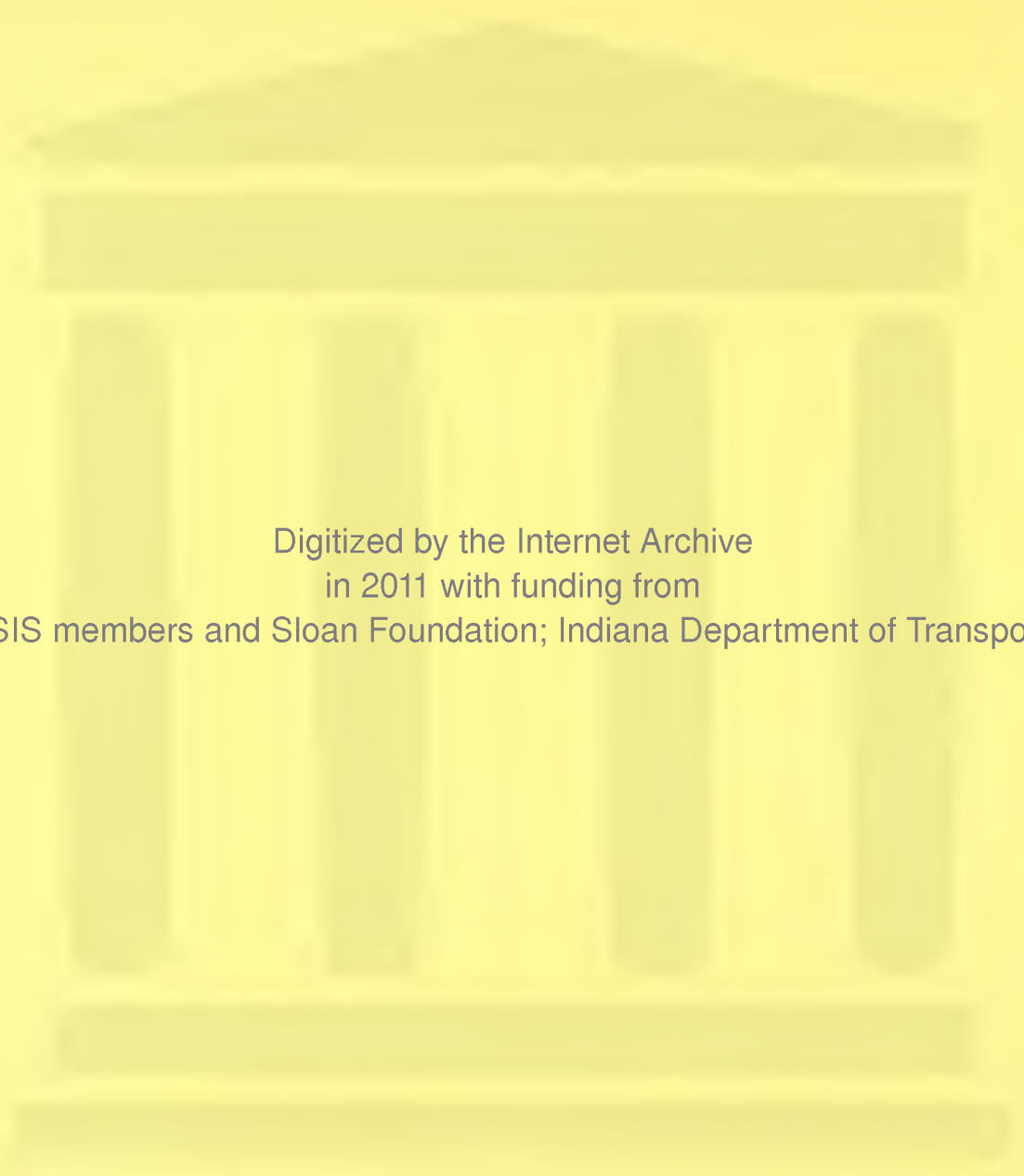
FROST HEAVING RATE OF
SILTY SOILS AS A FUNCTION OF
PORE SIZE DISTRIBUTION

Michael A. Reed

PURDUE UNIVERSITY
INDIANA STATE HIGHWAY COMMISSION

Interim Report

FROST HEAVING RATE OF SILTY SOILS

AS A FUNCTION OF PORE SIZE DISTRIBUTION

TO: J. F. McLaughlin, Director   September 7, 1977
        Joint Highway Research Project

                                      Project: C-36-5N

FROM: H. L. Michael, Assoicate Director
        Joint Highway Research Project   FIle: 6-6-14

      Attached is an Interim Report on the HPR-1(15) Part II Research Study
titled "The Effects of Pore Size Distribution on Permeability and Frost
Susceptibility of Selected Sub-Grade Materials". The Report is titled
"Frost Heaving Rate of Silty Soils as a Function of Pore Size Distribution".
It has been authored by Mr. Michael A. Reed, Graduate Instructor on our
staff, under the direction of C. W. Lovell, L. E. Wood and A. G. Altschaeffl
of our staff.

      The results given in the attached report indicate the usefulness of pore
size distribution parameters in the prediction of frost heaving and frost
susceptibility of fine-grained soils. Since these parameters predict differ-
ences in the compaction process, they have a much better frost prediction
potential than the currently used criteria based on grain size and soil tex-
ture. The report contains a statistical equation for frost heave rate in
terms of pore size distribution, which is valid for all the soils and com-
paction conditions tested.

      The Report is submitted as partial fulfillment of the objectives of
the Study. Copies of the Report will also be submitted to ISHC and FHWA for
their review, comment and similar acceptance.

                            Respectfully submitted,

                              Harold L. Michael

                              Harold L. Michael
                              Associate Director

HLM/ss

cc: W. L. Dolch   K. R. Hoover   C. F. Scholer
     R. L. Eskew   G. A. Leonards   M. B. Scott
     G. D. Gibson   R. F. Marsh   K. C. Sinha
     W. H. Goetz   R. D. Miles   C. A. Venable
     M. J. Gutzwiller   P. L. Owens   L. E. Wood
     G. K. Hallock   G. T. Satterly   E. J. Yoder
     D. E. Hancher   S. R. Yoder

Interim Report

FROST HEAVING RATE OF SILTY SOILS

AS A FUNCTION OF PORE SIZE DISTRIBUTION

by

Michael A. Reed
Graduate Instructor in Research

Joint Highway Research Project

Project No.: C-36-5N

File No.: 6-6-14

Prepared as Part of an Investigation

Conducted by

Joint Highway Research Project
Engineering Experiment Station
Purdue University

in cooperation with the

Indiana State Highway Commission
and the
U.S. Department of Transportation
Federal Highway Administration

Purdue University
West Lafayette, Indiana
September 7, 1977

1. Report No. JHRP-77-15	2. Government Accession No.	3. Recipient's Catalog No.
4. Title and Subtitle FROST HEAVING RATE OF SILTY SOILS AS A FUNCTION OF PORE SIZE DISTRIBUTION		5. Report Date September 7, 1977
		6. Performing Organization Code
7. Author(s) Michael A. Reed		8. Performing Organization Report No. JHRP-77-15
9. Performing Organization Name and Address Joint Highway Research Project Civil Engineering Building Purdue University W. Lafayette, Indiana 47907		10. Work Unit No.
		11. Contract or Grant No. HPR-1(15) Part II
		13. Type of Report and Period Covered
12. Sponsoring Agency Name and Address Indiana State Highway Commission State Office Building 100 North Senate Avenue Indianapolis, Indiana 46204		Interim Report #1
		14. Sponsoring Agency Code

15. Supplementary Notes
Prepared in cooperation with the U. S. Department of Transportation, Federal Highway Administration on Study "The Effects of Pore Size Distribution on Permeability and Frost Susceptibility of Selected Sub-Grade Materials".

16. Abstract The purpose of this study was to examine the relation of frost heave to pore size distribution of compacted silty soils, and to propose that frost susceptibility criteria based upon the distribution of porosity are more logical and versatile than those based upon texture and grain size.

Rapid freezing laboratory tests were conducted to evaluate the heaving rate. The soils were compacted at different energy levels and water contents, and consisted of three different combinations of silt and kaolin.

Mercury intrusion tests were performed to obtain the pore size distributions of the compacted soils. Since this procedure requires the soil to be free of moisture, the soil samples were freeze dried. This type of drying almost eliminated the volume change and structural modification expected from air or oven drying.

The relation of frost heave to pore size was obtained using the method or linear regression. The prediction equation ultimately selected had an R^2 value of 82.0%, and for the soils tested read:

$$\hat{Y} = -5.46 - 29.46 \left(\frac{X_{3.0}}{X_0 - X_{0.4}} \right) + 581.1 \, (X_{3.0})$$

where $\hat{Y}$ = frost heave rate in mm/day,

$X_{3.0}$ = cumulative porosity for pores > 3.0 μm but < 300 μm,

X_0 = total cumulative porosity,

$X_{0.4}$ = cumulative porosity for pores > 0.4 μm.

17. Key Words Pore size distribution; Frost heave; Frost susceptibility; Freeze drying; Compacted soil	18. Distribution Statement No restrictions. This document is available to the public through the National Technical Information Service, Springfield, Virginia 22161.		
19. Security Classif. (of this report) Unclassified	20. Security Classif. (of this page) Unclassified	21. No. of Pages 116	22. Price

Form DOT F 1700.7 (8-69)

ACKNOWLEDGEMENTS

TABLE OF CONTENTS

TABLE OF CONTENTS (Cont'd)

LIST OF TABLES

LIST OF FIGURES

LIST OF FIGURES (Cont'd)

LIST OF FIGURES (Cont'd)

LIST OF ABBREVIATIONS AND SYMBOLS

AASHTO   American Association of State Highway and Transportation Officials

ASCE   American Society of Civil Engineers

$\overset{\text{o}}{\text{A}}$ Angstrom (10^{-8} cm)

C   Celsius

cm   Centimeter

CRREL   Cold Regions Research and Engineering Laboratory, U.S. Army Corps of Engineers

o   Degree

F   Farenheit

ft lbs   Foot pounds

in.   Inch

μm   Micrometer (10^{-4} cm)

ml   Milliliter ($1 \ cm^3$)

mm   Millimeter (10^{-1} cm)

%   Percent

pcf   Pounds per cubic foot

psi   Pounds per square inch

SPSS   Statistical Package for the Social Sciences

U.S.   United States

HIGHLIGHT SUMMARY

The phenomena of frost heave and loss of strength on thawing produce serious highway damage in many areas of the United States. The frost susceptibility of soils is commonly predicted by grain size and textural criteria, which can not take into account the compacted soil conditions. A parameter which does change with the compaction variables is pore size distribution, and the present study focused on developing experimental relations between the distribution of porosity and frost heaving rate.

For this study, rapid freezing tests were conducted to evaluate the heaving rate of three different mixtures of an Indiana silt and Edgar plastic kaolin. Each soil mixture was compacted at two or three different energy levels, and at three moisture levels, viz., wet of optimum, optimum, and dry of optimum.

To obtain pore size distributions of the compacted soils, mercury intrusion tests were performed. Since this procedure requires the soil to be free of moisture, freeze drying techniques were used. This method almost eliminated the volume change and structural modification expected from air or oven drying.

To relate frost heave to pore size distribution, the method of linear regression was used. The prediction equation ultimately selected had an R^2 value of 82%, and for the soils tested read:

$$\hat{Y} = -5.46 - 29.46 \left(\frac{X_{3.0}}{X_0 - X_{0.4}} \right) + 581.1 \, (X_{3.0})$$

where $\hat{Y}$ = heave rate in mm/day,

$X_{3.0}$ = cumulative porosity for pores > 3.0 μm but < 300 μm,

X_0 = total cumulative porosity,

$X_{0.4}$ = cumulative porosity for pores > 0.4 μm.

The above equation applies to all test soil types and tested levels of compaction variables.

In physical explanation of the above equation, it is believed that the large pores, quantified by the value $X_{3.0}$, offer the least resistance for water to move to the freezing front, whereas the smaller pores represent the amount of available energy to do the work of frost heave. For soils of the same type, the fine pores are essentially independent of compaction and water contents and thus the larger pores will control the frost heave. However, when evaluating different soils, heave will be controlled by both fine and large pores.

INTRODUCTION

In many areas of the United States, the heaving of pavement due to freezing soil is a perplexing problem. Serious heaving of soils upon freezing is not due to the freezing of the local pore water in the soil, but to the phenomenon of water migration to the freezing front and formation of ice lenses. Loss of soil support on thawing is a problem which varies roughly with the amount of heave. For significant frost heave to occur, the soil must be frost susceptible, proper thermal conditions must exist, and a water table reasonably close to the freezing front must be present. The major concern in this study is the first of these requirements, that of soil frost susceptibility, and how its degree may be better predicted through correlation with the distribution of soil porosity.

Soils are directly evaluated as to frost susceptibility by their rates of heaving in freezing tests. More approximate predictions are based upon the soil texture or grain size distribution. The latter approach can not take into account variations in density and soil fabric. Furthermore, this method may be overly conservative for clayey soils. Due to the increasing use of clayey and potentially frost susceptible soils for highways, criteria better than the current grain size ones are needed.

Pore size controls the migration of water in soil and the mechanism of frost heave to a great degree. For this reason, it was felt that a study on the relation of frost heave to pore size distribution would be fruitful.

The determination of pore size distribution was accomplished with the method of mercury intrusion, which has been successfully used with soils in prior studies at Purdue by Ahmed, Lovell and Diamond (1974) and Bhasin (1975). Since mercury intrusion requires the soil to be dry, freeze drying techniques were used to minimize changes in the soil structure during its drying process.

As an indication of the ability of the soil to heave during freezing, rapid freezing tests were performed. The test method was developed by Kaplar (1968) and Zoller (1973), however, for this study modified procedures and apparatus were developed to better suit the clayey silt test soils.

To determine the relation of frost susceptibility to pore size distribution, the method of linear regression was used. This method allows a prediction equation to be developed, along with statistical measures of its reliability.

LITERATURE REVIEW

Frost Heave Theory

The theoretical reason and mechanism for soil heave upon freezing have been looked at for many years. However, due to the complexity of the chemical, thermal and molecular process of moisture migration during freezing, a completely accurate mathematical theory has yet to be developed. There are however, certain facets of frost heave theory that are widely accepted, and these will be discussed first.

The phenomenon of ice lens formation in frozen soils has been observed for many years. Beskow (1935) states that Runeberg observed clean ice in frozen soil in 1765. Another early work concerning frost heave was the "capillary theory of freezing pores" by Shtukenberg in 1885. Tsytovich (1975) states that Shtukenberg first recognized that frost heaving is caused by migration of moisture toward the freezing front, and proposed the above theory as an explanation.

An early concept in the modern explanation of frost heave is that a film of water separates the ice phase from the soil grains, and that the movement of water to feed ice lenses is through these thin films. This was postulated by Taber (1929) and Beskow (1935) around 1930, and is still fundamental to most water migration theories. Corte (1963) showed experimentally that such a film does exist by freezing water from the bottom upward in a transparent cylinder. Once the water was partially frozen, Corte sprinkled several size ranges of small soil

particles on top of the ice. As freezing continued, some particles were engulfed and others moved upward with the advancing front.

A second concept fundamental to most frost heave theories is the role of freezing point depression. The fact that large amounts of unfrozen water exist in colloidal soil can be shown by calorimetric studies. Lovell (1957a) found that even at temperatures as low as $-25^{\circ}C$, only 62% of the original moisture was frozen for a silty clay compacted at Standard Proctor optimum moisture content.

Schofield (1935) found that as the water content of the soil decreased during freezing, the freezing point was depressed further below $0^{\circ}C$. He also found that as the water content decreased, the soil suction increased. He therefore proposed the equation,

$$H = \frac{L}{T\,g}\,\Delta T \tag{1}$$

where H = suction,
L = latent heat of freezing,
ΔT = change in temperature
g = gravitational acceleration,

for the relation of pressure deficiency at a given water content and the temperature when the water begins to freeze.

Williams (1968) performed suction tests to give suction-moisture content relations and calorimeter studies for moisture content versus temperature depression. The results agreed closely with those of Schofield.

The freezing point depression is often attributed to the curvature of the ice-water interface. Osler (1967) gives the formula in finite difference form as

$$\Delta T = \frac{-2 \; \sigma_{iw} \; T}{\rho_i \; L \; r_{iw}} \tag{2}$$

where ΔT = freezing point depression,
σ_{iw} = ice-water interfacial energy,
T = freezing point with no curvature or interface,
ρ_i = density of ice,
L = latent heat of fusion,
r_{iw} = radius of curvature of the ice-water interface.

Williams (1968) points out that the equation is only good for pores large enough to have substantial amounts of free water, since σ_{iw} and L vary in a complex matter for the "bound" water close to the particle surface. He states that at -1.0°C, the adsorbed water is about 7% of r_{iw}, where r_{iw} is equal to 4.98×10^{-6} cm, and the thickness of the adsorbed water was considered to be about 7.0×10^{-7} cm. However, at -3.5°C, the adsorbed water accounts for about 2/3 of the calculated radius of the pore. Thus this formula is not good for predicting large freezing point depressions, as encountered in clay soils. The fact that the ice-water interface concept has its limitations was also brought up by Kolaian and Low (1963). They point out that there must be a significant lowering of the freezing point of adsorbed water due to its interaction with the mineral particle.

A more comprehensive freezing point relation was given by Low, Anderson and Hoekstra (1968) who related the freezing point depression to the partial molar free energy of the soil water. Their equation is rather involved, however with the use of the computer, they were able to calculate freezing point depression as a function of partial molar free energy and the negative of the relative partial molar heat content of the soil water.

In relating freezing point depression to frost heave theory, Scott (1969) states that for coarse, relatively uniform soils, the temperature depression will be only a few hundredths of a degree C. In such a soil, the pore water will freeze homogeneously throughout the soil mass, at near 0°C, and as a result, little heave will take place.

An entirely different situation arises with fine grained soils, where several degrees C of super cooling are required before nuclei form and grow in the soil pores. Once nucleation occurs in the pore, growth of the ice cluster proceeds until the ice almost fills the entire pore. During this time, the temperature in the pore either remains the same or rises, due to the release of latent heat on freezing. At this point, nucleation in the next lower pore may result, or the ice filling the pore may propagate through the small channel into the next pore. Either event requires a sufficient amount of super cooling. An alternative is for moisture to migrate to the freezing pore, with the resulting enlargement of the pore eventually forming an ice lens.

The relation of the geometry of the ice-water interface to frost heaving pressures has been used in theories by Everett and Haynes (1965), Penner (1973), Williams (1968) and many others. Williams uses the commonly accepted formula,

$$(p_i - p_w) = \frac{2\,\sigma_{iw}}{r_{iw}} \qquad (3)$$

where p_i = pressure on ice,
$\quad\;\; p_w$ = pressure on water.

He states that when,

$$(P_i - P_w) > \frac{2\,\sigma_{iw}}{r_c} \qquad (4)$$

where r_c = radius of connecting pore channel,

the ice front will pass through the pores. However if,

$$(P_i - P_w) < \frac{2\,\sigma_{iw}}{r_c} \qquad (5)$$

the ice front can not pass through the pore channels and ice lenses will form.

A different approach to the motive force for migration of water is the osmotic theory proposed by Cass and Miller (1959) and others. This theory is based on the idea that due to a concentration of ions in an electric double layer around soil, an osmotic pressure potential exists. The authors believe that an ice-water interface can be considered as a surface effectively midway between particles, and that an osmotic pressure difference exists between the interface and the less concentrated solution in underlying pores. Due to this difference, underlying pore water flows to, and then joins the ice lens, with heave resulting. Since ice forms as a pure phase without electrolytics, the concentration of ions below the ice lens tends to increase, whereas flow from pore water tends to dilute the concentration.

The authors also believe that the concentration of ions result in a depression of the double layer temperature, with the water freezing at a lower temperature. They state that ice lenses do not form in a coarse soil because water in the double layer is insignificant compared to the free water in the much larger pores.

With regards to the validity of the osmotic theory, Tstovich (1975) says that Bozhenova found that perceptible results of osmosis are observed only at rather high salt concentrations in the pore water.

Another driving force in the migration of water to the freezing front is that of chemical action. Tstovich (1975) describes work done under his direction by Nersisova, which considered the influence of physiochemical properties of soil surfaces on the migration of moisture and ice segregation. For the study, kaolin and montmorillonite clays were saturated with various exchange cations. It was found that greater migration of water and heaving were observed when the clays were saturated with multivalent cations and less with univalent cations.

An entirely different kind of moisture migration during freezing is from vapor transportation. Tsytovich (1975) says that Lebedev found experimentally that migration of moisture from moist, but unsaturated, soils is due to movement of vapor from locations of higher to those of lower vapor pressure. However, Jumikis (1957) found the amounts of soil moisture transferred upward to the freezing front in the form of vapor to be insignificant.

The basic adsorbed water film theory is probably the most widely accepted and is described in various ways by Kaplar (1970), Hoekstra, Chamberlain and Frate (1965), and by Keinonen (1973). According to this theory, water migrates from thick films with more mobile molecules toward thin films in the partially ice filled pores. The reason for this is that Gibbs' free energy is smaller for the thinner water films and water flows in the direction of decreasing free energy.

Keinonen (1973) expresses the Gibbs' free energy as,

$$G = u + pv - Ts \qquad (6)$$

where G = Gibbs' free energy,
     u = internal energy,
     p = pressure,
     v = volume,
     T = Temperature,
     s = entropy.

He states that when the soil water temperature decreases below $0^{\circ}C$, the outermost part of the adsorbed water freezes and the film becomes thinner. When the water molecule freezes, it loses its dipolar attraction to the soil particle. As a result, the inner pressure in the remaining water film decreases, and the Gibbs' free energy consequently decreases.

With regards to actual frost heaving, the difference between the free energy in free ground water and in freezing soil limits the total mechanical work done during the freezing process. The work in the freezing process is used both to draw up water to the freezing front and for frost heave pressures.

Kaplar (1970) prefers to let the soil physicists and physical chemists debate the actual motive force for the movement of water in films. Instead, he looks at the migrating-heaving system as a "jacking" process. The thin films serve as the jacks, lifting the overburden for the ice cluster to increase in size, and in the mean time "sucking" water to the cluster.

How involved one should get in various theories of frost heave and water migration is open to question, especially since there appears to be several motive forces behind the process. Possibly a quite adequate explanation for the principle of moisture migration in freezing soils is given by Tsytovich (1975) who says:

"...the migration of water in freezing moist soils is
a process of moisture transport that operates
consistently whenever the equilibrium state of the
soil's phases is disturbed and external factors
change (the presence of temperature, moisture content,
pressure, mineral particle surface energy, mobility
of molecules in water films, gradients, etc)."

In summarizing the theoretical and experimental work that has been
accomplished so far, there is still conflict and lack of understanding
in certain areas, however, certain concepts are considered essentially
true. Some of these are:

1) Heave in fine, frost susceptible soils is due to
migration of moisture and not just the slight
expansion of existing moisture when it freezes.

2) Coarse soils may not heave appreciably, due to
migrating forces being too small to transport
water to the freezing front. In some cases,
squeezing of water from the freezing front may
result.

3) Very plastic clays may only heave slightly, due to
excessive amounts of energy required to move water
to the freezing front.

4) A film of liquid separates the frozen water from
the soil particles, with the migration of water
to the ice front most likely being in these films.

5) Nucleation of water in pores is partly a function
of their curvature and size. In large pores,
nucleation will result at only a few hundredths of
a degree C below 0°C, whereas it may take several
degrees C below 0°C for nucleation in small pores.

6) The motive force for migration is a complicated
conglomerate, which may include chemical, osmotic,
vapor pressure, and other effects.

7) Although the heaving mechanism is complicated, it
is at least partially dependent on the size of
pores, the shape and size of pore channels, and
surface area of the particles.

Frost Heave Tests

An important tool for predicting frost heave has been the various laboratory frost heave tests. This area is again one in which there exists no complete agreement, and there seems to be no universal, standard test for all situations.

The U. S. Army CRREL heave test developed in the early 1950's is probably the most widely known one in the U. S. As described by Kaplar (1974), the test is based on one-dimensional heave of samples frozen from the top down at a rate of penetration of the $0^{o}C$ isotherm of about 0.25 to 0.5 inches per day. The soil samples are frozen in acrylic tubes, tapered so that the inside diameter is 5.75 in. at the top and 5.5 in. at the bottom. Before being placed in the acrylic tubes, the soil is compacted in steel cylinders using the Providence Vibrated Density method for coarse soils, and AASHTO test procedure T-180-570, method "A" or "D", for the fine grained soils. Saturation is accomplished using deaired water and a vacuum.

A disadvantage with this method is it is very time consuming, with a freezing test time of 15 to 20 days. Also, the soil may freeze to the sides of the acrylic containers, thus limiting heave. Kapler (1968) believes that with adfreezing to the sides, a more rapid penetration rate will result, due to less latent heat release at the freezing front. Since the operator controls the rate of penetration of the $0^{o}C$ isotherm, once an increasing rate of penetration was noticed, he would raise the freezing temperature, thus further decreasing the heat extraction and freezing rate.

Based on tests carried out by CRREL, Casagrande proposed the test criteria shown in Table 1.

Table 1. CRREL Frost Heave Classification

Average Rate of Heave (mm / day)	Relative Frost Susceptibility Classification
0 - 0.5	Negligible
0.5 - 1.0	Very Low
1.0 - 2.0	Low
2.0 - 4.0	Medium
4.0 - 8.0	High
> 8.0	Very High

Table 2. TRRL Frost Heave Classification

Total Heave (cm for 250 hours)	Relative Frost Susceptibility Classification
< 1.27	Satisfactory
1.27 - 1.78	Marginal
> 1.78	Unsatisfactory

Table 3. UNH Frost Heave Classification

Average Rate of Heave (mm / day)	Relative Frost Susceptibility Classification
0 - 6.5	Negligible
6.5 - 8.0	Very Low
8.0 - 10.3	Low
10.3 - 13.0	Medium
13.0 - 15.0	High
> 15.0	Very High

The British Transportation and Road Research Laboratory (TRRL) frost heave test, as described by Jacobs (1965), is another test widely used for evaluation of freezing conditions. As in the CRREL test, freezing is unidirectional, however, it is at a constant temperature.

The soil samples used in the TRRL test are 4 in. diameter by 6 in. high cylinders which are wrapped in polythene. The top of the samples are exposed to a temperature of -17°C and the bottoms rest on porous ceramic discs in contact with water at 4°C, with the space between samples filled with sand. The actual test is carried out for a period of ten days, although Sutherland and Gaskin (1970) have found experimentally that the test time could probably be reduced to about 50 hours.

The heave criterion for the TRRL test was based on field experience gained during severe frosts of 1940 and 1947. The frost susceptibility criteria are listed in Table 2.

To compare the CRREL and TRRL criteria and results, Sutherland and Gaskin (1973) tested four mixtures of stabilized pulverized fly ash, using both test procedures. Both tests classified the four mixes in the same increasing order of frost susceptibility. Three of the mixes were classified identically, with the remaining mix classified as "unsatisfactory" by TRRL and "very low" by CRREL.

Due to the limitations of the CRREL test, work on a rapid freeze test was performed by Kaplar (1968, 1971) and later Zoller (1973).

Kaplar found that with a faster freezing rate, heave rate increases to a maximum and then drops off, eventually reaching a point where heave is due solely to volume expansion during phase change. He therefore suggested that the 0.25 in. to 0.5 in. freezing penetration rate of the

CRREL test was unnecessarily slow, and more useful information concerning maximum heave could be obtained by using a higher rate of frost penetration, along with a constant temperature.

Kaplar also believed a major problem with the existing CRREL test was that soil froze to the acrylic tube, thus impeding heave. To reduce this side-wall friction, Kaplar used a series of acrylic rings, designed to separate during freezing.

The University of New Hampshire (UNH) test developed by Zoller (1973) and his students also is a rapid freeze test using Lucite rings to reduce sidewall friction. The test procedure used at UNH is slightly different than Kaplar's, since a Peltier battery serves as a heat sink during freezing. The battery is adjusted to a heat pumping capacity of about 65 BTU per hour, with the top of the samples stabilizing to a temperature of about $-4^{\circ}C$.

A problem with the use of rings is that it is difficult to saturate samples with low permeability. If a vacuum or large gradient is applied during saturation, the sample containers will leak. Zoller's method of saturating the sample by raising the water level to the top of the sample may work for fine sand and some silts. However, it is questionable whether a very high degree of saturation can be obtained with soils containing much clay.

The purpose of the UNH test program was not so much to consider a different laboratory freezing method as to correlate it with freezing in the field. From their testing program, the UNH criteria shown in Table 3 were developed. Zoller reports that of the many base course materials tested during the project life, no instances have been

reported in which materials classified as "low to negligible" in the UNH rapid freeze test have subsequently heaved detrimentally in the field.

Penner (1972) has also carried out experiments using a rapid freeze setup similar to the UNH test. However Penner suggests using rates of freezing that are related to actual field conditions, rather than at one arbitrary applied temperature.

In other frost action tests carried out by Hoekstra, Chamberlain, and Frate (1965), Osler (1967), and Martin and Wissa (1973), the soil samples were completely constrained and heaving pressures were measured. Hoekstra et al. and others state that the one-dimensional heaving pressure, p, is given by

$$p = \frac{2 \, \sigma_{iw}}{r_{iw}} \tag{7}$$

where σ_{iw} = surface tension between ice and water,
r_{iw} = effective radius of ice-water interface.

The researchers believe that heaving pressures may be a way of predicting frost susceptibility. However, the role of permeability in transporting water to the freezing front does not seem to enter into the heaving pressure. As a result, soils with very low permeabilities may have high heaving pressures, yet heave very little.

Frost Heave Criteria

Before closing the discussion on frost heave, it is worthwhile to discuss some of the frost susceptibility criteria and related factors that are based on soil parameters.

In the U. S., probably the most widely known frost susceptibility criterion is based on Casagrande's (1932) famous discussion in 1932, where he gave the following rule of thumb for identifying frost-susceptible soils:

> "Under natural freezing conditions and with sufficient water supply one should expect considerable ice segregation in non-uniform soils containing more than 3 percent of grains smaller than 0.02 mm, and in very uniform soils containing more than 10 percent smaller than 0.02 mm. No ice segregation was observed in soils containing less than 1 percent of grains smaller than 0.02 mm, even if the ground water level was as high as the frost level."

A variation of Casagrande's frost susceptibility criterion is the Corps of Engineers frost design classification system {Johnson (1975)}, which is listed in Table 4. This test was developed to account for the reduced stability of the various types of frost susceptible soils during the thaw-weakened period. Frost susceptible soils are classified into four groups (F1, F2, F3, F4) of increasing susceptibility to frost heaving and/or weakening as a result of frost melting. With the groups, F1 is the least susceptible, F4 the most, and F2 and F3 falling between the two. Groups F1 and F2 may both experience equal ice segregation, however, F1 material may be expected to show higher bearing capacity than F2 material during thaw.

A logical extension of textural and grain size criteria is the pore size distribution of the soil. Hoekstra, Chamberlain and Frate (1965) stated that pore size distribution could be a more fundamental parameter. They point out that although grain size and pore size are related, this relationship is obscured by factors such as gradation and grain shape. As a measure of pore size, the authors used soil tension and were able to identify trends between the frost heaving process and soil tension.

Table 4. U.S. Army Corps of Engineers Frost Design Soil Classification

Frost Group	Soil Type	Percentage Finer Than 0.02 mm, by weight	Typical Soil Types Under Unified Soil Classification
F1	Gravelly soils	3 to 10	GW, GP, GW-GM, GP-GM
F2	(a) Gravelly soils	10 to 20	GM, GW-GM, GP-GM
	(b) Sands	3 to 15	SW, SP, SM, SW-SM, SP-SM
F3	(a) Gravelly soils	> 20	GM, GC
	(b) Sands, except very fine silty sands	> 15	SM, SC
	(c) Clays, PL > 12	–	CL, CH
F4	(a) All silts	–	ML, MH
	(b) Very fine silty sands	> 15	SM
	(c) Clays, PL < 12	–	CL, CL-CM
	(d) Varved clays and other fine-grained banded sediments	–	CL and ML; CL, ML, and SM; CL, CH, and ML; CL, CH, ML, and SM

Csathy and Townsend (1962) used a capillary rise test as a basis for determination of pore size distribution, and compared results with actual field frost behavior. From the comparison, they proposed the following criterion,

1) soils with P_u < 6 are frost susceptible, and

2) soils with P_u > 6 are non frost susceptible,

where $P_u = P_{90}/P_{70}$,
P_{90} = the pore diameter such that 90% of the pores are smaller than P_{90},
P_{70} = the pore diameter such that 70% of the pores are smaller than P_{70}.

Csathy and Townsend concluded that the pore size criterion was considerably more efficient than the currently used particle size criterion. However, Gaskin and Raymond (1973) point out that Csathy and Townsend extrapolated some of their curves to obtain a P_{90} value. They believe that this procedure is of doubtful validity, and state that if only curves that actually contain both P_{90} and P_{70} values are used, Csathy and Townsend's criterion has no real advantage over currently used particle criterion.

Gaskin and Raymond (1973) have also looked at pore size distribution from samples of actual field soils and tried to correlate them to the field frost performance. However, instead of using capillary rise methods, which take four weeks per test, they used the pressure plate suction test, along with the mercury intrusion test. Based on their tests, the authors found no correlations which were more efficient than the currently used criterion based on particle size.

Two objections might be raised against Gaskin and Raymond's experimentation. The first is the question of disturbance of the pore

structure due to sampling and drying that took place before measurement of the structure. The second is that the pore size distribution was only carried down to about the 10 micron size range. For some of the soils tested, less than 60% of the pores were larger than this size. Therefore, the actual complete pore size distribution was not always truly represented.

When considering the effects of density and compaction on frost heave, Zoller (1973) postulates that there is approximately a linear relationship between heave rate and percent compaction, and that the zero percent compaction intercept is approximately the same heave rate value for all materials tested. Thus he says that the calculated heave rate at a given percent compaction for any material is a simple function of its heave rate at any other compaction as expressed by the equation:

$$HR = S(PC) - 15.40 \qquad (8)$$

where HR = heave rate, in mm,
    PC = percent compaction,
    S = slope of percent compaction - heave rate line.

The above relation is somewhat contrary to results of an early study by Winn and Rutledge (1940). Their data indicated that for the soils tested, there is one density at which frost heave occurs most readily, while at higher or lower densities the action is not so pronounced.

Pore Size Determination

The present study is based on past work with pore size done at Purdue University and is geared more toward the useful applications of pore size distribution rather than refinement of the technique. For this reason, the present literature review on pore size distribution is brief,

and the reader is referred to Ahmed (1971) and Bhasin (1975) for a much more comprehensive review.

The method used for the present study is mercury intrusion, which was first proposed by Washburn (1921). Washburn suggested that the absolute pressure, p, required to intrude a cylinderical pore of diameter, d, is related by

$$p = - \frac{4 \sigma_m \cos \theta}{d} \tag{9}$$

where σ_m = surface tension of mercury,
 θ^m = contact angle between the mercury and the pore wall.

Since the proposal of the above equation, there has been much discussion about the "correct" contact angles and surface tension values, along with development of practical mercury intrusion apparatus. However, the basic equation, along with its limitations is still used.

A primary limitation with mercury intrusion is that it measures the diameter of the channel leading into the pore, and not the actual pore diameter. Many researchers {Ahmed (1971), Orr (1969)} point out the "ink bottle" effect, where mercury does not flow into a large pore with a small opening until the pressure is sufficient to intrude the pore opening. When related to frost heave, this problem may not be so major, since the advancing ice front and moisture migration to the freezing front must both pass through, and be restricted by, the pore channels.

A second problem with the Washburn equation is that cylindrical pores are assumed. As pointed out by Bhasin (1975), this assumption may be fairly reasonable since differences due to pore shapes are within an order of magnitude while the pore size range of compacted soils normally extends over five orders of magnitude.

Sample Drying Methods

For mercury intrusion to be effective, the soil sample must be almost completely free of moisture. Since air or oven drying often produces excessive shrinkage, critical region drying and freeze drying methods have been developed to allow dehydration at essentially constant volume.

The critical region drying method is based on the idea that a fluid at temperatures and pressures below the critical point can occur in two coexisting phases, with different specific volumes. However, at temperatures above the critical point, a fluid can exist only as a single phase with no latent heat of vaporization and no change in specific volume. Using this concept, the critical region drying process begins by raising the temperature and pressure such that changes in the specific volume are slow in the compressed liquid region. Once the critical point is reached, the soil water is transformed into vapor and then is removed in the superheated vapor region.

Using the critical region drying method, Bhasin (1975) successfully dried Edgar plastic kaolin, Grundite, Crosby silty clay, and a reddish-brown limestone residual clay with little or no volume change. He also tried Volclay bentonite, but found that the essentially montmorillonitic clay shrank appreciably.

A second method of drying is the freeze drying method. With this method, the soil sample is quickly frozen in liquid nitrogen and then placed in a vacuum where the moisture in the form of ice is removed by sublimation. Drying takes place when the partial pressure of water vapor at the frozen surface exceeds that of the surroundings. As Ahmed

(1971) points out, the vacuum does not "suck" water out, but merely reduces the concentration of gas molecules present in the pores and thus reduces the resistance to water vapor flow.

Using the freeze drying process, Ahmed dried Grundite at various compacted water contents. He found that freeze drying produced less than 5% reduction of volume.

Zimmie and Almaleh (1976) also used freeze drying, and found from some 100 tests that the mean volume shrinkage was less than about 7% for both a kaolinite and sodium montmorillonite clay. The clays were compacted with a static pressure, at water contents between 10 and 40% for the kaolinite and 120% to slightly over 250% for the montmorillonite.

Pore Size Distribution of Compacted Clays

From work done by Sridharan, Altschaeffl and Diamond (1971), Ahmed, Lovell, and Diamond (1974), and Bhasin (1975), the following conclusions can be drawn about pore size distribution and its relation to compaction variables.

1) It is generally agreed that most soils compacted on the dry side of optimum exhibit greater space in relatively large pores than that present in soils compacted at optimum or on the wet side. Bhasin believes that this results from dry side specimens retaining after compaction much of the structure of the individual aggregations, with large spaces present between the aggregations. However, the interaggregation spaces are completely eliminated by the time the water content is increased to the wet side.

2) Bhasin found that increasing the compactive effort on the dry side of optimum water content diminished the quantity of the larger pores, whereas increasing the compactive effort had little effect on the pore size distribution for soils compacted on the wet side.

3) For the Grundite samples tested by Ahmed, the pore size distributions were affected very little when samples were compacted to the <u>same</u> moisture-unit weight conditions by <u>different</u> methods of compaction.

SOILS STUDIED

The soils were selected based on projected frost heave and fac-
ility of pore size distribution tests. With regards to frost heave,
silt generally is the highest heaving of any soil. Therefore, it was
decided to use a relatively pure silt and observe the effects of
different water contents and clay contents on frost heave and pore size
distribution. A second factor favoring the choice of a clay-silt soil
was the requirement that the porosimeter sample be very small. Thus,
soils containing particles larger than fine sand are not really practical
with this equipment.

The silt was obtained from a natural loess deposit at the second
bench level on the east side of US 41, just south of Patoka, Indiana.
For the frost heave and pore size tests the silt was air dried and
passed through a number 40 sieve. The silt was found to have a specific
gravity of 2.73, liquid limit of 24 and no plasticity. The AASHTO
classification of this type of soil is A-4. A grain size distribution
for the natural silt is shown in Figure 1.

The clay that was mixed with the silt so as to give different soil
combinations was Edgar plastic kaolin. This clay is commercially
processed to remove material coarser than 40 micrometers, dried in a
tunnel dryer at temperatures ranging from 300° to 450°F, and then
pulverized. The manufacturer states that the clay mineral composition
is 99.5% kaolinite, with the remainder as micro sized alpha quartz and

mica. The specific gravity of the clay is 2.65.

Three silt-clay mixtures were used: 90% silt, 10% kaolin; 70% silt, 30% kaolin; and 50% silt, 50% kaolin. Grain size distribution curves for the three soil mixtures are plotted on Figure 1. Listed in Table 5 are the Atterberg limits and AASHTO classification for the soil mixes.
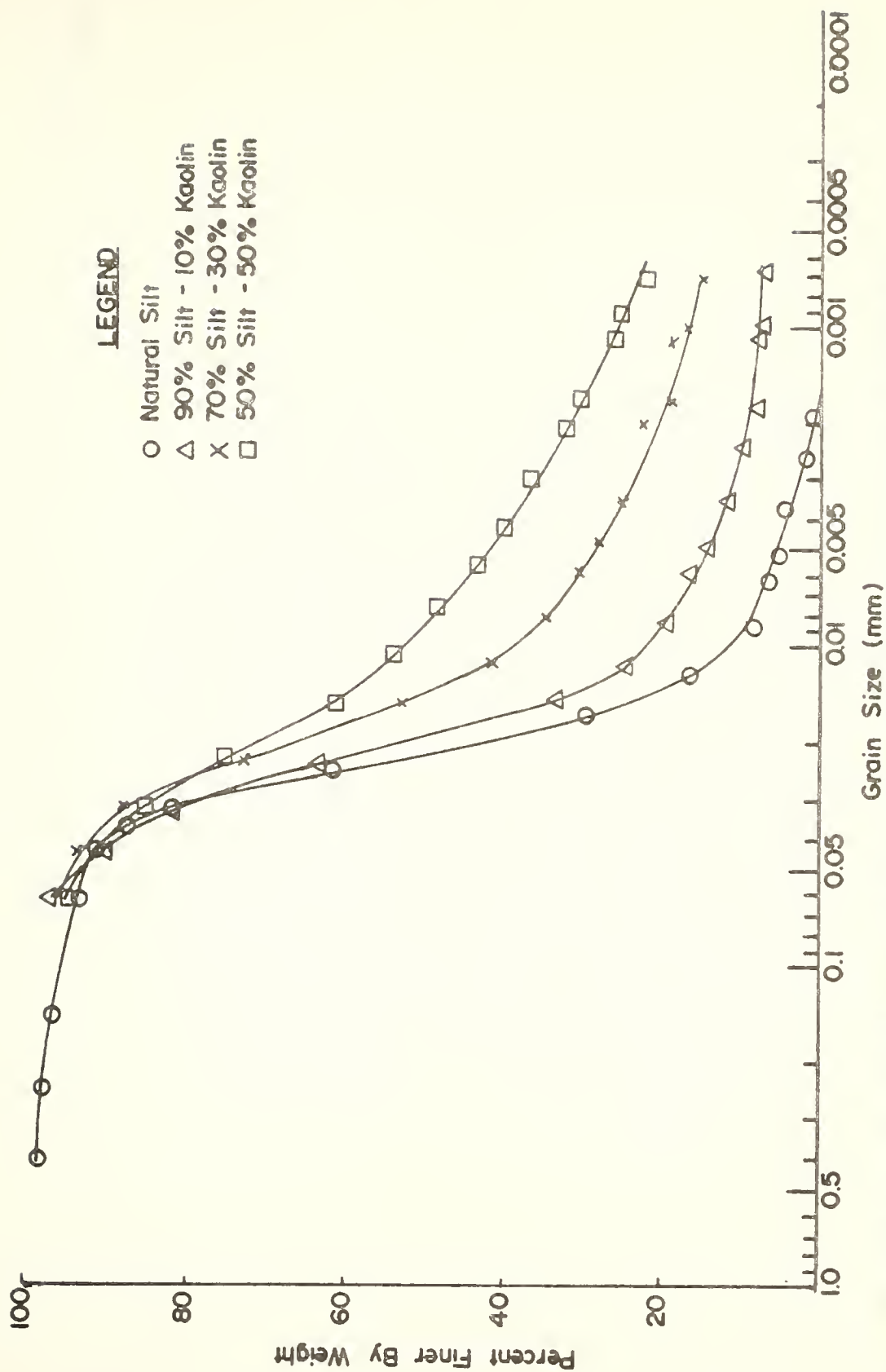
FIGURE I GRAIN SIZE DISTRIBUTIONS FOR SILT AND SILT-KAOLIN MIXTURES

Table 5. Atterberg Limits and Classification of Soil Mixtures

% Silt - % Kaolin	Liquid Limit	Plastic Limit	Plastic Index	AASHTO Soil Classification	Unified Soil Classification
90 - 10	19.7	19.7	0	A-4 (0)	ML
70 - 30	25.3	18.3	7.0	A-4 (5)	CL - ML
50 - 50	36.7	21.0	9.7	A-4 (11)	ML

APPARATUR AND EXPERIMENTAL PROCEDURES

Soil Mixing and Curing

The selected mix of clay and silt was both dry mixed and mixed to the desired moisture content using a Patterson Kelly twin shell liquid solid blender. The blender, shown in Figure 2, consists of a rotating V shell which keeps the soil in continual motion. Inside the shell is a high speed rotating dispersion bar from which dionized water is sprayed. Connected to the dispersion bar is a graduated cylinder and stopcock which controls the amount of water to be sprayed.

To use the blender, 4 kg of the desired air dried silt-clay combination was first dry mixed for about 10 minutes. Water was then added at a rate of about 50 to 100 ml per minute, after which the blender was stopped and the sides of the shell scraped to remove sticking soil. Following scraping, the mixer was run for 7 minutes, stopped, and again the sides were scraped. The mixer was run for 7 additional minutes, after which the soil was sealed inside a polyethylene bag and cured in a high humidity barrel for two days. When adding water to the mix at hygroscopic water content, experimentation indicated that adding 0.5% less water than calculated gave within 0.25% of the desired moisture content.

It should be noted that enough soil was mixed at one time so that two samples could be compacted. Thus one sample could be used for the frost heave test and the other cut up for freeze drying.
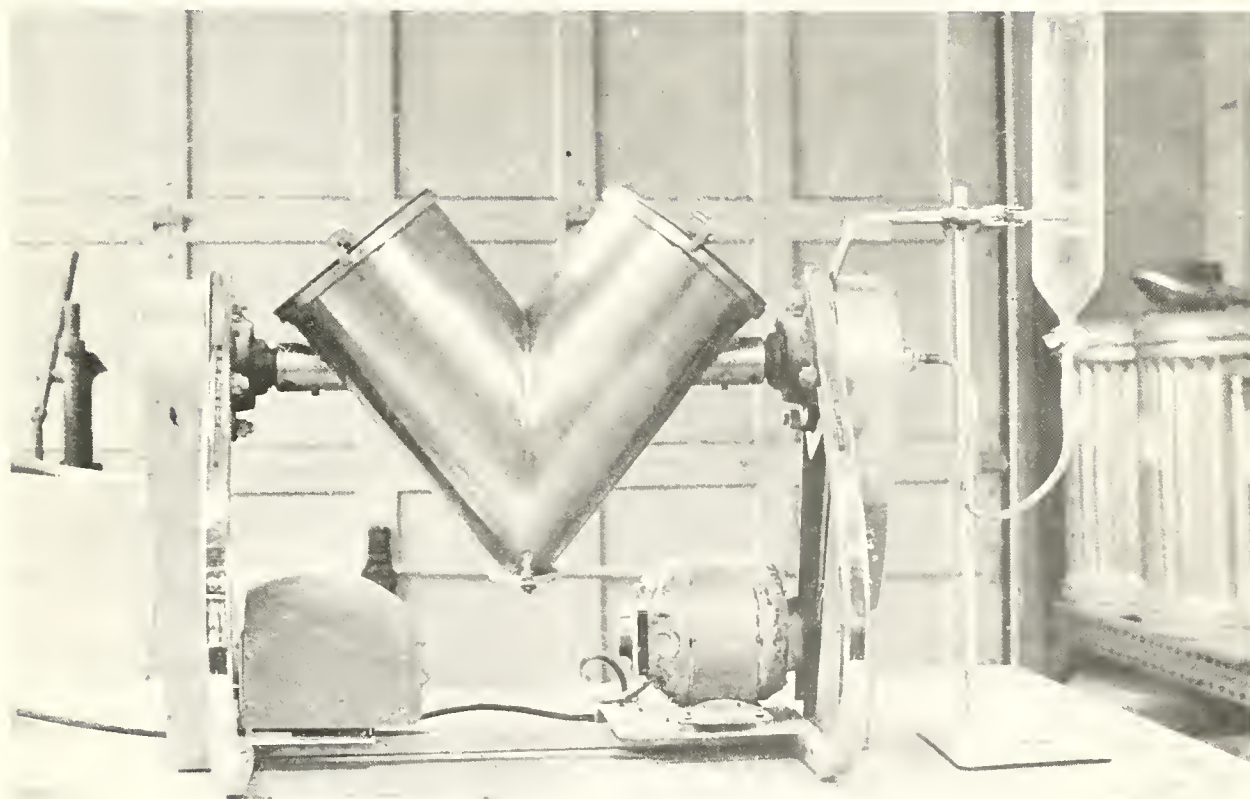
FIGURE 2   PATTERSON KELLY BLENDER

3R

Compaction

Description of Compactor

As shown in Figure 3, an electrically driven semi-automatic kneading compactor made by the August Manufacturing Company was used. As mentioned by Bailey (1976), this type of compactor seems to simulate actual field compaction conditions. Also, since it is mechanized, the compaction foot gives very repetitious foot pressures, and hopefully a very uniform sample. This is highly desirable where very small samples are to be taken from the compacted soil for pore size distribution studies.

Soil samples were compacted by a triangular shaped foot with the sample rotated 60° between application. The foot pressure was varied by a pneumatic-hydraulic control system using a standard air regulator and pressure gauge. At the present time, the actual foot pressure versus gauge pressure is somewhat difficult to accurately quantify. However, the maximum dynamic foot pressure versus gauge pressure could be determined using a proving ring. This relation is plotted in Figure 4. Since this calibration varies with time and use of the compactor, the reported foot pressures should be viewed as approximate.

Compaction Procedure

Three nominal energy levels of compaction were used to give a range of soil density conditions. The gauge readings for the compactive levels are as follows:

1) 3.5 and 40 psi for 90% silt - 10% kaolin
2) 4, 8.5 and 40 psi for 70% silt - 30% kaolin
3) 4 and 8.5 psi for 50% silt - 50% kaolin.
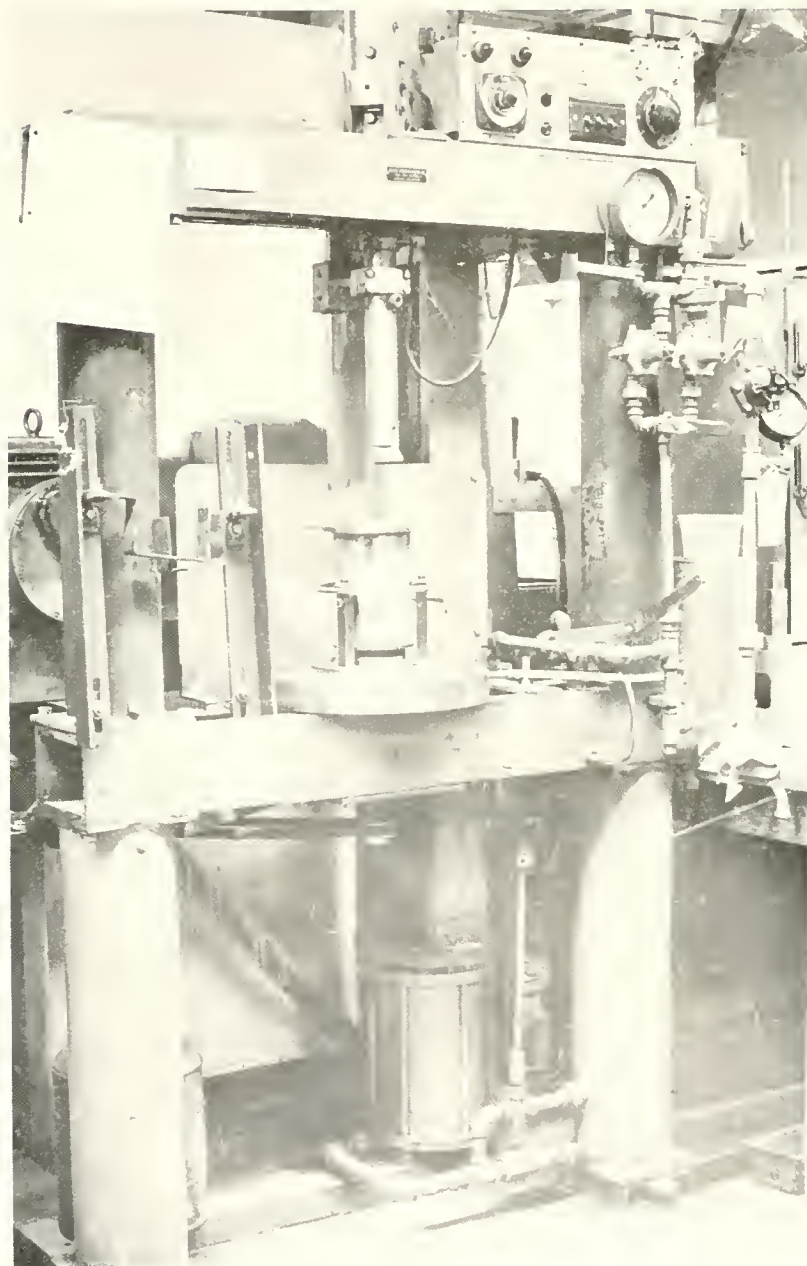
FIGURE 3   AUGUST MANUFACTURING COMPANY
            KNEADING COMPACTOR
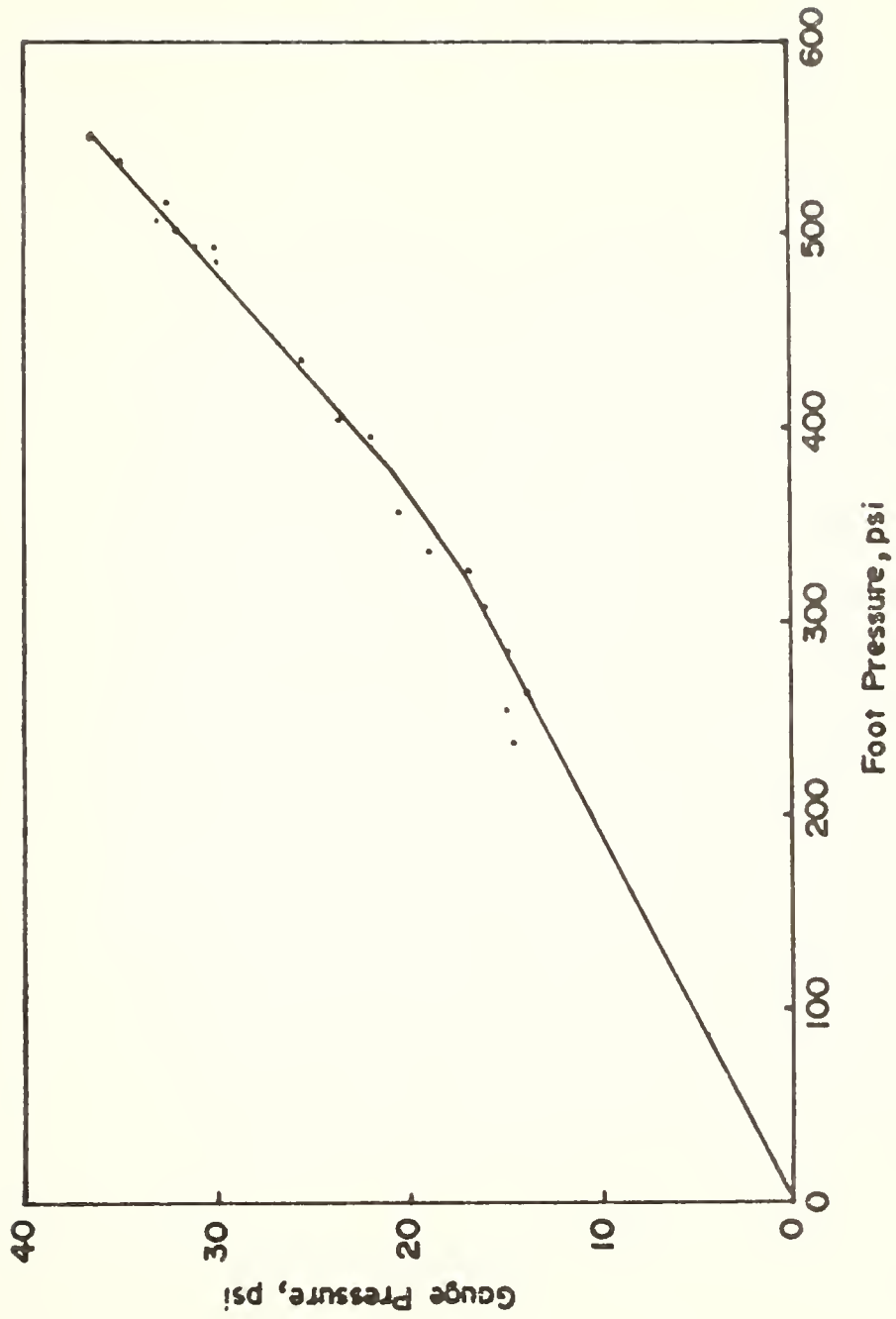
FIGURE 4 DYNAMIC FOOT PRESSURE VS GAUGE PRESSURE

The middle range (8.5 psi) of compactive effort was selected so that the maximum dry density for the 90% silt - 10% kaolin mixture closely approximated that obtained by an impact hammer using AASHTO test procedure T99-70, method "A", except that fresh soil samples were used for each point.

As mentioned by Bailey (1976), there is no standard method for this type of compaction with soil. Therefore, the following procedure was used. The sample was compacted in a Lucite mold 4.0 in. in diameter by 4.58 in. high, which was supported in a ring as shown in Figure 5. The soil sample was compacted in 5 equal layers with 30 blows per layer. Before compaction, each layer was lightly tamped with a piston. After the layer was compacted, the top of it was scarified before compacting the next layer. If this was not done, cracking tended to appear between layers for soil compacted on the wet side of optimum. Once compaction was completed, the sample and mold were removed from the compaction holder and the soil was ready for saturation.

<div align="center">Saturation</div>

To maximize the frost heave, the freezing samples were brought as close to complete saturation as practicable while still retaining a constant volume condition. To accomplish this, the saturation device shown in Figures 6 and 7 was used.

To saturate the sample enclosed in the Lucite tube, caps containing porous stones and quicklock connections were placed on each end. The assembly was then connected for two days to an inflow and outflow reservoir of the saturation device. The device was designed so that both reservoirs could be independently pressurized and also so that a
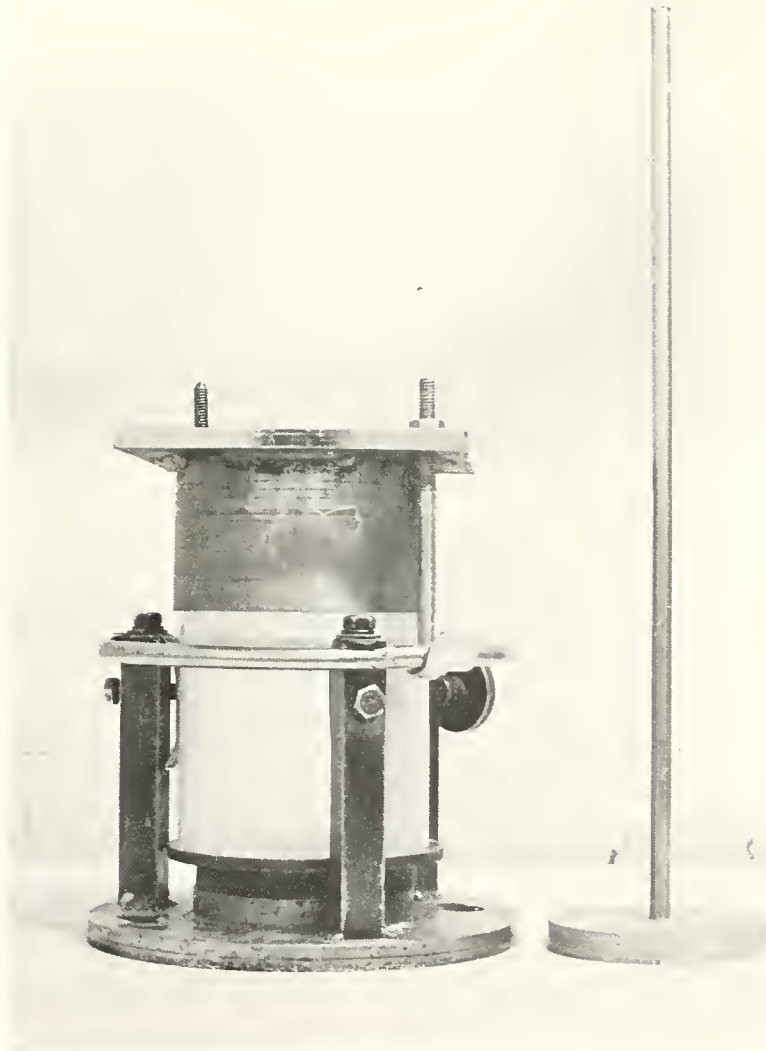
FIGURE 5   COMPACTION MOLD, HOLDER, AND PISTON
TAMPER

FIGURE 6   COMPACTION MOLD AND END CAPS USED FOR
SATURATION
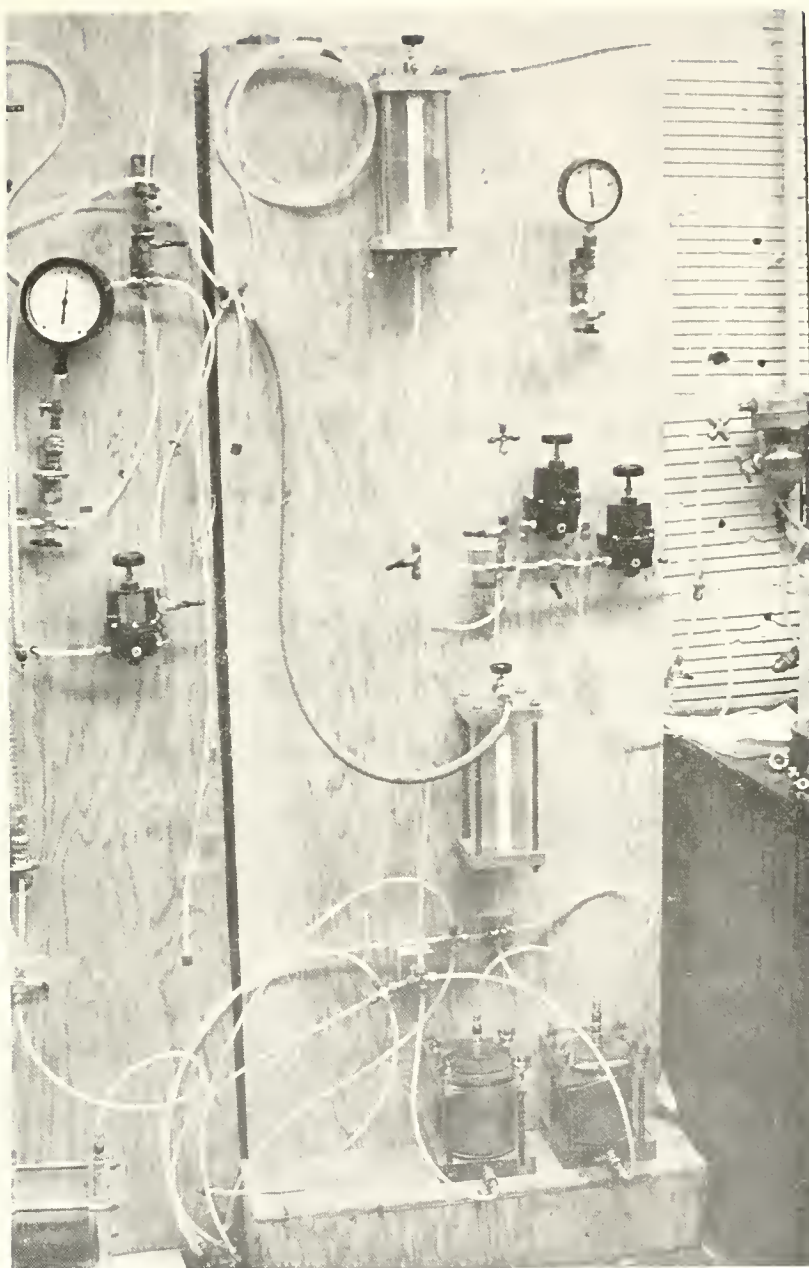
FIGURE 7   SATURATION DEVICE

vacuum could be connected to the outflow reservoir.

The usual procedure was to apply a pressure to the inflow reservoir so that a gradient would exist in the sample. In some cases, the inflow and outflow reservoirs were both pressurized, so that air bubbles in the sample would be compressed and hopefully flow out of the sample. The gradient used for saturation depended on the soil, but in no case exceeded about 5 psi. For some soils, it was found that applying a vacuum at the top of the sample also aided in saturation.

For almost all the soil mixes it was possible to obtain saturation of 95% or better. Some problems were encountered with the 90% silt - 10% kaolin mixture compacted on the wet side. However, soil mixtures of 70% silt - 30% kaolin and 50% silt - 50% kaolin compacted at optimum and the wet side had initial compacted saturations of close to 95%, and thus no problems were encountered. Soil mixes compacted on the dry side seemed to saturate well by using a vacuum.

Frost Heave Test

At the present time there is no universal, simple, frost heave test. The U. S. Army Cold Regions Research and Engineering Laboratory (CRREL) test seems to be the most universal, however it is very time consuming. The test is based on a slowly descending frost line, controlled by constantly adjusting the room temperature.

A more practical test is the rapid freeze test developed by Kaplar (1968) and Zoller (1973). This test uses a constant room temperature to freeze the sample and only takes 2 days. A problem with the setup that these gentlemen used is that the sample was compacted and frozen in Lucite rings. The rings were selected to reduce side wall friction,

however, they cause problems in saturating soils of low permeability.
Since some of the soil mixes used in this study are of low permeability,
different sample containers were designed.

The sample container, shown in Figures 8 and 9, consists of a 17 in.
by 17 in. by 6.75 in. block of Dow Styrofoam in which two 4 in. diameter
cylinders were bored to hold the samples. In order to prevent friction
between the cylinder and sample, the sides were lined with teflon tape.
Attached to the top of the Styrofoam were two brackets which held dial
gauges to measure sample heave. Also, porous stones were mounted in the
cylinder, so that the top of the soil sample protruded slightly above
the top of the Styrofoam block. Styrofoam was used as the container
because of its low thermal conductivity, and thus it was felt that the
sample would be less likely to freeze to the side of the cylinder, as is
possibly the case when using a Lucite cylinder.

The freezing container with samples enclosed, was placed inside a
Styrofoam lined box which contained deionized water at $4^{o}C$. The height
of the sample container was designed so that it would float in the water
bath with a water level of approximately 0.75 in. above the bottom of
the sample. Floating the container gave a very simple and constant
regulated water supply. To maintain the water temperature of $4^{o}C$, a
temperature control bath and circulator were used. The complete setup
is shown in Figure 10.

The entire assembly was placed inside a cold room at $-6^{o}C$ for
freezing. The average temperature of the cold room was monitored by
placing thermocouples inside a glycerol filled bottle which rested on
the sample container. The water bath temperature was also monitored
using thermocouples. To read the thermocouples a digital voltmeter and
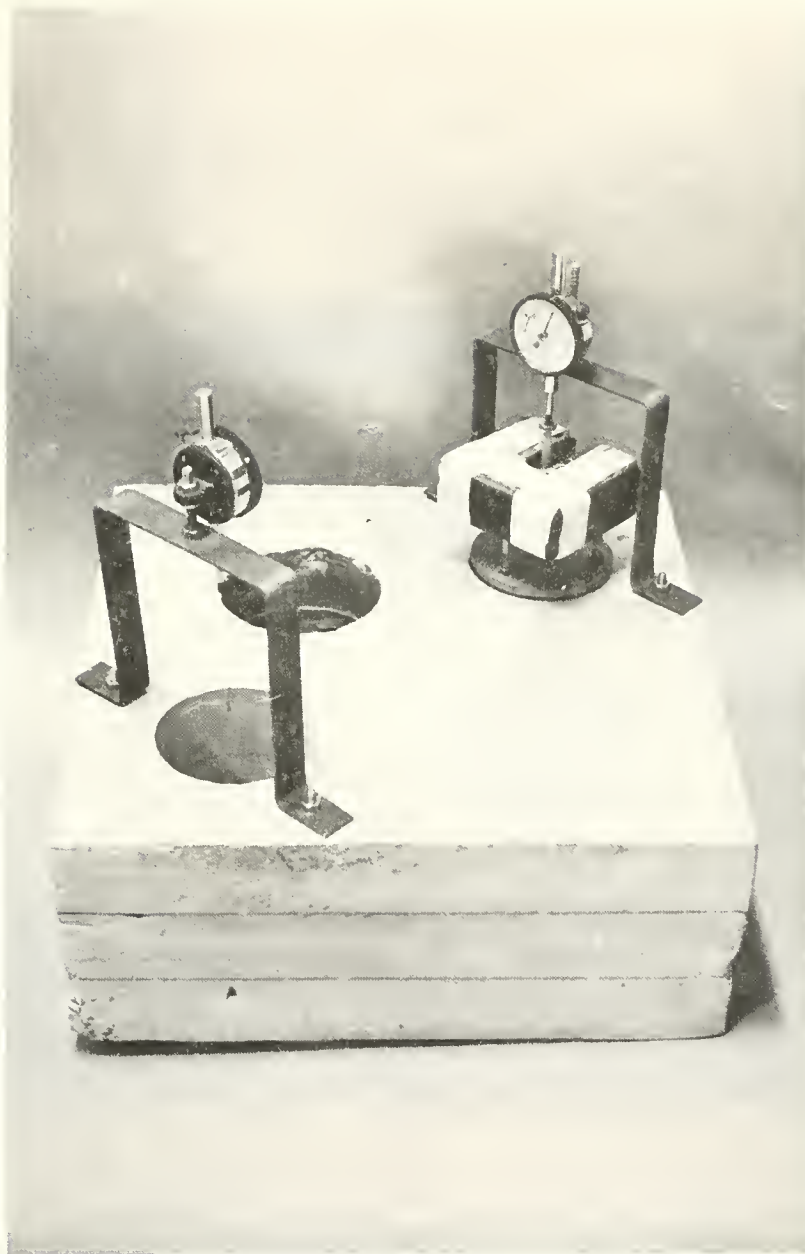
FIGURE 8   FROST HEAVE SAMPLE CONTAINER WITH DIAL
GAUGES MOUNTED
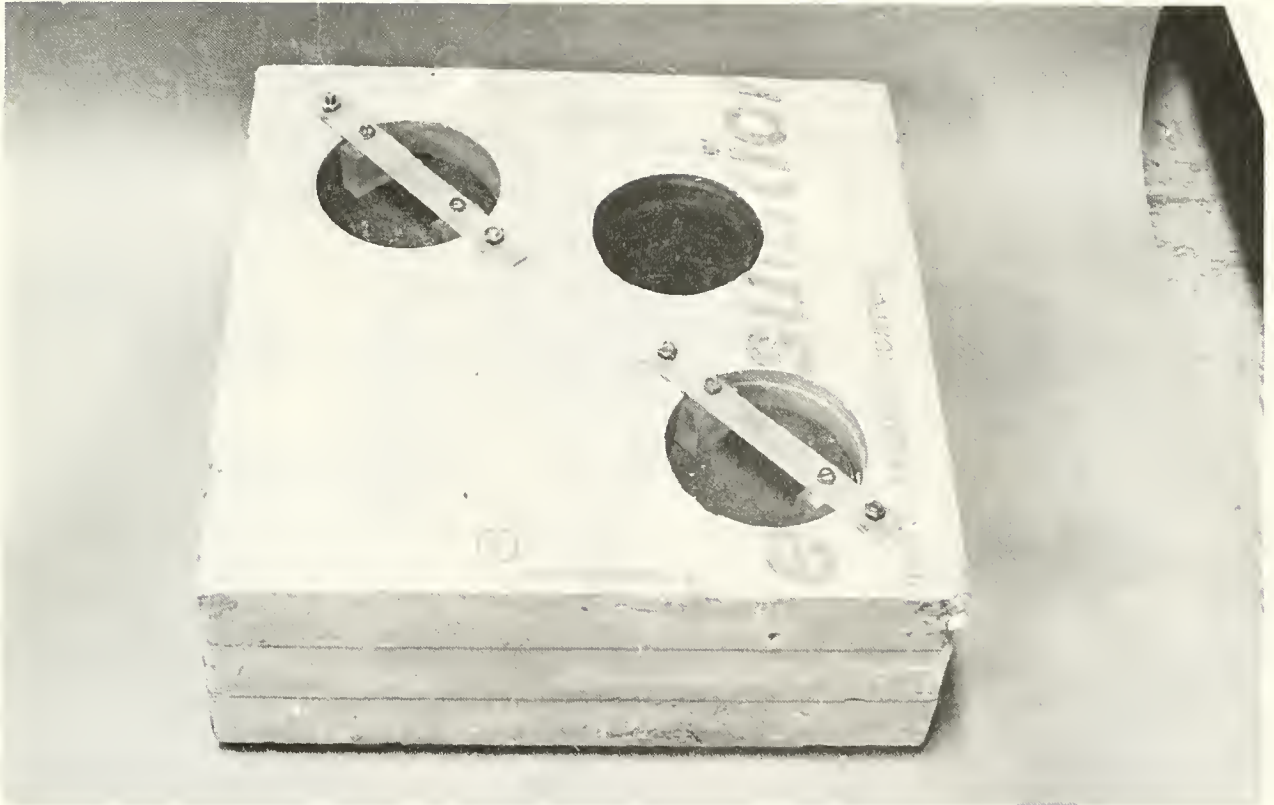
FIGURE 9   POROUS STONES MOUNTED IN FROST
HEAVE CONTAINER
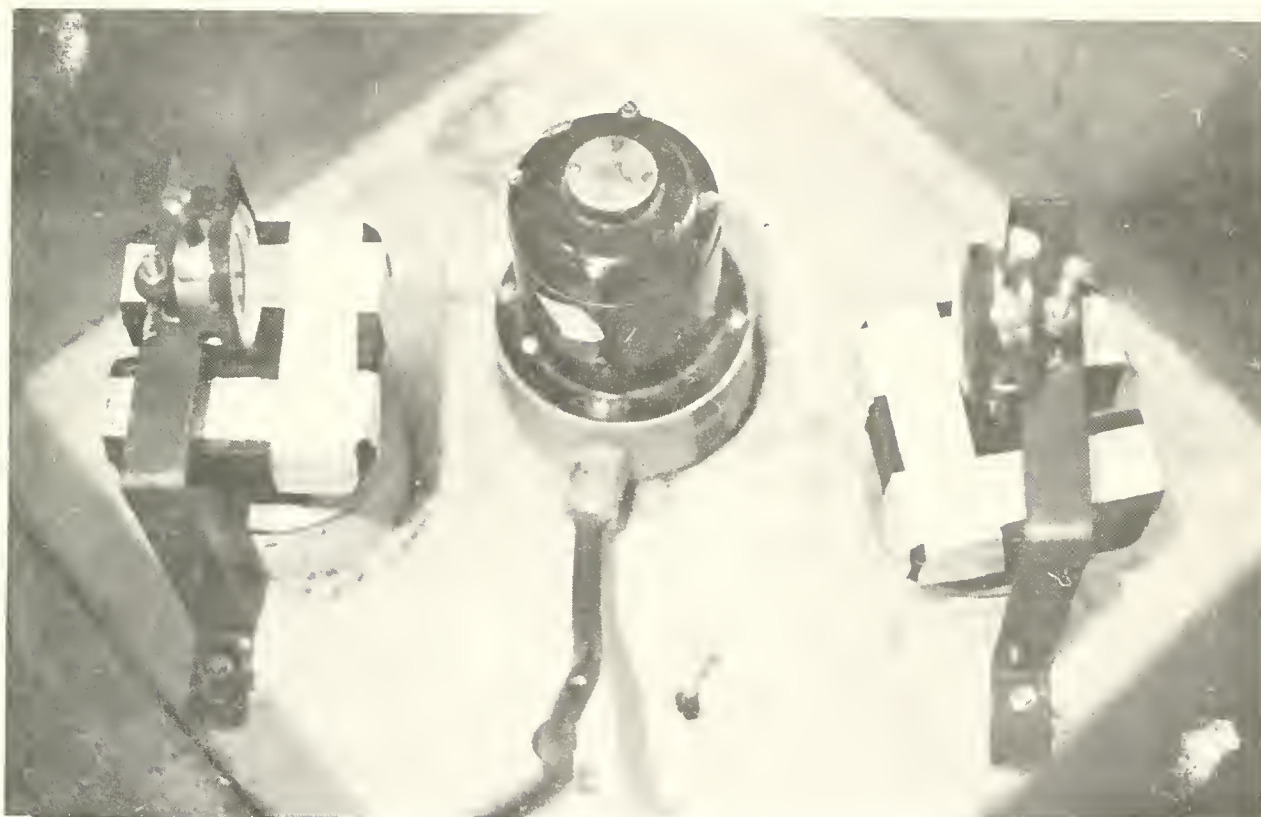
FIGURE 10   CONTAINER AND SAMPLES DURING
             FROST HEAVE TEST

Omega Engineering Inc. cold junction compensator were used. The compensator serves as an electronic zero degree reference, thus taking the place of an ice bath.

Testing Procedure

After completion of saturation, the sample and end caps were disconnected from the saturation device and placed inside a refrigerator set at 4°C. After tempering overnight, the end caps were taken off the sample and the soil was extruded from the Lucite mold. The sample was then pushed inside the Styrofoam cylinder. The cylinder had essentially the same diameter as the sample, however, very slight pressure was needed to insert the sample. To aid in insertion, the teflon cylinder liner was lightly coated with silicon grease.

Following insertion of the soil, dial gauges were mounted above the sample and freezing was begun. Freezing at the top of the sample was initiated by leaving the soil exposed for one hour. After an hour had passed, a brass cover plate along with a surcharge load of 0.5 psi to simulate pavement weight was placed on top of the sample. The surcharge weights were mounted in an elevated position to allow better thermal transfer between the soil, brass plate, and ambient temperature of -6°C. On initiation of freezing, heave readings were normally noted at about 4 hour increments.

After freezing for 2 days, the sample and container were removed from the cold room. The soil was removed from the container, with photographs of the soil and ice lenses and water contents then being taken. Following this, two new samples were placed in the Styrofoam container and the process was repeated.

Freeze Drying

The Process

For effective measurement of pore size distribution using mercury intrusion the soil must be almost completely dry. If compacted soil is dried by air or oven, surface tension forces produced by the air-water menisci generally causes large amounts of shrinkage and thus structural disturbance. To avoid this problem, critical region drying or freeze drying may be used.

The critical region process, as used by Bhasin (1975), subjects the soil sample to increasing pressure and temperature such that the moisture remains in a liquid state until it passes the critical point of water, where it is transformed into a vapor. Since no phase interface occurs within the critical region, there are no surface tension forces to cause disturbance to the sample. For the present study, this method was initially used, however destruction of the soil structure resulted due to a reaction between dolomite in the silt and kaolinite. See Appendix B for further details.

With freeze drying, the soil sample is quickly frozen in liquid nitrogen and then placed in a vacuum where moisture in the form of ice is removed by sublimation. Since there are no surface tension forces from air-water menisci, the sample should display little shrinkage by this method of drying. Freeze drying was successfully used by Ahmed, Lovell and Diamond (1974) and has been simplified by Zimmie and Almaleh (1976). For this study the procedure used by Zimmie et al. seemed to work well.

<p style="text-align:center">Apparatus</p>

As shown in Figures 11 and 12, the basic components of the freeze
drying apparatus consist of:

1) Wire cage to hold samples during freezing and sublimation.

2) Large Dewar flask containing liquid nitrogen into which the
   sample and cage are dipped.

3) Desiccator with inside wire support from which sample cage
   is suspended during sublimation.

4) Vacuum pump, capable of evacuating to less than 0.01 mm of
   mercury.

5) Condenser, which is hooked between the desiccator and vacuum
   pump in order to prevent vapor from the soil entering the
   pump. Liquid nitrogen contained in a Dewar flask was used to
   cool the condenser.

<p style="text-align:center">Procedure</p>

Samples used for freeze drying were obtained by quartering the
compacted soil with a knife and then carefully trimming a cube of soil
with a razor blade. It was felt that a razor blade produced less
disturbance than the small tube sampler used by Ahmed (1971). After
trimming the sample, the cubes were placed in the cage and dipped into
liquid nitrogen for about 5 minutes. It was found that to freeze dry
the cubes successfully, they could be no larger than about 8 mm square.
Larger samples often cracked during freezing, and displayed greater
shrinkage. The small size was not a handicap since samples to be used
in the mercury porosimeter could be no larger than about 0.4 cm^3 in
volume.
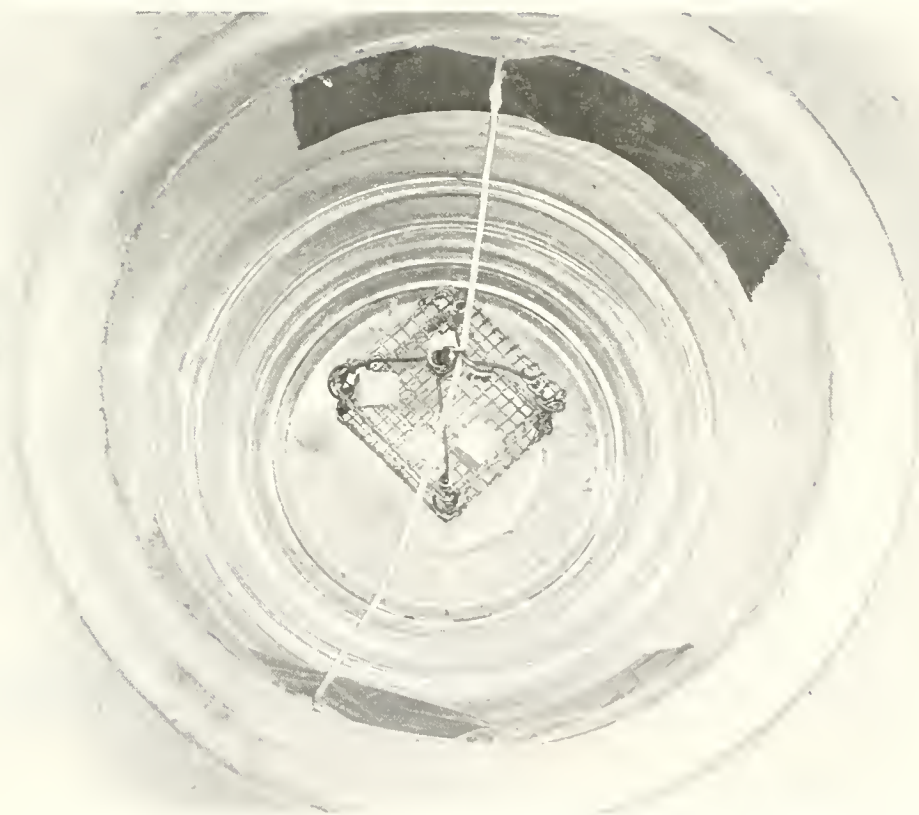
FIGURE II   SAMPLE CAGE SUSPENDED IN DESICCATOR
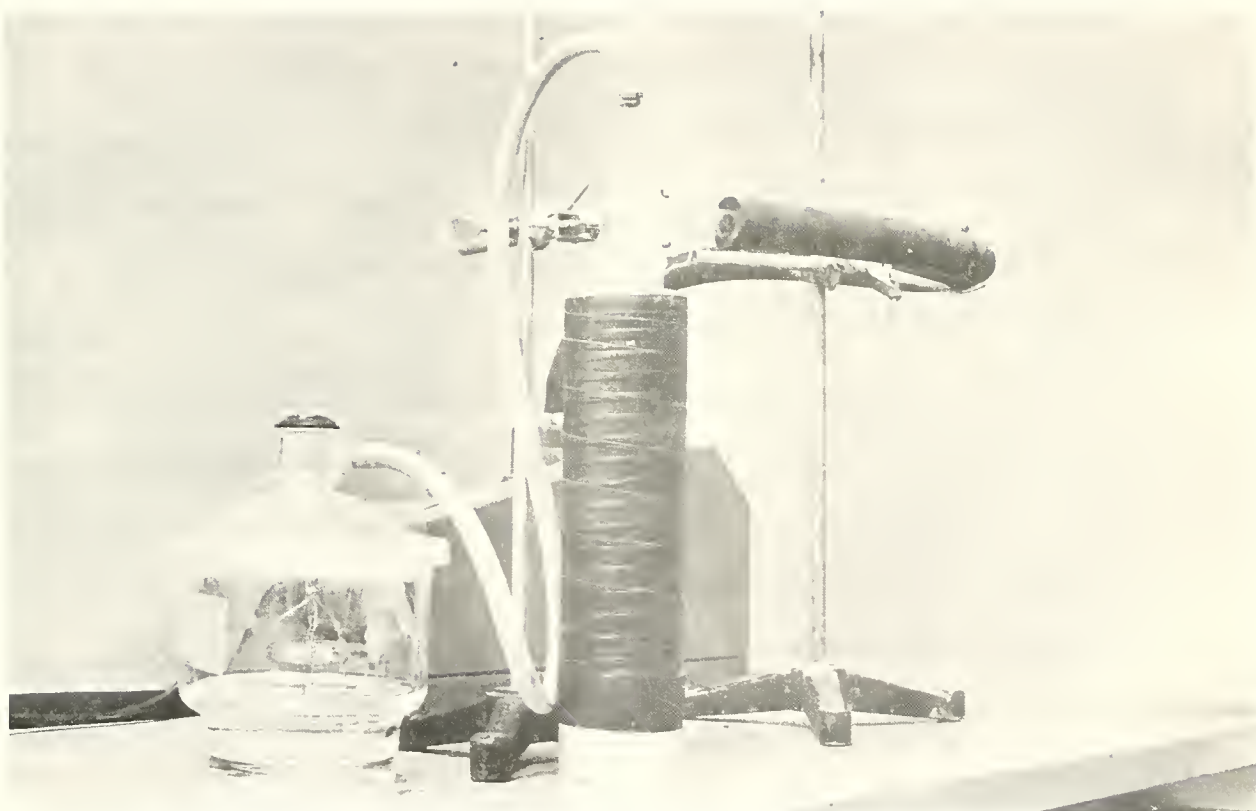
FIGURE 12   FREEZE DRYING APPARATUS WITH VACUUM PUMP, CONDENSER AND DESICCATOR

After freezing, the sample and cage were quickly placed in the desiccator, which was then evacuated by a vacuum pump and sublimation had thus begun. The vacuum pump was left running for 10 hours with the Dewar flask for the condenser being periodically refilled with liquid nitrogen. Zimmie et al. (1976) found for kaolinitic clay that only about 5 to 6 hours were needed for sublimation. However, to be conservative, 10 hours was used in this study.

The basic difference between the method used by Zimmie et al. and Ahmed was that Ahmed kept his sample container cooled to below 0°C during sublimation. However, as Zimmie et al. point out "... sublimation is an evaporative process accompanied by cooling, so although the specimen container is exposed to room temperature, the sample temperature will remain well below freezing". It is important though, that the sample not touch the glass desiccator since heat conducted through the glass could cause melting of the sample. For this reason, the sample cage was suspended in the desiccator. The advantage of not cooling the sample during sublimation is that sublimation will proceed at a much faster rate at higher temperatures.

Once sublimation had been completed, the sample was removed, placed in a labeled glass jar and stored in a desiccator containing anhydrous magnesium perchlorate, so as to remove any remaining moisture.

The degree of shrinkage of freeze dried samples could be determined by mercury displacement in the porosimeter device. For the soils studied, it was found that not more than 3% volume change resulted from the freeze drying process.

Pore Size Determination

Concept

Pore size distribution determination using mercury intrusion is based on the concept that a non-wetting liquid, such as mercury with soil, enters an empty capillary only under pressure, with increasing pressures needed to intrude smaller pores. If cylindrical pore shape is assumed, then knowing the contact angle between soil and mercury and the surface tension of mercury, the absolute pressure of intrusion can be used to calculate pore diameter using the Washburn (1921) equation:

$$d = \frac{-4 \, \sigma_m \, \cos \theta}{p} \tag{9}$$

where d = pore diameter in cm,
σ_m = surface tension of mercury in dynes/cm,
θ = contact angle between mercury and soil,
p = absolute pressure in dynes/cm^2.

Diamond (1970) measured the contact angle between mercury and kaolinitic and illitic soils by the sessile drop method and found it to be within a degree of an average value of 147 degrees. For the surface tension of mercury, the value found by Kembell (1946) of 484 dynes/cm at 25°C was used for this study.

Based on the computed pore size diameter and the amount of mercury intruded at the desired pressure, a pore size distribution can then be calculated.

Apparatus

The apparatus used in mercury pore size determination consists of a penetrometer; filling device, vacuum pump, McLeod gauge, mercury

manometer and control board; and an Aminco porosimeter.

The glass penetrometer consists of a bulb to hold the sample and a graduated stem. The stem is marked in increments of 0.002 ml so as to measure a total of 0.200 ml intrusion of mercury into the sample. The bulb of the penetrometer is sealed using a stainless steel end cap and teflon locking ring. Figure 13 illustrates the assembled penetrometer and separate parts.

Shown in Figure 14 is the filling device, McLeod gauge and control board. The filling device consists of a two chambered glass tube in which the penetrometer is inserted and sealed. Connected to the device is a control board which is also connected to a mercury manometer, McLeod gauge and vacuum pump. The mercury manometer is used to measure vacuum pressures from atmospheric down to 1 mm of mercury, whereas the McLeod gauge is used to measure pressures below 1 mm of mercury. Also fastened to the filling device is a side arm containing mercury, along with a reserve mercury reservoir connected via a teflon stopcock.

The final piece of equipment is an Aminco Porosimeter, which measures mercury intrusion at pressures greater than atmospheric. Pressure for intrusion is generated by the porosimeter using an electrically driven hydraulic pump, and is measured by two Bourdon pressure gauges of 1000 and 15,000 psi capacity. The amount of intrusion is measured by a stainless steel needle which follows the position of the mercury meniscus in the capillary stem of the penetrometer.

Test Procedure

The test procedure used in this study was similar to that used by Ahmed (1971) and Bhasin (1975). Therefore, the method is only briefly described here.
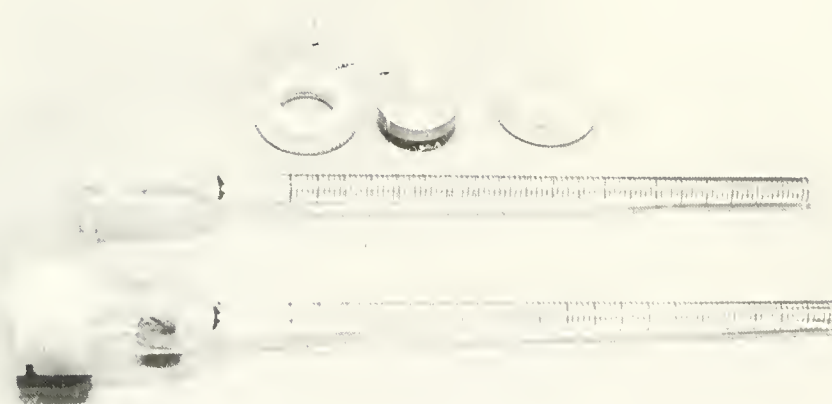
FIGURE 13   PENETROMETER : DISASSEMBLED AND ASSEMBLED
WITH SAMPLE
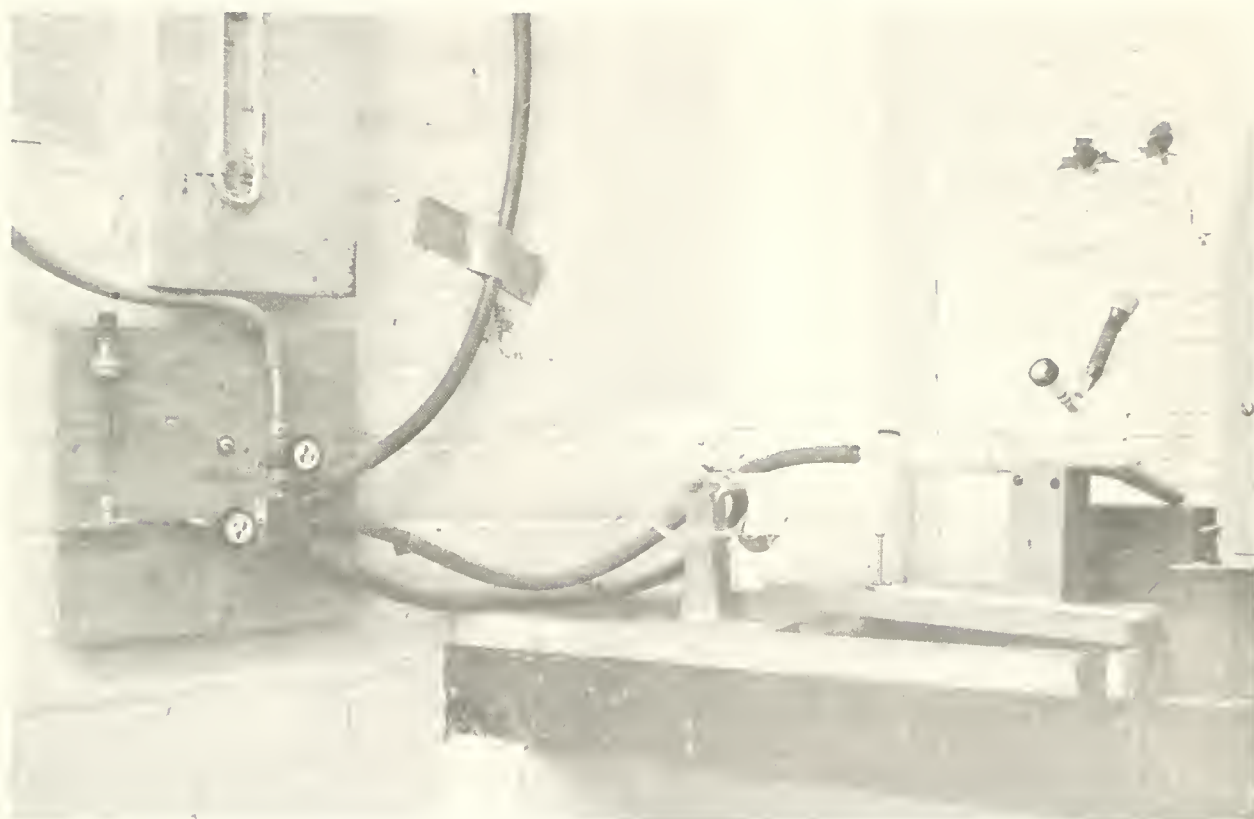
FIGURE 14   FILLING DEVICE, McLEOD GUAGE AND CONTROL
BOARD

A sample to be intruded was first trimmed with a razor blade so as to have a void volume less than 0.200 ml. Following trimming, the sample was weighed, placed in the penetrometer, and then weighed again. The penetrometer was inserted in the filling device and the complete assembly was evacuated to between 0.01 and 0.02 mm of mercury, which normally took about 20 minutes. Once filling pressure had been reached, the arm of the device was raised such that mercury completely covered the penetrometer. The device was then shut off from the vacuum, and air was let in to raise the pressure to 20 to 40 mm of mercury, which resulted in mercury flowing into and filling the penetrometer. After filling the penetrometer the arm was lowered, and pressure was incrementally increased in the device with the mercury meniscus noted for each pressure.

Upon reaching atmospheric pressure, the penetrometer was removed from the filling device, weighed, and placed stem down inside the porosimeter. The pressure of the porosimeter was then incrementally raised until it reached its maximum of between 13,900 and 14,300 psi, with penetrometer probe readings noted for each pressure increment. It should be noted that the weight of the mercury in a "stem down" position caused the sample to be at less than atmospheric at initiation of the test. Therefore, to start the test at atmospheric, the pressure in the porosimeter had to be raised to about 4 psi. Following completion of the porosimeter run, the mercury was removed from the penetrometer and both were cleaned before reusing.

RESULTS AND DISCUSSION OF RESULTS

Compaction

As mentioned previously, three levels of kneading compactive effort were used. The compaction efforts were selected such that, for the 90% silt - 10% kaolin mixture, the maximum dry density for the middle effort (8.5 psi gauge pressure), closely approximated that obtained in AASHTO test procedure T99-70, Method "A". The preliminary compaction curves for each of the three soil mixtures are shown in Figures 15, 16 and 17. It should be noted that the compactive effort referred to in the Figures and throughout the study are gauge pressures for the kneading compactor.

During the course of the study there was sometimes a slight difference between the preliminary compaction curves and the water content-density values obtained during the actual frost heave test program. This difference is probably due to the varying room temperature and humidity conditions at the time of compaction. The changing room conditions were a result of the preliminary curves being obtained during the winter, whereas some of the freezing test samples were compacted in the early spring. Listed in Table 6 are the water contents and dry densities for the samples tested during the freezing program.

Although sample densities for similar water contents varied slightly over the course of the study, there was little variance in
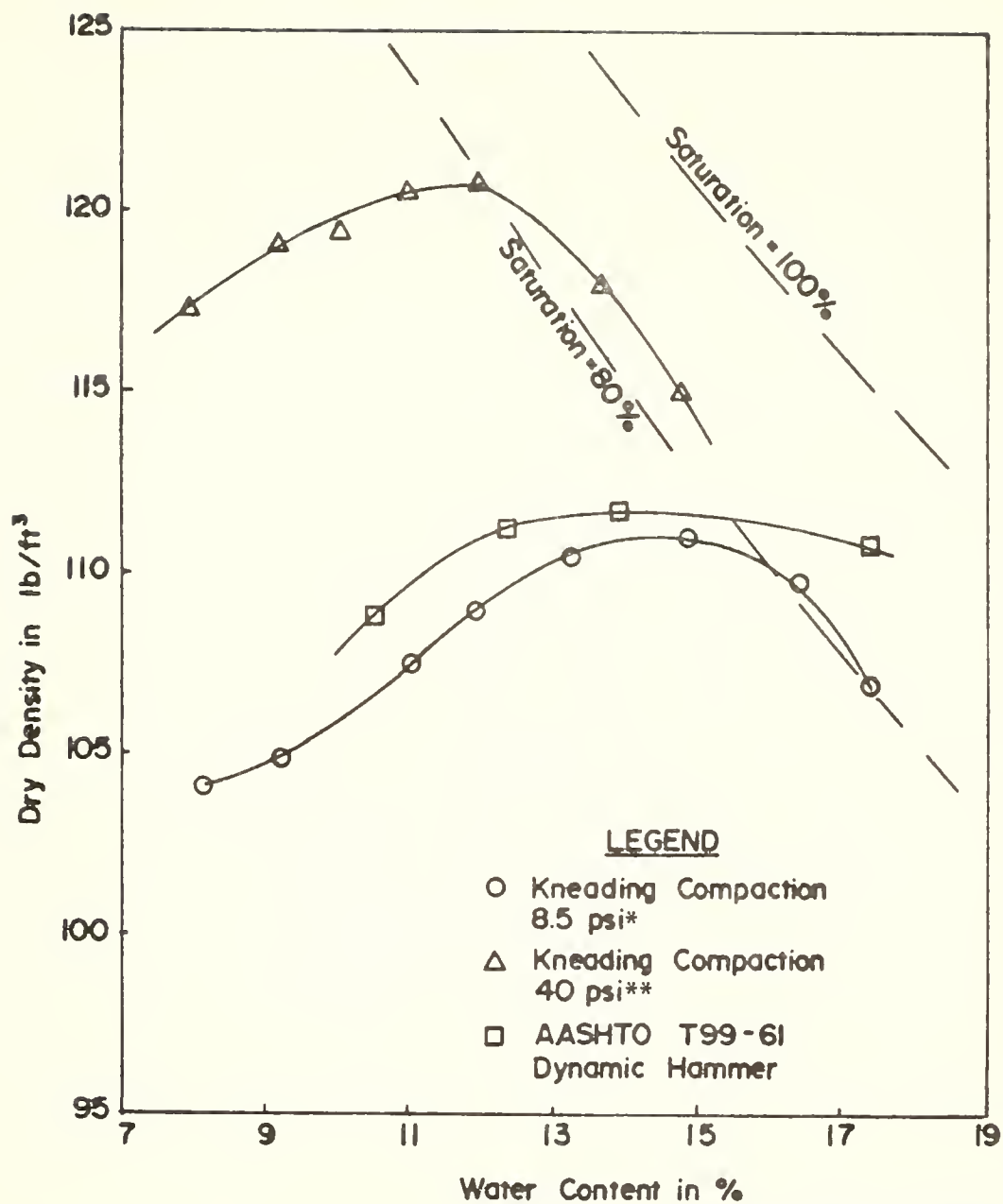
FIGURE 15 COMPACTION CURVES FOR 90% SILT-
10% KAOLIN

FIGURE 16   COMPACTION CURVES FOR 70% SILT -
30% KAOLIN
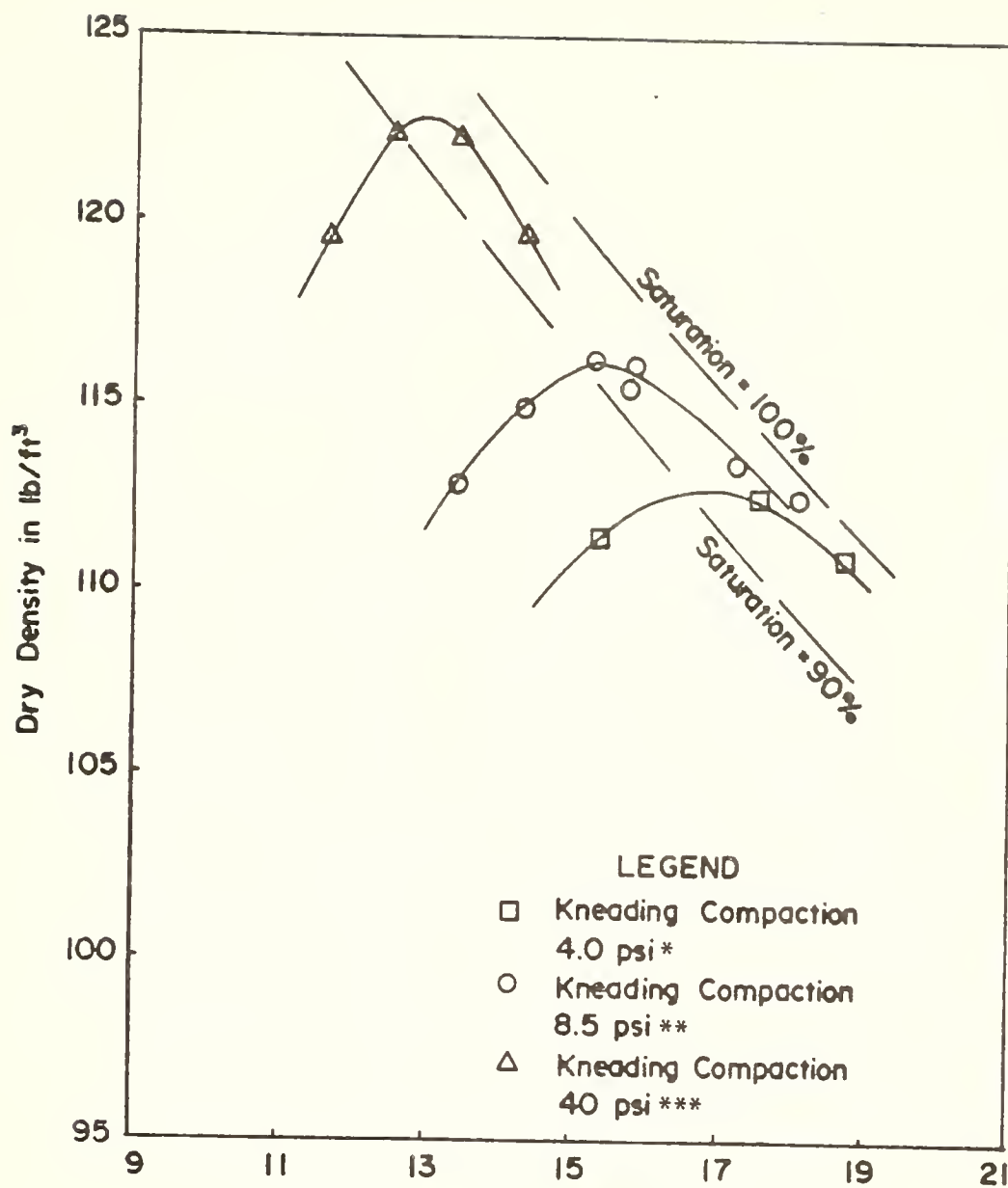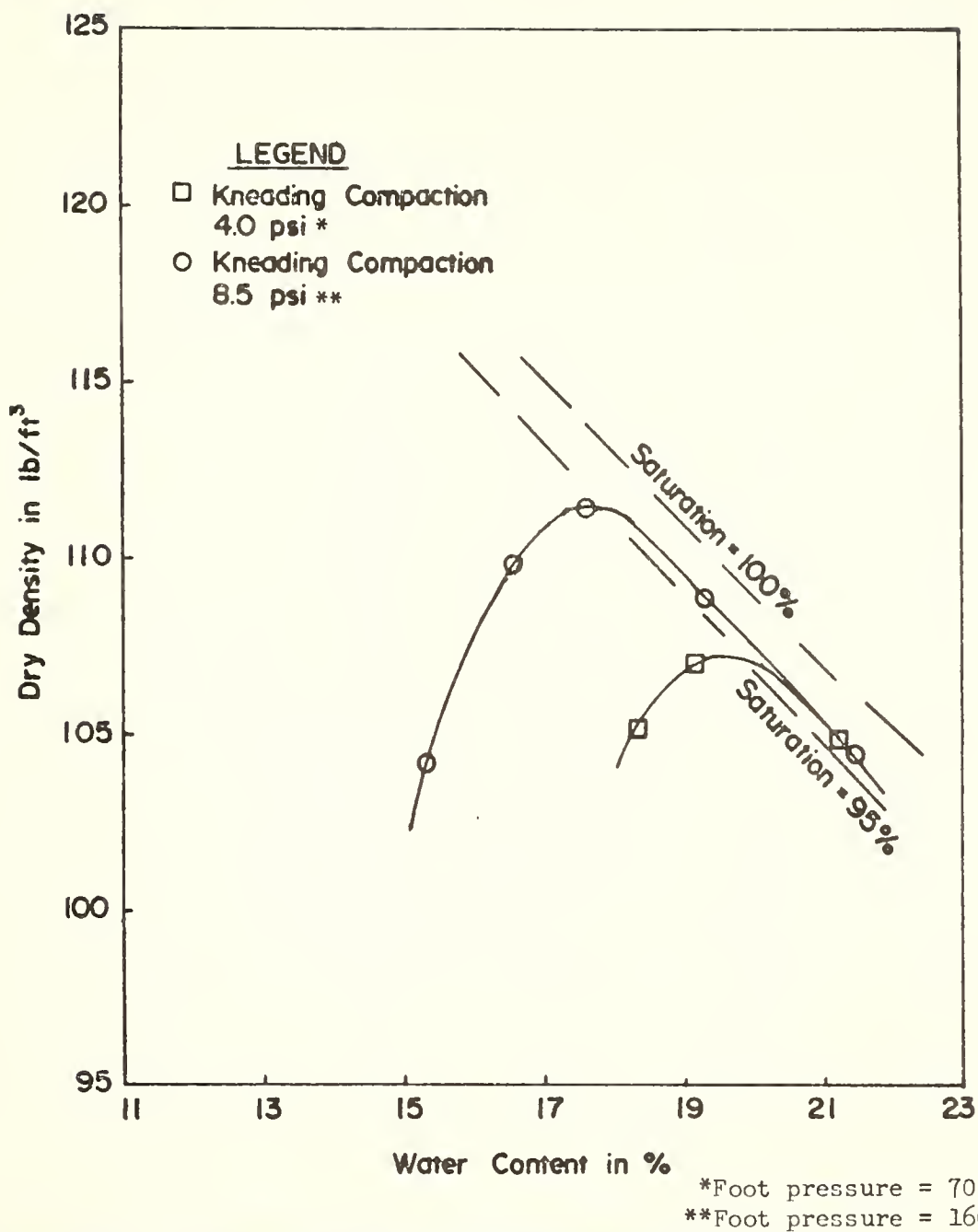
FIGURE 17   COMPACTION CURVES FOR 50% SILT-
50% KAOLIN

*Foot pressure = 70 psi
**Foot pressure = 160 psi

Table 6. Compaction Parameters For Soil Samples Tested

Sample Number	%Silt-%Kaolin	Compactive Effort (psi Gauge Pressure)	Water Content (%)	Dry Density (pcf)	Dry Density After Saturation (pcf)
1	90-10	8.5	18.0	108.7	110.8
2	90-10	8.5	17.1	110.3	-
3	90-10	8.5	14.6	110.8	-
4	90-10	8.5	14.6	111.0	-
5	90-10	8.5	11.5	108.6	-
6	90-10	8.5	11.2	108.5	-
7	90-10	8.5	10.5	106.9	-
8	90-10	40	14.0	114.5	-
9	90-10	40	12.1	120.1	-
10	90-10	40	8.6	118.0	-
11	90-10	40	8.2	117.2	-
12	70-30	4.0	18.7	110.8	113.5
13	70-30	4.0	17.5	112.9	114.5
14	70-30	4.0	17.6	112.5	113.4
15	70-30	4.0	15.3	111.4	-
16	70-30	4.0	14.8	103.3	-
17	70-30	8.5	18.1	112.7	-
18	70-30	8.5	17.4	113.4	-
19	70-30	8.5	15.7	115.4	117.6
20	70-30	8.5	15.8	116.1	-
21	70-30	8.5	13.4	115.0	-
22	70-30	8.5	13.7	114.4	-
23	70-30	40	14.1	119.4	-
24	70-30	40	13.1	121.2	-
25	70-30	40	11.9	120.0	-
26	50-50	4.0	21.2	104.8	107.1
27	50-50	4.0	19.1	106.8	-
28	50-50	4.0	18.3	103.6	-
29	50-50	8.5	20.4	108.4	-
30	50-50	8.5	20.3	107.3	108.1
31	50-50	8.5	18.2	111.4	-
32	50-50	8.5	18.0	111.5	-
33	50-50	8.5	16.7	104.7	-
34	50-50	8.5	17.4	106.1	-

density between the freeze drying and frost heave samples that were
compacted at the same time. In almost all cases there was less than
0.5 lbs/ft^3 difference between the two samples, with typical differences
of 0.2 lbs/ft^3 or less. The closeness of the freeze drying and frost
heave sample densities is due to the samples coming from soil mixed
and cured in a single batch, and also because of the high degree of
replication of the kneading compactor.

Saturation

As listed in Table 7, almost all soil samples were saturated to a
degree of saturation of 95% or better. The only soil samples which could
not be brought to a high degree of saturation were the 90% silt - 10%
kaolin soil mixtures at wet of optimum, using 8.5 psi compactive effort,
and wet of optimum and optimum for the 40 psi compactive effort.

Table 6 shows that seven of the samples displayed higher densities
at the end of saturation. This was due to the sample consolidating
slightly when saturation pressures were applied. Determination of any
change of volume after saturation was accomplished by trimming two
sections of the freeze drying sample. These sections were weighed,
coated with wax, and then weighed both in air and submerged in water,
so that the sample volume, density, and degree of saturation could be
calculated.

Freeze Drying

Table 7 lists the void ratios for samples both before and after
freeze drying. The post-freeze drying void ratios were determined
during the mercury intrusion runs, based on the amount of mercury

Table 7. Compaction and Frost Heave Parameters For Soil Samples Tested

Sample Number	Saturation (%)	Void Ratio After Saturation	Void Ratio After Freeze Drying	Volume Change (%)	24 Hour Frost Heave (mm)
1	89	0.53	0.54	0.8	12.2
2	95	0.54	0.51	-2.0	11.2
3	96	0.53	0.54	0.2	31.8
4	99	0.53	0.56	2.2	33.5
5	99	0.56	0.59	1.7	39.4
6	95	0.57	0.60	2.0	30.0
7	99	0.59	0.63	2.3	46.7
8	84	0.48	0.43	-3.8	8.4
9	84	0.41	0.44	1.8	11.3
10	99	0.44	0.45	0.7	33.0
11	95	0.45	0.47	1.5	24.6
12	95	0.49	0.47	-1.3	10.7
13	97	0.47	0.42	-3.7	9.4
14	93	0.49	0.48	-0.8	9.0
15	98	0.52	0.49	-2.1	34.8
16	?	0.63	0.63	-0.3	45.7
17	98	0.50	0.46	-2.6	9.3
18	96	0.49	0.49	0.3	6.9
19	94	0.44	0.42	-1.5	6.6
20	95	0.45	0.43	-1.5	5.7
21	100	0.47	0.46	-0.8	23.6
22	97	0.48	0.49	1.3	16.8
23	94	0.41	0.43	0.8	5.1
24	94	0.39	0.38	-1.0	5.1
25	89	0.41	0.44	2.4	3.2
26	95	0.57	0.57	0.4	8.5
27	96	0.57	0.53	-2.6	6.7
28	95	0.62	0.62	-0.1	23.6
29	97	0.55	0.51	-2.3	9.9
30	97	0.55	0.55	-0.2	5.2
31	98	0.51	0.49	-1.4	5.6
32	95	0.50	0.50	-0.2	6.1
33	95	0.60	0.56	-2.5	14.7
34	96	0.58	0.61	1.7	15.7

enclosing the sample at initiation of the test. This method assumes that at the mercury intrusion filling pressure, no pores were filled. For the soils used, this assumption was valid. As can be seen from the Table there was less than 3% volume change for all but two of the samples. These two samples showed volume decreases of 3.7% and 3.8%, but these values may reflect experimental error rather than shrinkage due to freeze drying.

Frost Heave

Freezing Results

During the freezing test program, frost heave versus time curves were plotted for all soil samples. Typical heaving curves are shown in Figures 18 through 21. The curves are fairly linear for all soil combinations, although some of them depart slightly from linear due to decreasing heave. This is probably caused by changing thermal conditions as the freezing front penetrated the sample.

For correlation of frost heave with pore size distribution, an arbitrary heaving value and criterion were selected. Since the frost heave versus time curves were particularly linear during the first 24 hours, the frost heave after 24 hours was selected as the evaluating factor. These values are shown in Table 7. To group the 24 hour heave values into frost susceptible categories, the classification listed in Table 8, relative to the soils and procedures used, was chosen.

The effects of water content and compaction on frost heaving rate are shown in Figures 18 through 21, where the high, medium, and low water contents are wet of optimum, at optimum, and dry of optimum,

FIGURE 18 TYPICAL FROST HEAVE CURVES FOR 90% SILT - 10% KAOLIN

*Foot pressure = 160 psi
**Foot pressure = 590 psi
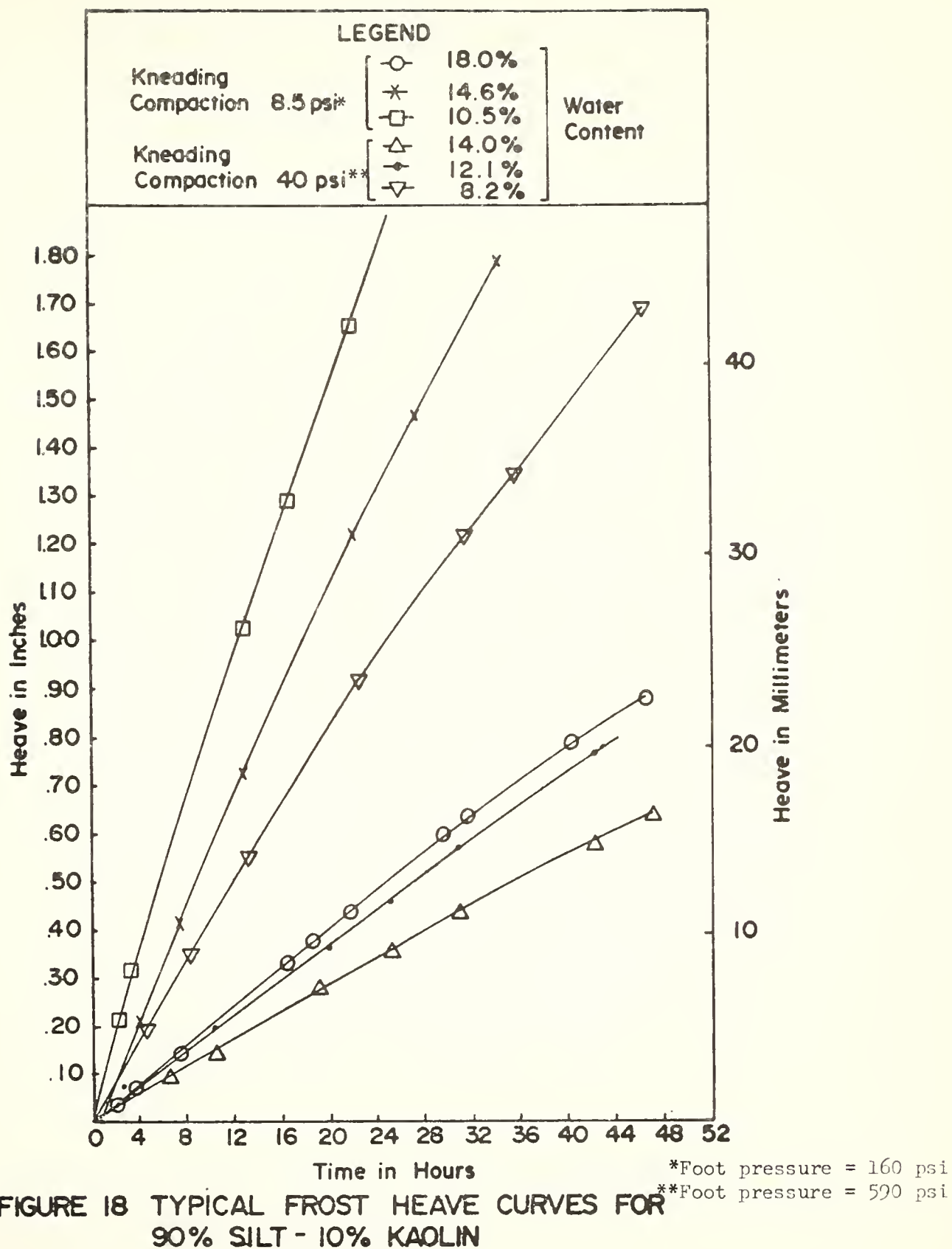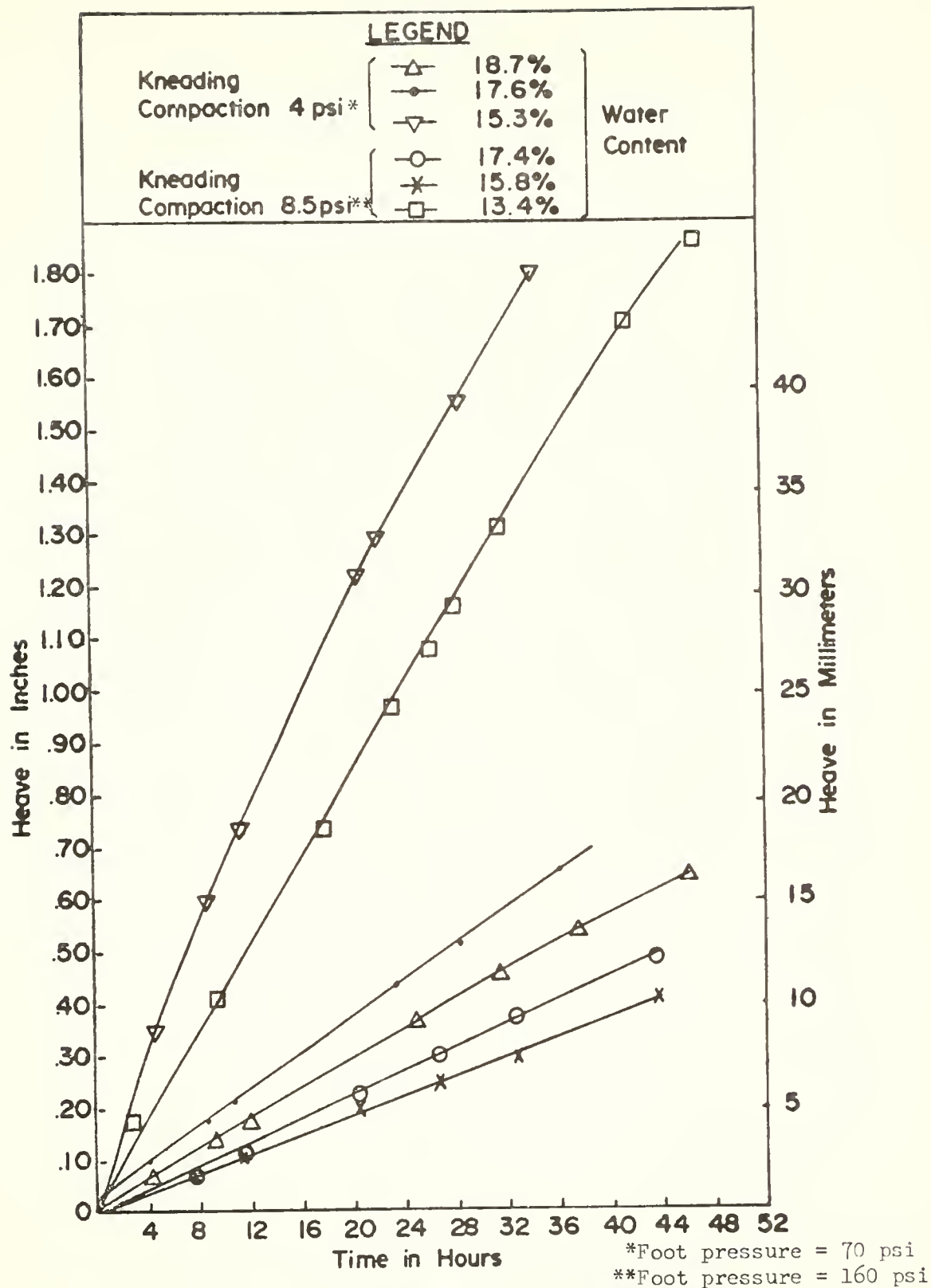
FIGURE 19 TYPICAL FROST HEAVE CURVES FOR
70% SILT-30% KAOLIN
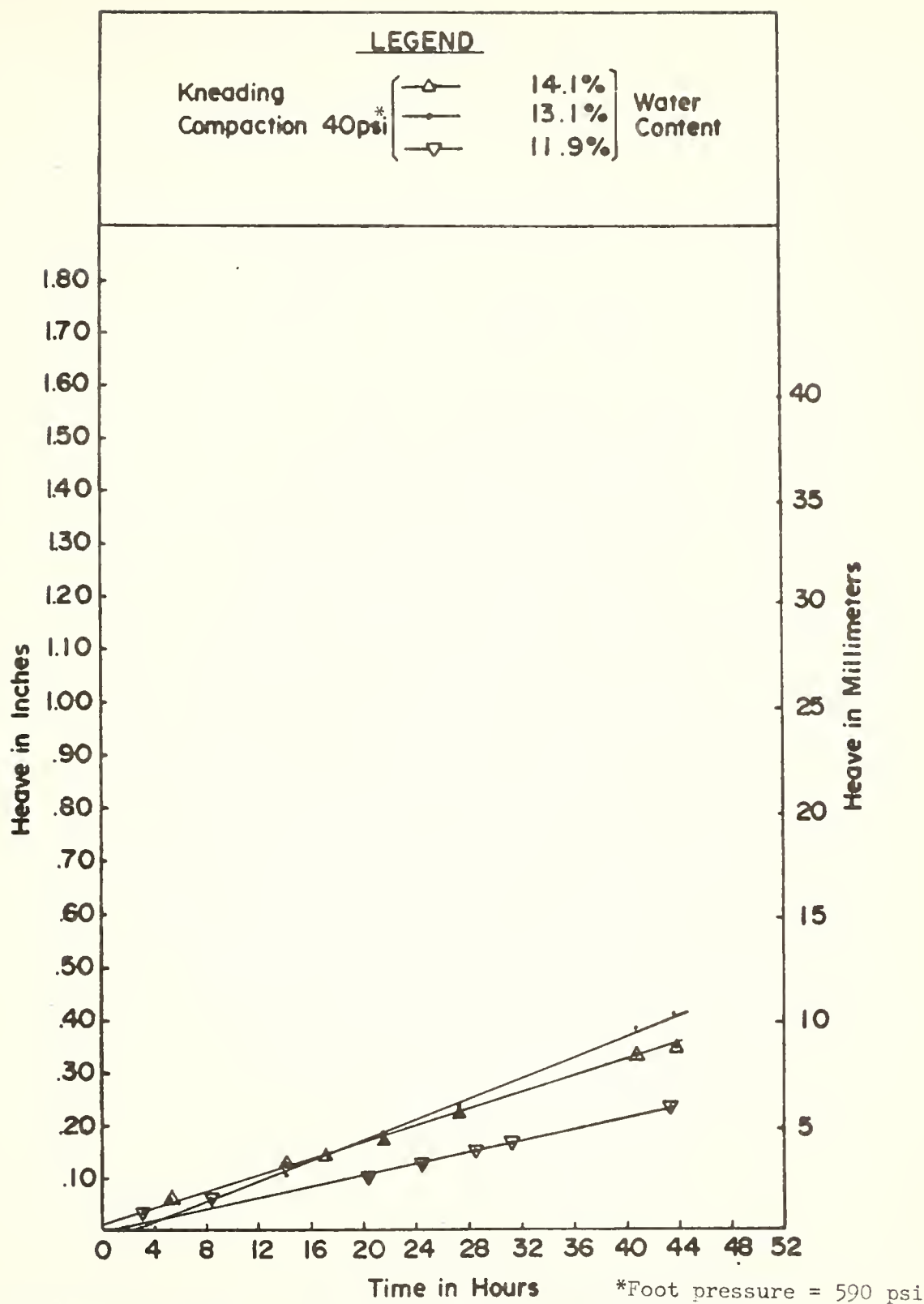
FIGURE 20 TYPICAL FROST HEAVE CURVES FOR
70% SILT-30% KAOLIN
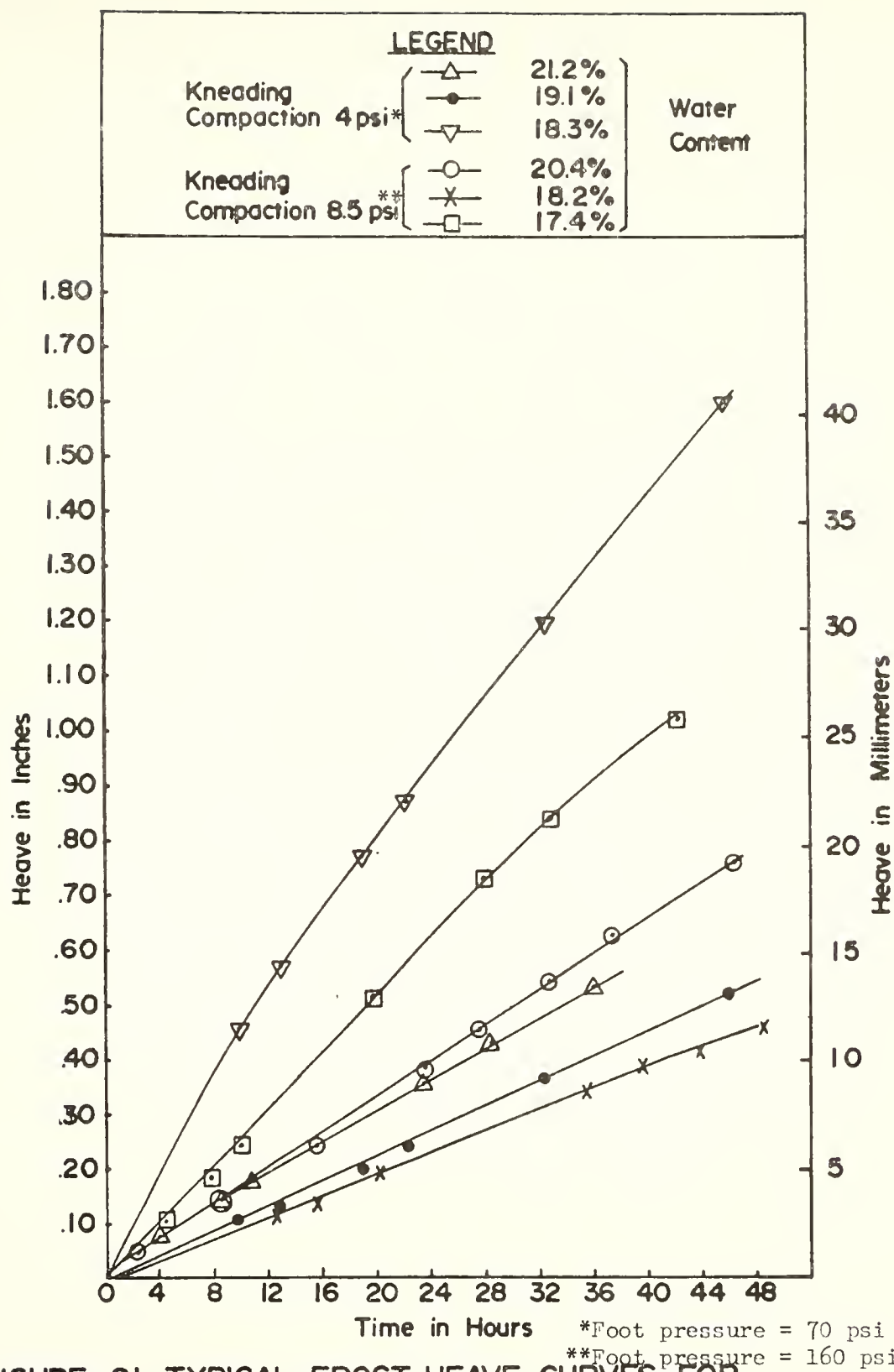
FIGURE 21 TYPICAL FROST HEAVE CURVES FOR
50% SILT-50% KAOLIN

Table 8. Frost Susceptibility Classification Used for Purposes
          of Rating the Tested Soils

24 Hour Frost Heave (mm)	Frost Susceptibility Rating
< 6	Very low
6 – 11	Low
11 – 20	Medium
20 – 30	High
> 30	Very High

respectively. Table 9 summarizes the frost susceptibility classifications of each soil by the Casagrande criteria, U. S. Army Corps of Engineers "F" rating, and the authors system.

For the 90% silt - 10% kaolin soil compacted at 8.5 psi, both the dry side of optimum and optimum had "very high" heave, with heave increasing somewhat as water contents decreased. When water contents were increased to the wet side of optimum, the heave decreased to the lower "medium" range.

By increasing the compactive effort to 40 psi, the heave for 90% silt - 10% kaolin compacted at optimum, decreased to the "medium" range. However, the heave for the wet side samples decreased only slightly and the heave for the dry side samples were still in the "very high" range.

For the 70% silt - 30% kaolin samples, the dry side samples had "very high" heave for 4 psi, decreasing to "medium" to "high" heave at 8.5 psi, and "very low" at 40 psi compactive effort. The optimum and wet sample heave also decreased slightly with increasing compactive effort. However, unlike the 90% silt - 10% kaolin mixture, the wet side heave was slightly higher than that at optimum, with both much less than the dry side for 4 and 8.5 psi compactive effort.

The 50% silt - 50% kaolin mix behaved much like the 70% silt - 30% kaolin mix, with samples compacted on the dry side having much greater heave than those compacted at optimum or wet of optimum. Again, the wet side sample heave was greater than that of optimum. Also, increasing the compactive effort from 4 psi to 8.5 psi decreased heave on the dry side, but had little effect on samples compacted at optimum or wet of optimum.

Table 9. Frost Susceptibility Ratings of Soils Tested

Sample Number*	%Silt-%Kaolin	Casagrande's Soil Classification	Corps of Engineers Soil Classification	Author's Frost Heave Rating***
1	90 - 10	FS**	F4	Medium
2	90 - 10	FS	F4	Medium
3	90 - 10	FS	F4	Very High
4	90 - 10	FS	F4	Very High
5	90 - 10	FS	F4	Very High
6	90 - 10	FS	F4	High
7	90 - 10	FS	F4	Very High
8	90 - 10	FS	F4	Low
9	90 - 10	FS	F4	Medium
10	90 - 10	FS	F4	Very High
11	90 - 10	FS	F4	High
12	70 - 30	FS	F4	Medium
13	70 - 30	FS	F4	Low
14	70 - 30	FS	F4	Low
15	70 - 30	FS	F4	Very High
16	70 - 30	FS	F4	Very High
17	70 - 30	FS	F4	Low
18	70 - 30	FS	F4	Low
19	70 - 30	FS	F4	Low
20	70 - 30	FS	F4	Very High
21	70 - 30	FS	F4	High
22	70 - 30	FS	F4	Medium
23	70 - 30	FS	F4	Very Low
24	70 - 30	FS	F4	Very Low
25	70 - 30	FS	F4	Very Low
26	50 - 50	FS	F3(c)	Low
27	50 - 50	FS	F3(c)	Low
28	50 - 50	FS	F3(c)	High
29	50 - 50	FS	F3(c)	Low
30	50 - 50	FS	F3(c)	Very Low
31	50 - 50	FS	F3(c)	Very Low
32	50 - 50	FS	F3(c)	Low
33	50 - 50	FS	F3(c)	Medium
34	50 - 50	FS	F3(c)	Medium

* See Table 6 for compaction variables. Sample numbers correspond to those in Tables 6 and 7.
** FS: Frost susceptible soil
*** The reader is reminded that this rating has not been applied to field frost susceptibility. It applies only to the laboratory tests described herein.

In summary, the dry side samples tended to have greater heave and be more frost susceptible. Increasing the compactive effort did decrease heave for soils on the dry side, but not always for optimum or wet side samples. In comparison of wet side with optimum, greater heave may be displayed for either, depending on the soil.

Description of Frozen Soil

As can be seen in Figures 22 and 23, ice lenses tended to be much more prevalent, although slightly smaller, for the dry side samples rather than optimum and wet side samples. With increasing clay contents, the samples tended to have somewhat thicker lenses, but they were spaced much further apart. Also, ice lenses for samples at optimum or wet of optimum and with high clay contents, tended to be more irregularly oriented.

Pore Size Distribution

Determination of Pore Size

For all mercury intrusion runs, the pressure and intrusion data were punched on computer cards and programmed on the Purdue CDC-6500 Dual Mace computer, using the programs given in Appendix A. The computer tabulated pore size diameter and cumulative intrusion, and also plotted limiting pore size diameter, both with respect to cumulative voids per weight, and cumulative voids per volume.

Drake and Ritter (1945) introduced the concept of plotting cumulative voids per gram versus pore diameter, and this method was also used by Bhasin (1975) and Ahmed (1971). However, for this study it was felt that the amount of pores per given volume would be more relevant,

Dry of Optimum   Optimum   Wet of Optimum
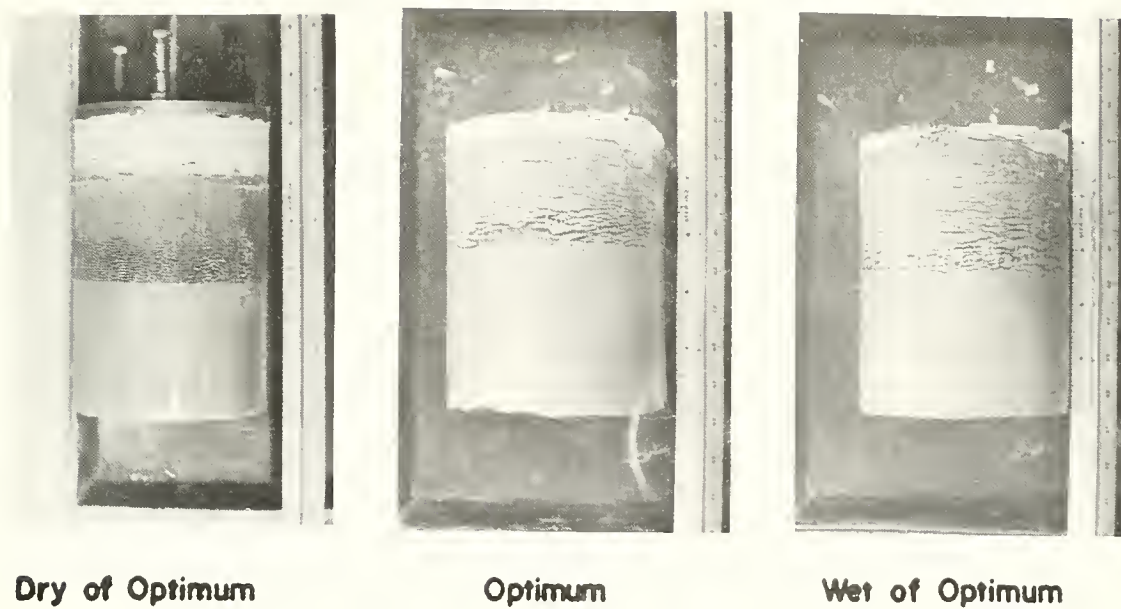
FIGURE 22   FROST HEAVE SAMPLES OF 70% SILT-
30% KAOLIN COMPACTED AT 8.5 PSI

Dry of Optimum   Optimum   Wet of Optimum
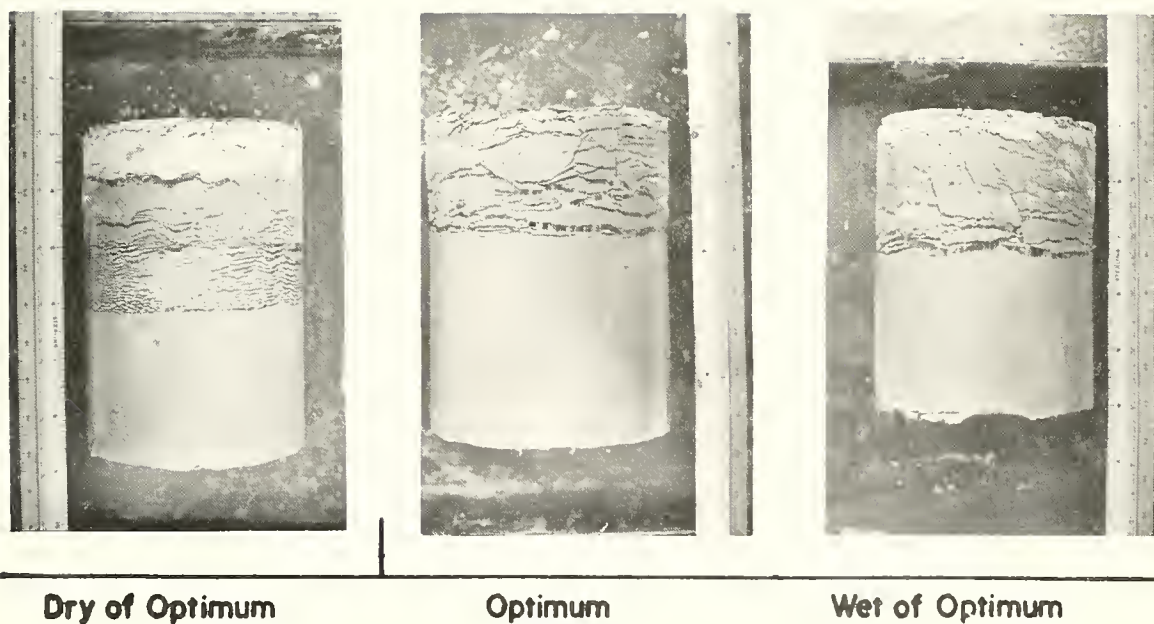
**FIGURE 23   FROST HEAVE SAMPLES OF 50% SILT-
50% KAOLIN COMPACTED AT 8.5 PSI**

and the final analysis was based on plots of cumulative voids per volume, or "cumulative porosity" versus limiting pore size diameter.

For each compacted sample, there were two or more porosimeter runs. Prior to the freeze drying process, two samples were taken from the top and two from the bottom of each compacted soil sample. It was found that the pore size distribution curves were essentially the same, regardless of the location of the sample. At times total porosities were different in replicate mercury intrusion runs, in which case additional runs were made. From the multiple runs for each compacted sample, a representative pore size distribution curve was selected for analysis.

Comparison of Pore Size Curves

The pore size distribution curves are given in Figures 24 through 34, where the high, medium and low water contents represent wet of optimum, at optimum, and dry of optimum, respectively. Comparison of these curves shows that the distribution of fine pores below 0.1 μm was consistent for each soil. Significant differences in distributions of porosity due to compactive effort and water content did not begin to appear until about the 0.4 μm size. This is in agreement with Sridharan, Altschaeffl and Diamond (1971), Bhasin (1975), Diamond (1971), and Ahmed (1971), who worked with soils ranging from Edgar plastic kaolin and Grundite to Boston blue clay and Crosby silty clay.

Bhasin (1975) suggests that the fine pores (< 0.1 μm) occur either within individual particles or within domains of roughly face to face oriented clay particles. Furthermore, Bhasin points out that this size range conforms roughly to the intradomainal pore size range of 300Å to 800Å as determined by Diamond (1971) for Edgar plastic kaolin. Since

the pore size below 0.1 μm is almost in direct proportion with the kaolin content of the three mixes, one might conclude that this pore size range is due to the clay particles, with the silt contributing little.

Pore Size Distribution on Dry Side of Optimum

Figures 24 through 34 show that for the soil samples compacted on the dry side of optimum, there was a high percentage of large pores (> 2 μm), relative to samples compacted at optimum or the wet side of optimum. Again, this is in agreement with Bhasin (1975), Ahmed (1971) and Diamond (1971).

It is interesting to note that for the 90% silt - 10% kaolin soil mixture when compacted on the dry side of optimum (Figures 24, 25, 26), a high percentage of large pores was in a relatively narrow band of pore size. For instance, for the soil compacted at 8.5 psi, about 50% of the pores were in a band between 7 and 9 μm. This might suggest a very orderly packing between silt particles and silt-clay aggregations for the largely silt soil.

For the soil mixtures compacted on the dry side, increasing the compactive effort tended to decrease the amount of large pores. Again, the 90% silt, 10% kaolin soil showed a large number of large pores in a relatively narrow band, however, this band had shifted to a smaller size in comparison to the lower compactive effort.

Pore Size Distribution of Optimum and Wet Side Samples

At a compactive effort of 8.5 psi, the 90% silt - 10% kaolin samples displayed larger amounts of pore space between 1 to 8 μm for the soil compacted at optimum in comparison to wet of optimum. By increasing the
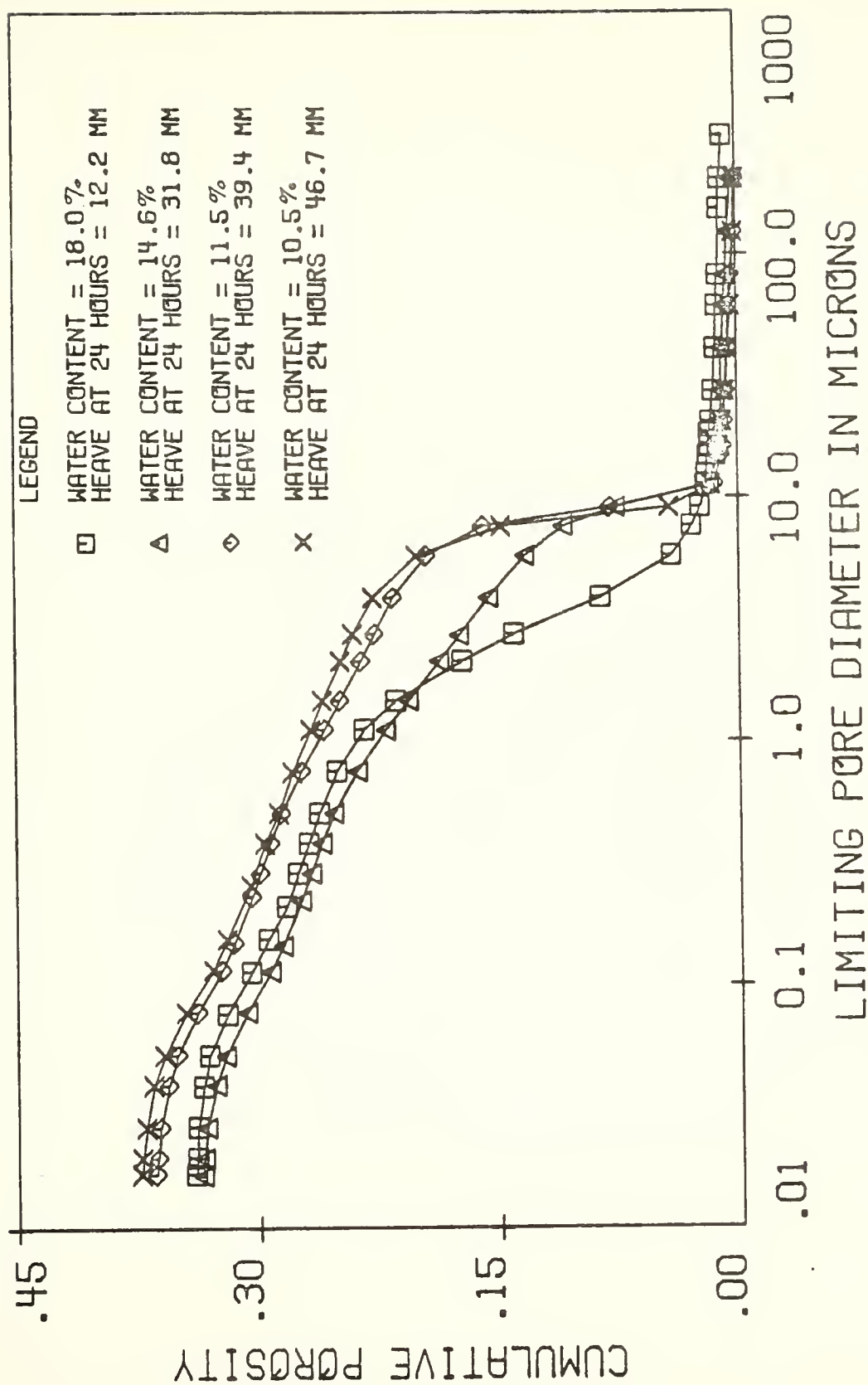
FIGURE 24 PORE SIZE DISTRIBUTION FOR 90% SILT –
10% KAOLIN COMPACTED AT 8.5 PSI*

*Foot pressure = 160 psi
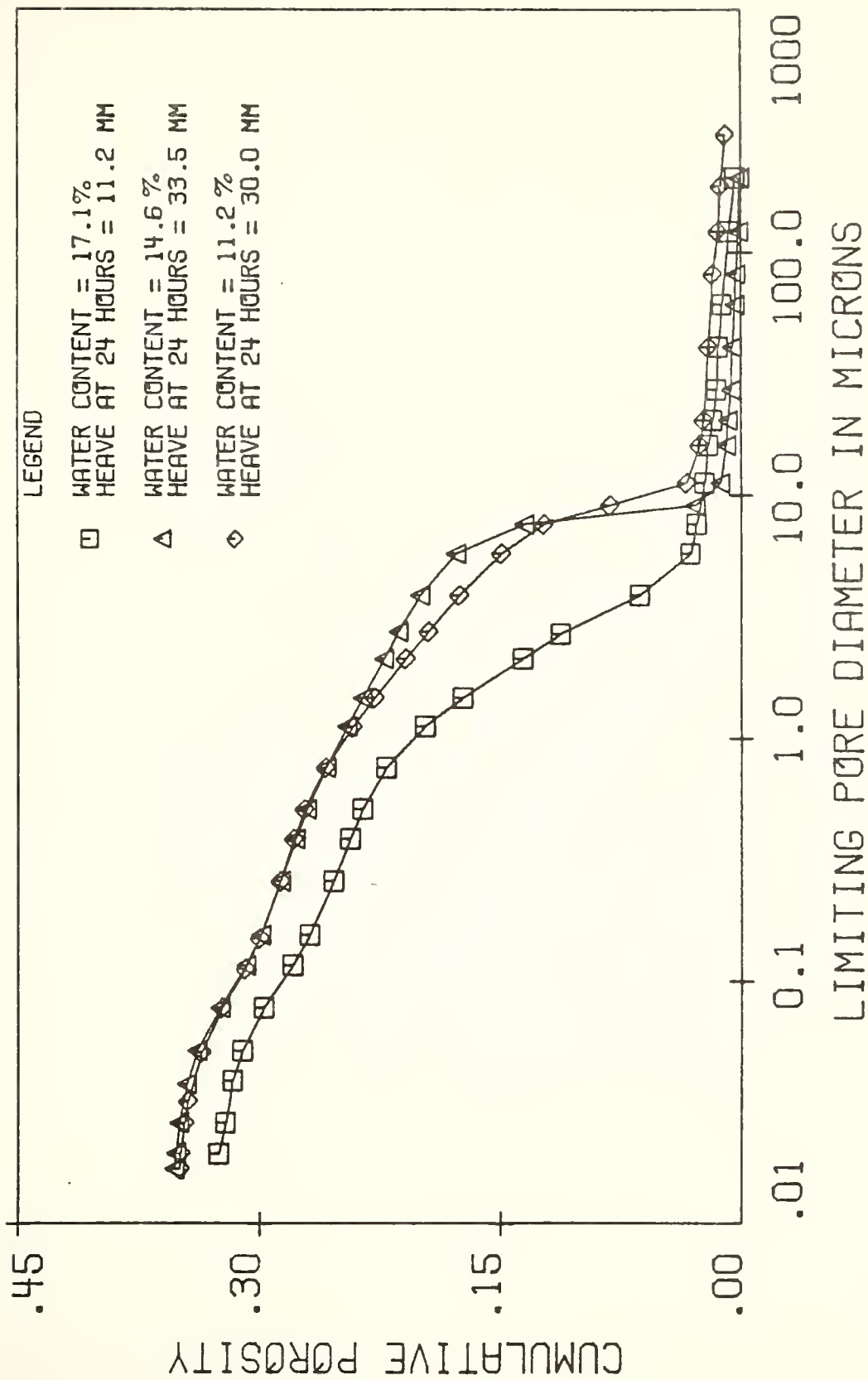
FIGURE 25 PORE SIZE DISTRIBUTION FOR 90% SILT — 10% KAOLIN COMPACTED AT 8.5 PSI*

*Foot pressure = 160 psi
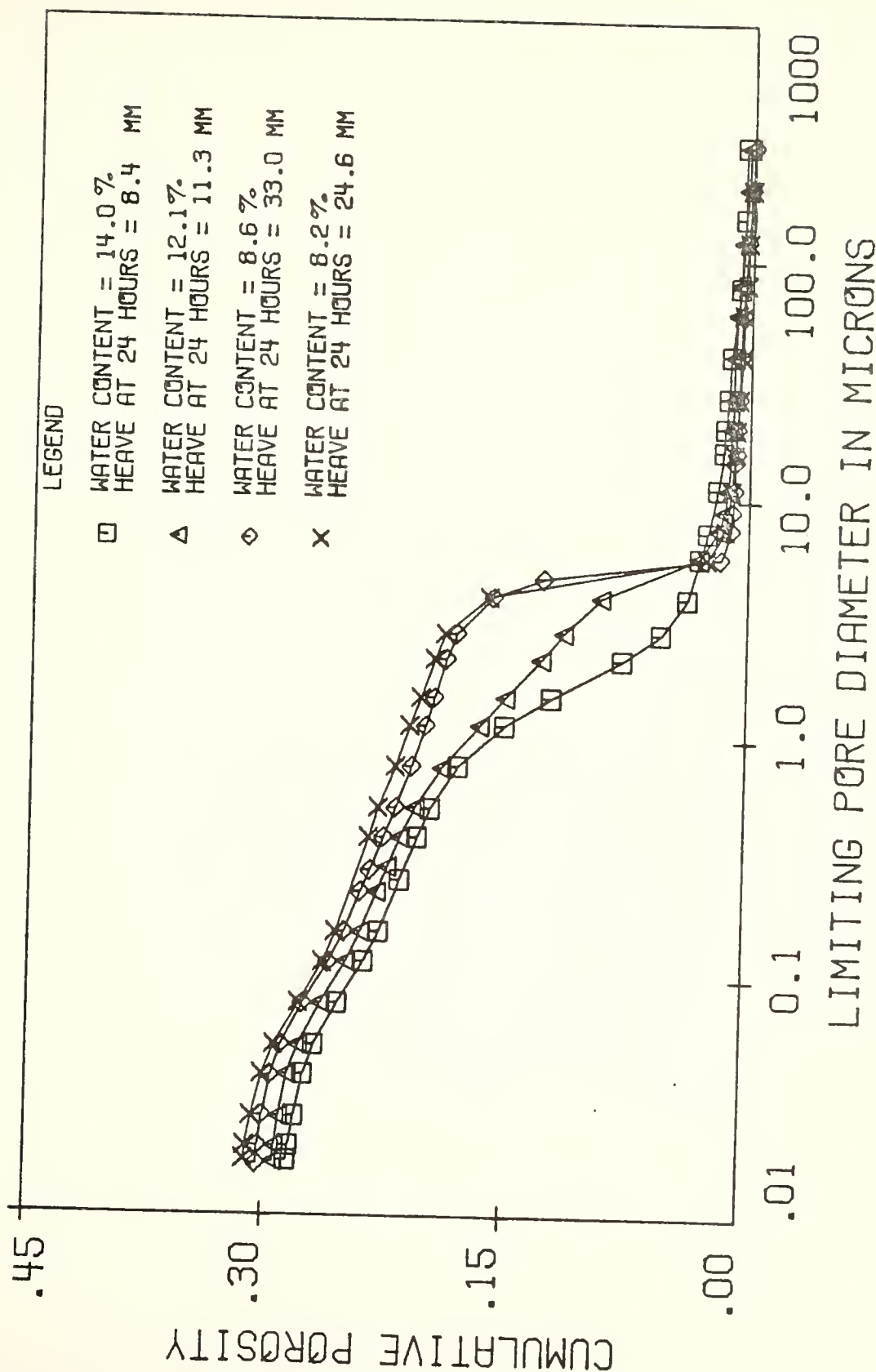
FIGURE 26   PORE SIZE DISTRIBUTION FOR 90% SILT –
10% KAOLIN COMPACTED AT 40 PSI*

*Foot pressure = 590 psi
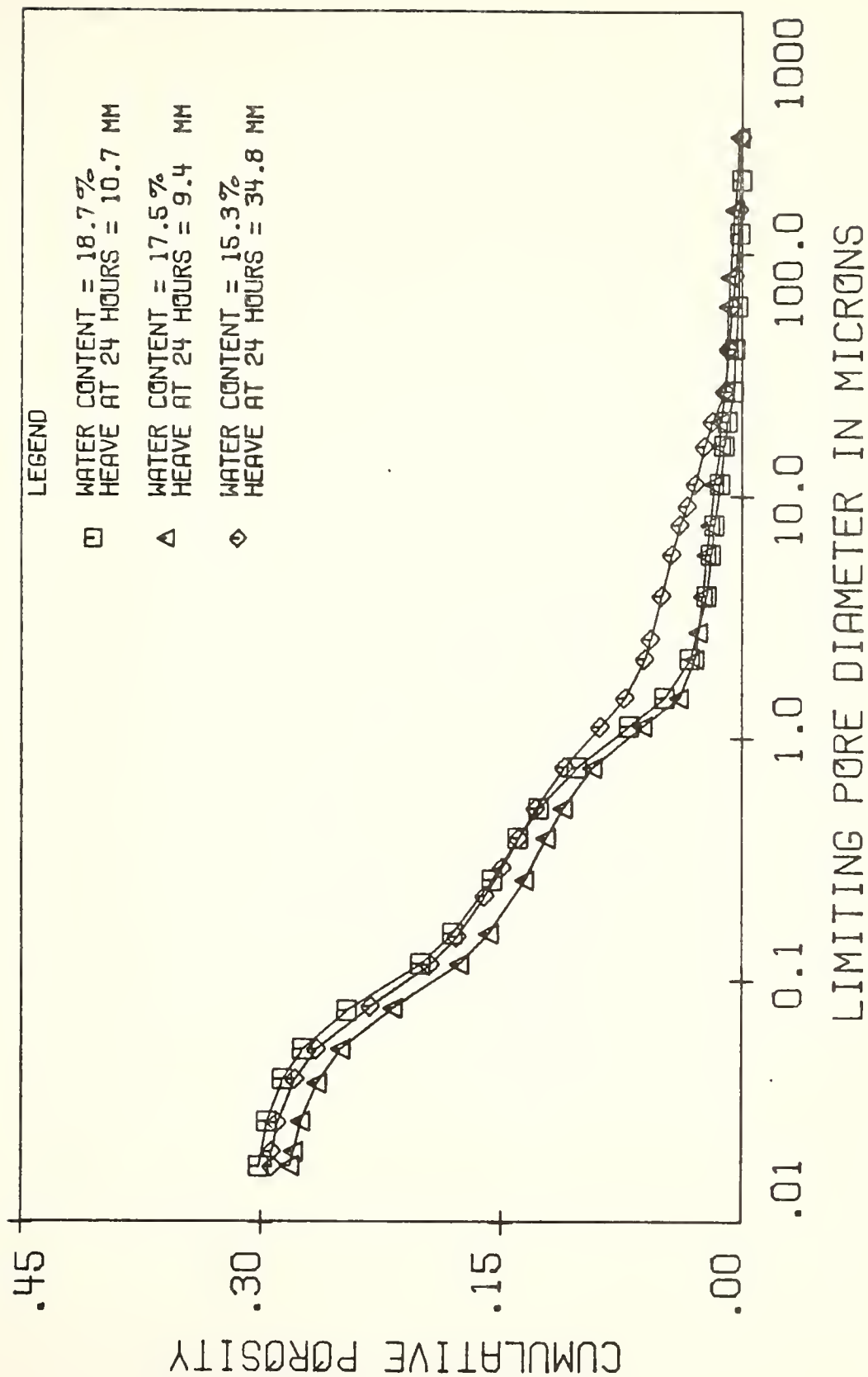
FIGURE 27 PORE SIZE DISTRIBUTION FOR 70% SILT – 30% KAOLIN COMPACTED AT 4.0 PSI*

*Foot pressure = 70 psi

LEGEND

□ WATER CONTENT = 18.7%
   HEAVE AT 24 HOURS = 10.7 MM

△ WATER CONTENT = 17.5%
   HEAVE AT 24 HOURS = 9.4 MM

◇ WATER CONTENT = 15.3%
   HEAVE AT 24 HOURS = 34.8 MM

LIMITING PORE DIAMETER IN MICRONS

CUMULATIVE POROSITY
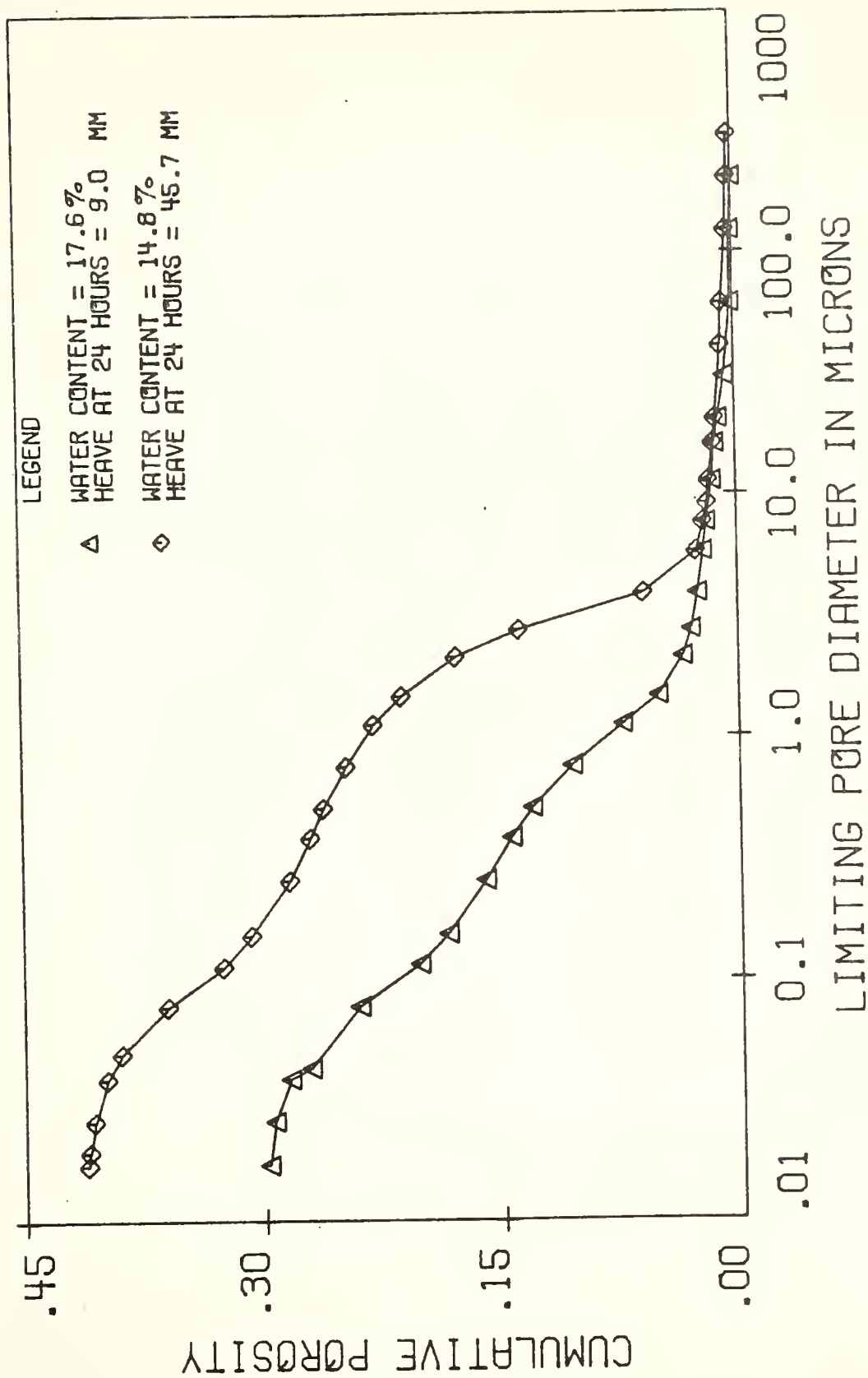
FIGURE 28   PORE SIZE DISTRIBUTION FOR 70% SILT —
30% KAOLIN COMPACTED AT 4.0 PSI*

*Foot pressure = 70 psi
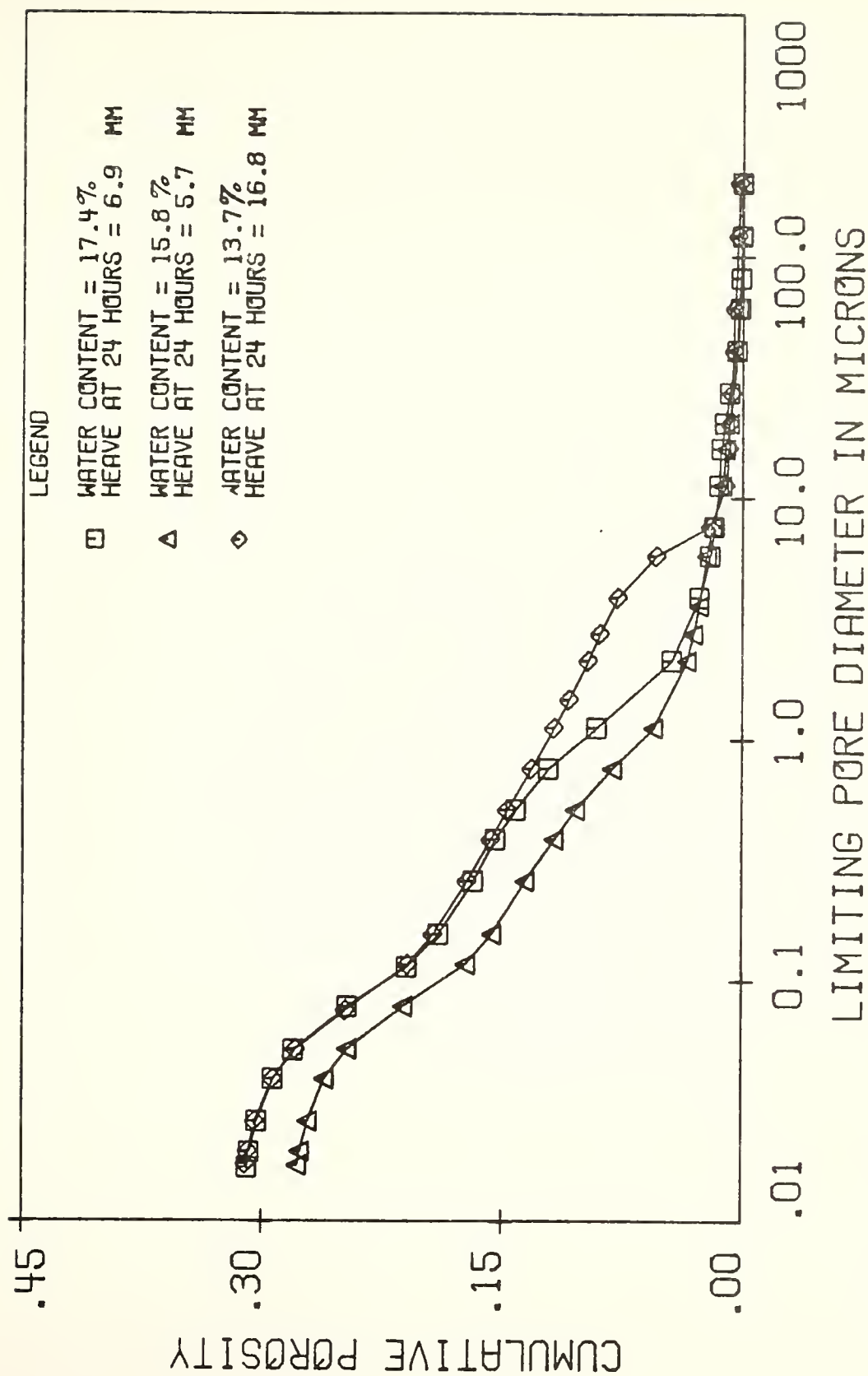
FIGURE 29 PORE SIZE DISTRIBUTION FOR 70% SILT -
30% KAOLIN COMPACTED AT 8.5 PSI*

*Foot pressure = 160 psi
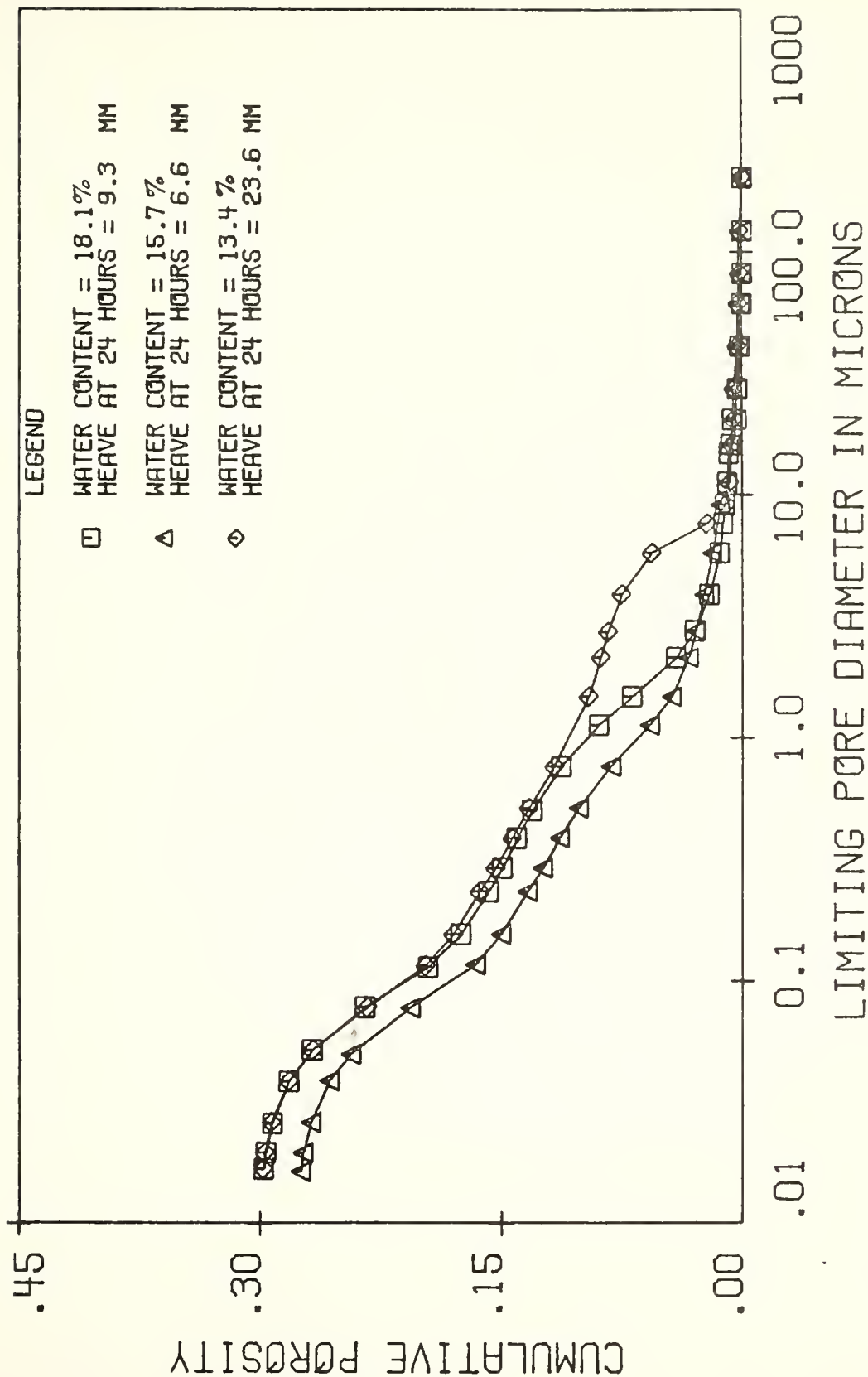
FIGURE 30   PORE SIZE DISTRIBUTION FOR 70% SILT – 30% KAOLIN COMPACTED AT 8.5 PSI*

*Foot pressure = 160 psi
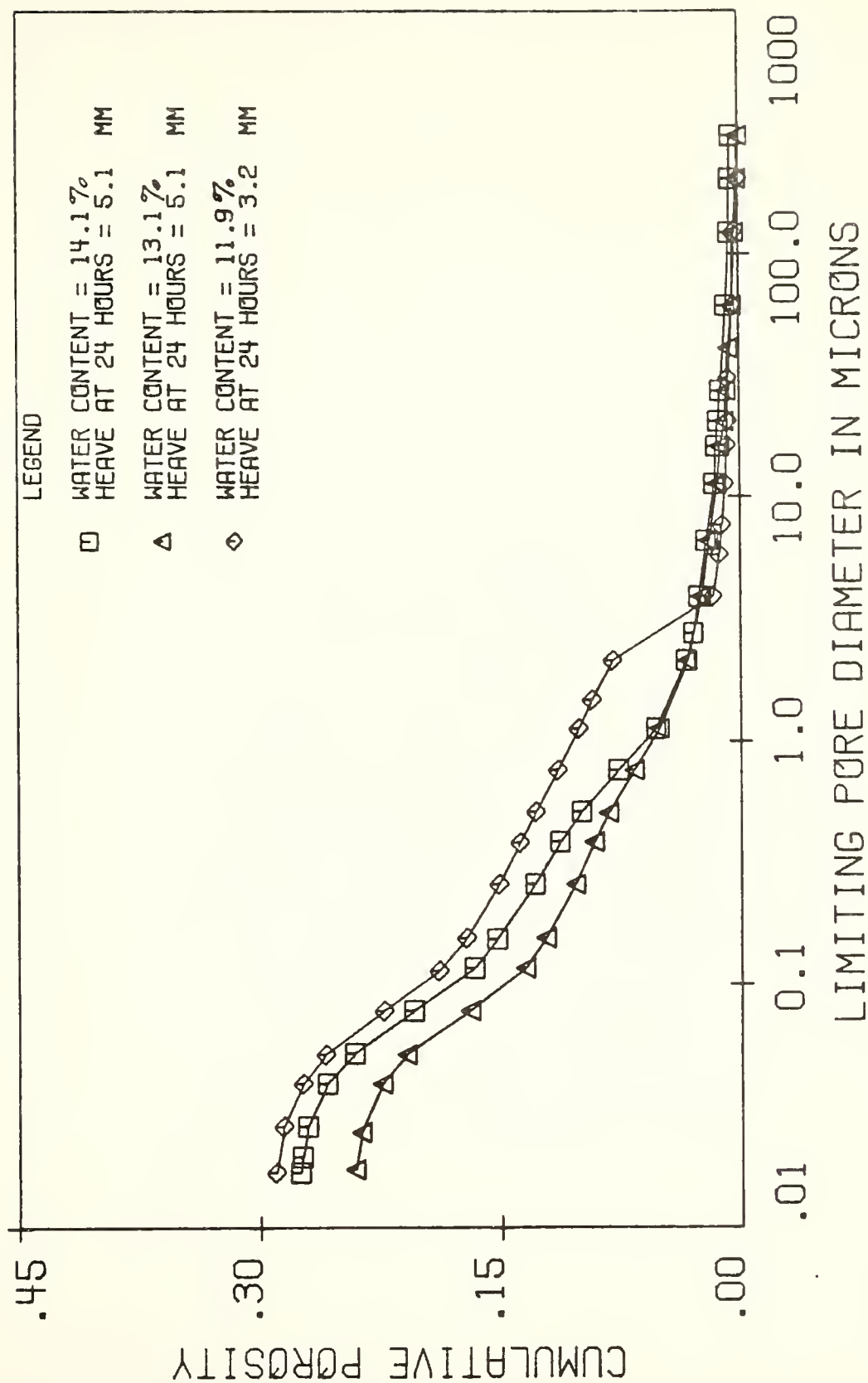
FIGURE 31   PORE SIZE DISTRIBUTION FOR 70% SILT –
30% KAOLIN COMPACTED AT 40 PSI*

LIMITING PORE DIAMETER IN MICRONS

*Foot pressure = 590 psi

LEGEND

WATER CONTENT = 14.1%
HEAVE AT 24 HOURS = 5.1   MM

WATER CONTENT = 13.1%
HEAVE AT 24 HOURS = 5.1   MM

WATER CONTENT = 11.9%
HEAVE AT 24 HOURS = 3.2   MM

CUMULATIVE POROSITY
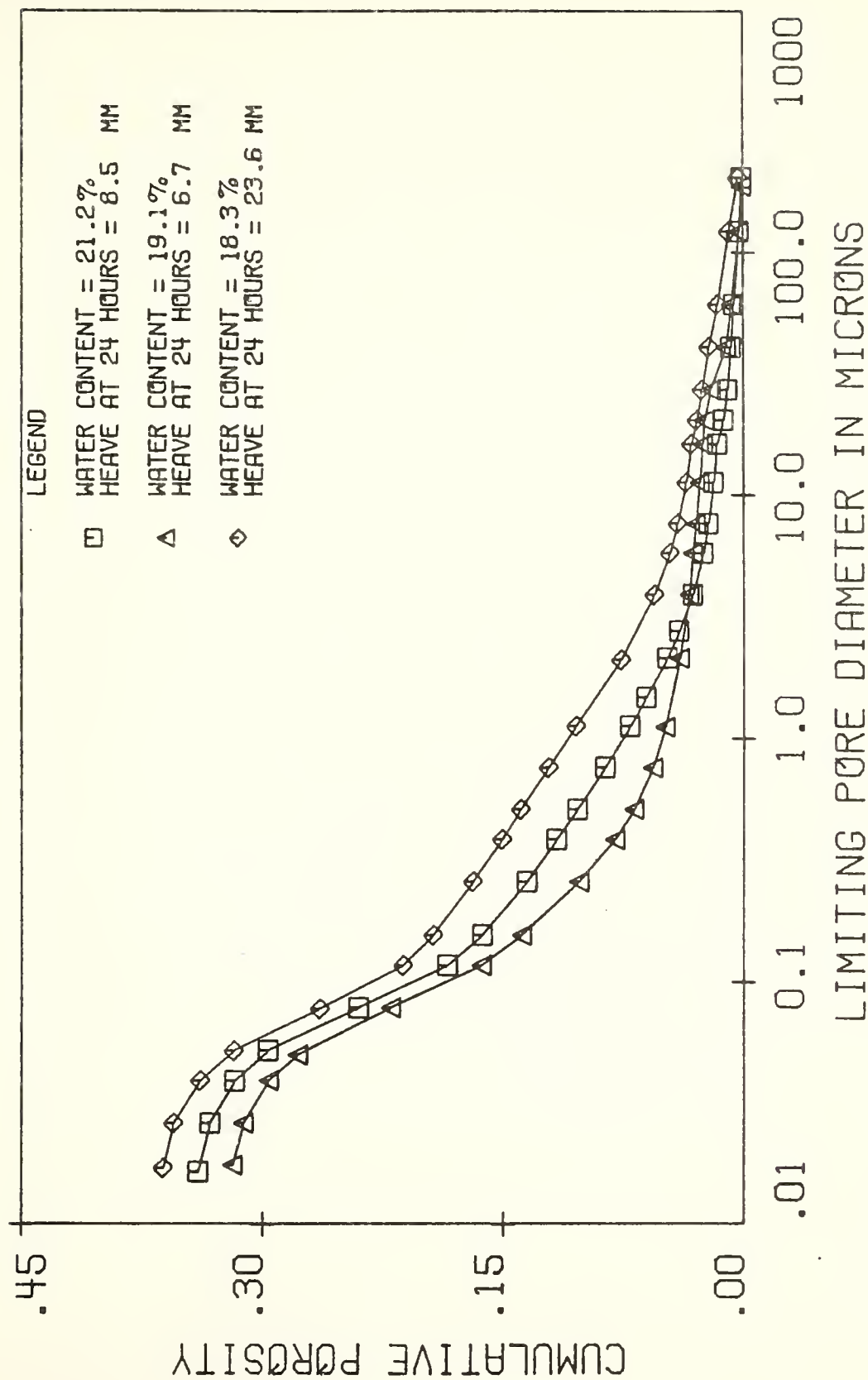
FIGURE 32   PORE SIZE DISTRIBUTION FOR 50% SILT –
50% KAOLIN COMPACTED AT 4.0 PSI*

*Foot pressure = 70 psi
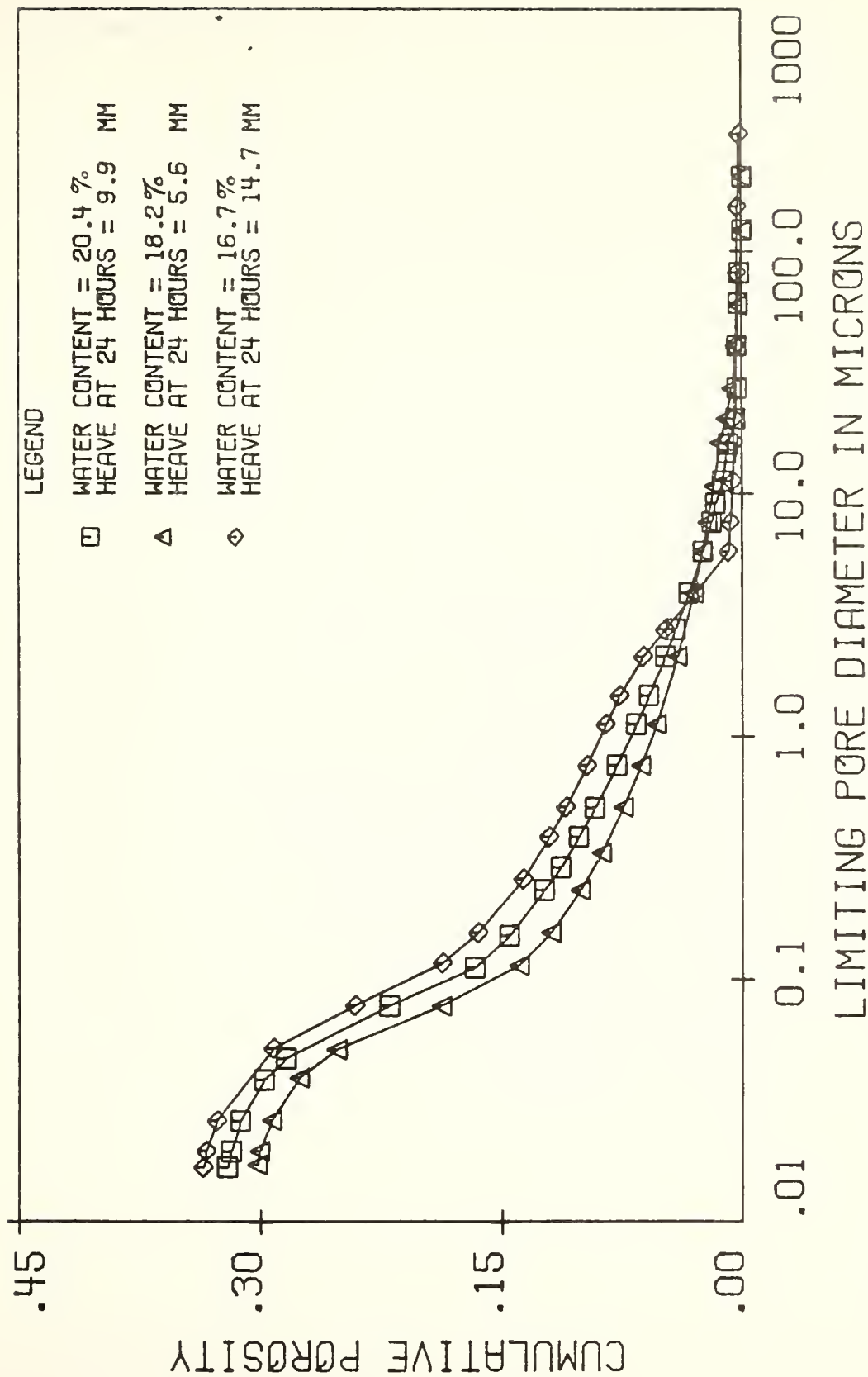
FIGURE 33 PORE SIZE DISTRIBUTION FOR 50% SILT —
50% KAOLIN COMPACTED AT 8.5 PSI*

*Foot pressure = 160 psi
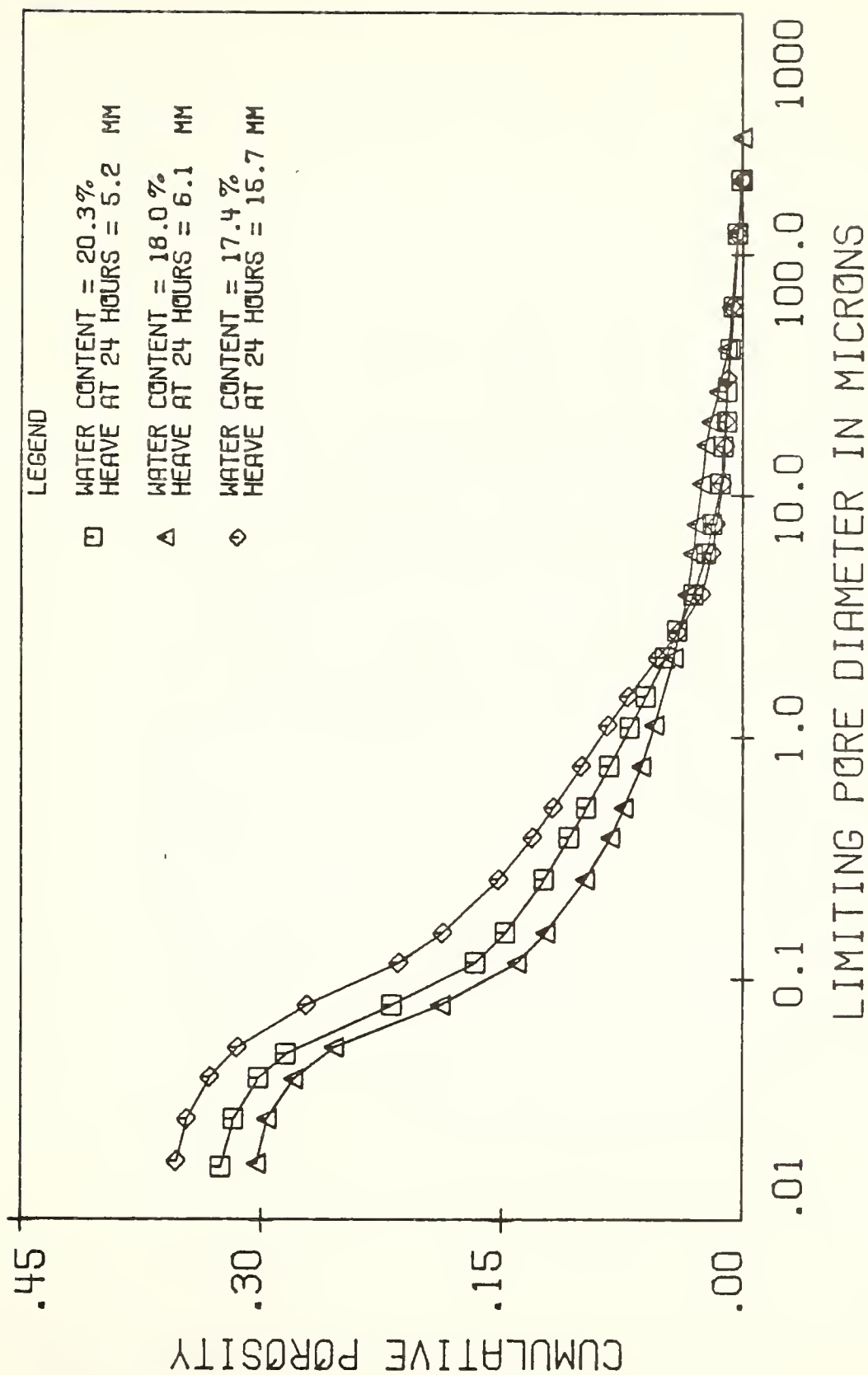
FIGURE 34 PORE SIZE DISTRIBUTION FOR 50% SILT – 50% KAOLIN COMPACTED AT 8.5 PSI*

*Foot pressure = 160 psi

compactive effort to 40 psi, this range was reduced to 1 to 6 µm.

In contrast to the above, the 70% silt - 30% kaolin mixtures
(Figures 27 through 31) displayed larger amounts of soil pores in the
0.4 to 3 µm range for the 8.5 psi compactive effort, and in the 0.4 to
1 µm range for soil compacted at 40 psi. Outside of the above
mentioned ranges, the amount of pores was essentially the same,
whether the soil was compacted at optimum or wet of optimum.

For the 50% silt - 50% kaolin mixture, the wet side of optimum
displayed larger amounts of pores than the optimum for the range of
0.1 to 3 µm at the 4 psi compactive effort and in the range of 0.4 to
3 µm for soil compacted at 8.5 psi. See Figures 32, 33 and 34.

Relation of Frost Heave to Pore Size

Regression Analysis

To derive a prediction equation for frost heave as a function of
pore size, the method of linear regression was used. This method is
based on a model, which in the case of a first order relation is

$$Y_i = \beta_o + \beta_1 X_i + \varepsilon_i \qquad (10)$$

where β_o and β_1 are parameters of the model, X_i is the independent
variable, Y_i is the corresponding observation, or dependent variable,
and ε_i is the departure from the regression line, or random error.

In the above model, β_o, β_1 and ε_i are unknown, with ε_i changing
for each observation Y_i. Although ε_i is impossible to predict, β_o and
β_1 can be estimated by use of the method of least squares, which is
based on minimizing the sum of squares of errors. The sum of squares
of errors is equal to

$$S = \sum_{i=1}^{n} \varepsilon_i^2 = \sum_{i=1}^{n} (Y_i - \beta_0 - \beta_1 X_i)^2 \qquad (11)$$

To use the least squares methods, estimates of β_0 and β_1, denoted by b_0 and b_1, are picked so that when substituted for β_0 and β_1, the sum of squares of errors is minimized. Once the estimates b_0 and b_1 are determined, the prediction equation is written as

$$Y = b_0 + b_1 X \qquad (12)$$

where Y is the predicted value of Y.

For the above prediction equation, the following assumptions have been made.

1) ε_i are random variables with mean 0 and variance σ^2.

2) ε_i and ε_j are uncorrelated, $i \neq j$, so that cov $(e_i, e_j) = 0$.

3) For the F test, used as a method of evaluation of the model, ε_i is a normally distributed variable with mean 0 and variance σ^2.

A measure of how well the prediction equation fits the actual data is the coefficient of determination, R^2, which is defined as

$$R^2 = \frac{\text{Sum of squares due to regression}}{\text{Total (corrected) sum of squares}}$$

$$= \frac{\Sigma(\hat{Y}_i - \bar{Y})^2}{\Sigma(Y_i - \bar{Y})^2} \qquad (13)$$

The coefficient of determination is usually expressed as a percentage, $100\ R^2$, and is the percent variation explained by the regression line.

If R^2 is 0%, then no variation is explained by the prediction equation. On the other hand, if R^2 is 100%, then all variation is explained by the equation.

A second test for the applicability of the model is the F test, which tests whether β_1 can be considered non zero or not. For this test, the ratio

$$F = \frac{\text{Mean Square due to regression}}{\text{Mean Square due to residual variation}}$$

is compared with the 100 $(1 - \alpha)$% point of the F $\{1, (n - 2)\}$ distribution in order to determine if β_1 can be considered non zero for the available data. If it cannot, then the regression equation has little value. A complete explanation of the F test is given in Draper and Smith (1966).

For the actual regression analysis for this study, prediction equations were developed using the Statistical Package for the Social Sciences (SPSS) computer program REGRESSION, developed by Nie et al. (1975). The equations were then evaluated for their accuracy by

(1) The coefficient of determination R^2.

(2) The overall F test, with the test being significant at $\alpha = 0.5$.

(3) The partial F test for each β_1, with the test being significant at $\alpha = 0.05$.

Prediction of Frost Heave

The pore size distribution curves shown in Figures 24 through 34 were evaluated in the following ways:

(1) Calculation of a mean and standard deviation for
each curve.

(2) Division of the curves into percentage-of-intrusion
bands. These bands indicated the pore size for
which 10%, 20%, ... 90% of the pores were larger.

(3) Division of the curves into bands of pertinent pore size
diameters. From these bands, the cumulative porosities
were obtained for pore size diameters of 0.05, 0.08,
0.1, 0.2, 0.4, 1.0, 1.5, 2.0, 3.0, 4.0 and 8.0 μm.

Table 10 presents the data for methods (2) and (3). The maximum pore
size that was measured was 300 μm.

For the frost heave prediction equations, parameters from one of
the above three cases were picked as the independent variables, with
frost heave as the dependent variable. Regression analysis was then
used to formulate and evaluate the prediction equations.

The first parameters to be evaluated were the mean and standard
deviation, since these values could be calculated using the same
computer program for tabulating and plotting the pore size curves.
However, the two parameters turned out to be essentially useless for
predicting frost heave. It was noted that the mean and standard
deviation could be greatly altered by a few very large pores. Thus,
this method of prediction was abandoned.

The second method of prediction was to consider the pore diameters
for selected percentages of intrusion. This method resulted in fairly
good results. For a one order linear model, the best prediction was
obtained by the equation

Table 10. Pore Size Distribution Values Used in Prediction Equations

Sample Number*	Total Cumulative Porosity	Cumulative Porosity for Pore Diameters > Indicated Diameter (in µm), but < 300 µm										
		0.05	0.08	0.10	0.20	0.40	1.0	1.5	2.0	3.0	4.0	8.0
1	.340	.331	.319	.310	.285	.267	.239	.210	.179	.125	.081	.027
2	.326	.312	.295	.286	.261	.242	.203	.170	.140	.097	.060	.027
3	.336	.322	.307	.298	.276	.259	.225	.204	.190	.169	.153	.100
4	.353	.340	.324	.313	.292	.277	.249	.235	.225	.209	.198	.110
5	.365	.352	.337	.328	.308	.290	.261	.247	.238	.224	.212	.135
6	.350	.338	.322	.313	.292	.277	.248	.226	.211	.190	.173	.110
7	.374	.359	.343	.334	.312	.294	.270	.258	.249	.236	.225	.115
8	.284	.261	.253	.244	.222	.204	.160	.121	.085	.050	.037	.025
9	.292	.280	.263	.255	.234	.213	.173	.152	.132	.110	.086	.018
10	.303	.290	.275	.266	.245	.266	.203	.196	.190	.177	.152	.011
11	.311	.294	.277	.270	.249	.235	.212	.203	.198	.182	.147	.014
12	.301	.277	.240	.217	.169	.137	.079	.046	.035	.027	.022	.018
13	.282	.251	.214	.192	.146	.121	.070	.039	.030	.027	.025	.020
14	.298	.262	.237	.216	.172	.140	.080	.049	.037	.028	.024	.018
15	.293	.267	.229	.208	.165	.137	.095	.071	.062	.055	.050	.038
16	.413	.389	.358	.338	.294	.268	.235	.209	.182	.117	.055	.020
17	.298	.270	.231	.210	.164	.139	.096	.066	.045	.026	.020	.012
18	.309	.282	.243	.222	.178	.152	.100	.069	.048	.034	.026	.017
19	.275	.243	.303	.181	.140	.112	.064	.044	.035	.027	.023	.017
20	.278	.248	.209	.189	.146	.115	.063	.046	.037	.029	.026	.017
21	.298	.270	.231	.210	.170	.141	.109	.096	.089	.080	.073	.018
22	.310	.282	.242	.222	.182	.156	.122	.107	.098	.086	.075	.017
23	.276	.243	.205	.180	.140	.111	.060	.044	.035	.029	.026	.020
24	.241	.210	.170	.148	.112	.090	.057	.043	.035	.029	.025	.019
25	.290	.261	.222	.200	.160	.136	.105	.092	.082	.044	.017	.011
26	.339	.299	.237	.205	.148	.114	.074	.060	.050	.038	.031	.022
27	.319	.278	.218	.184	.120	.079	.051	.045	.040	.037	.033	.029
28	.362	.321	.260	.230	.180	.149	.110	.092	.078	.064	.055	.040
29	.321	.277	.212	.181	.131	.100	.070	.058	.049	.040	.032	.019
30	.325	.281	.215	.187	.136	.107	.072	.058	.050	.039	.029	.019
31	.302	.255	.180	.156	.108	.082	.057	.049	.041	.034	.030	.021
32	.303	.255	.185	.160	.110	.081	.057	.050	.044	.039	.034	.029
33	.335	.294	.238	.209	.150	.119	.088	.075	.064	.042	.028	.008
34	.353	.315	.268	.237	.170	.130	.099	.069	.055	.037	.025	.018

* See Table 6 for Compaction variables. Sample numbers correspond to those in Tables 6,7 and 9.

Table 10.   (Cont'd)

Sample Number*	Pore Diameter for Indicated Percentage of Intrusion (in µm)								
	90%	80%	70%	60%	50%	40%	30%	20%	10%
1	0.113	0.34	1.02	1.58	2.17	2.77	3.45	4.55	6.90
2	0.087	0.212	0.64	1.15	1.63	2.23	2.97	3.75	5.60
3	0.087	0.280	0.81	1.56	3.00	5.55	7.90	9.30	10.5
4	0.091	0.323	1.06	2.90	5.70	7.30	8.00	8.50	9.00
5	0.101	0.405	1.20	3.45	6.30	7.80	8.40	9.20	10.3
6	0.097	0.380	1.07	1.98	3.80	6.10	8.10	9.40	10.8
7	0.096	0.340	1.35	3.93	6.10	7.50	8.10	8.60	9.60
8	0.073	0.169	0.495	0.86	1.21	1.56	1.99	2.70	6.80
9	0.082	0.217	0.55	0.97	1.63	2.67	4.00	4.80	6.10
10	0.083	0.215	0.67	2.67	3.95	4.60	4.90	5.20	5.60
11	0.074	0.217	0.84	2.82	3.80	4.25	4.70	5.10	5.70
12	0.053	0.077	0.104	0.150	0.29	0.54	0.86	1.25	2.45
13	0.046	0.068	0.092	0.126	0.222	0.48	0.81	1.17	2.13
14	0.047	0.078	0.106	0.169	0.333	0.59	0.90	1.28	2.58
15	0.052	0.074	0.102	0.151	0.310	0.66	1.12	2.27	11.3
16	0.065	0.107	0.224	0.73	1.54	2.25	2.90	3.43	4.70
17	0.050	0.075	0.099	0.142	0.29	0.64	1.10	1.62	2.68
18	0.052	0.077	0.103	0.168	0.385	0.71	1.10	1.63	3.30
19	0.045	0.065	0.078	0.117	0.214	0.42	0.74	1.18	3.13
20	0.047	0.068	0.092	0.127	0.230	0.43	0.72	1.12	3.50
21	0.050	0.071	0.100	0.160	0.330	0.72	1.90	5.60	7.30
22	0.050	0.073	0.103	0.180	0.405	0.90	2.32	5.00	7.00
23	0.046	0.064	0.088	0.120	0.212	0.41	0.68	1.10	3.25
24	0.042	0.059	0.077	0.101	0.152	0.318	0.66	1.22	4.25
25	0.048	0.070	0.096	0.147	0.310	0.71	1.72	2.62	3.48
26	0.048	0.062	0.077	0.100	0.138	0.250	0.53	1.17	3.45
27	0.044	0.058	0.074	0.094	0.120	0.178	0.290	0.58	5.70
28	0.045	0.063	0.083	0.110	0.198	0.44	1.02	2.40	10.1
29	0.044	0.056	0.074	0.092	0.120	0.21	0.45	1.22	4.20
30	0.042	0.057	0.071	0.091	0.123	0.24	0.50	1.28	3.55
31	0.040	0.055	0.066	0.080	0.103	0.152	0.31	0.88	3.90
32	0.041	0.055	0.066	0.081	0.103	0.158	0.31	0.85	6.60
33	0.041	0.062	0.081	0.103	0.148	0.270	0.68	1.88	3.52
34	0.048	0.069	0.093	0.120	0.180	0.315	0.66	1.47	3.00

$$\hat{Y} = -0.3805 + 1.6940 \left(\frac{D_{40}}{D_{80}}\right) \quad\quad (14)$$

where $\hat{Y}$ = predicted frost heave rate in mm/day,
$\quad D_{40}$ = pore diameter such that 40% of the pores are larger,
$\quad D_{80}$ = pore diameter such that 80% of the pores are larger.

For the above prediction equation, R^2 = 69.0%, and the residuals (ϵ) are plotted in Figure 35.

The last, and most fruitful, method of analysis was to consider the cumulative porosity for pertinent pore size bands. The approach was to first run a one order regression analysis for each soil, looking at all eleven selected pore size diameters. Based on these prediction equations, listed in Table 11, this approach seemed promising.

The next step was to run regression analyses for all data combined. When considering each soil, the prediction equation depended only on the large pores. This is partly due to the earlier mentioned fact that the amount of smaller pores was essentially constant. Therefore, it seems reasonable that a prediction equation for all soils would also have to take account of the small pores. Based on this premise, various two order models were tried, and the best results were obtained by the prediction equations listed in Table 12. The residuals for these equations are plotted in Figures 36, 37 and 38.

Proposal and Discussion of Frost Heave Prediction Equation

Based on the results discussed in the preceding paragraph, the equation

$$\hat{Y} = -5.46 - 29.46 \left(\frac{X_{3.0}}{X_0 - X_{0.4}}\right) + 581.1 \ (X_{3.0}) \quad\quad (15)$$
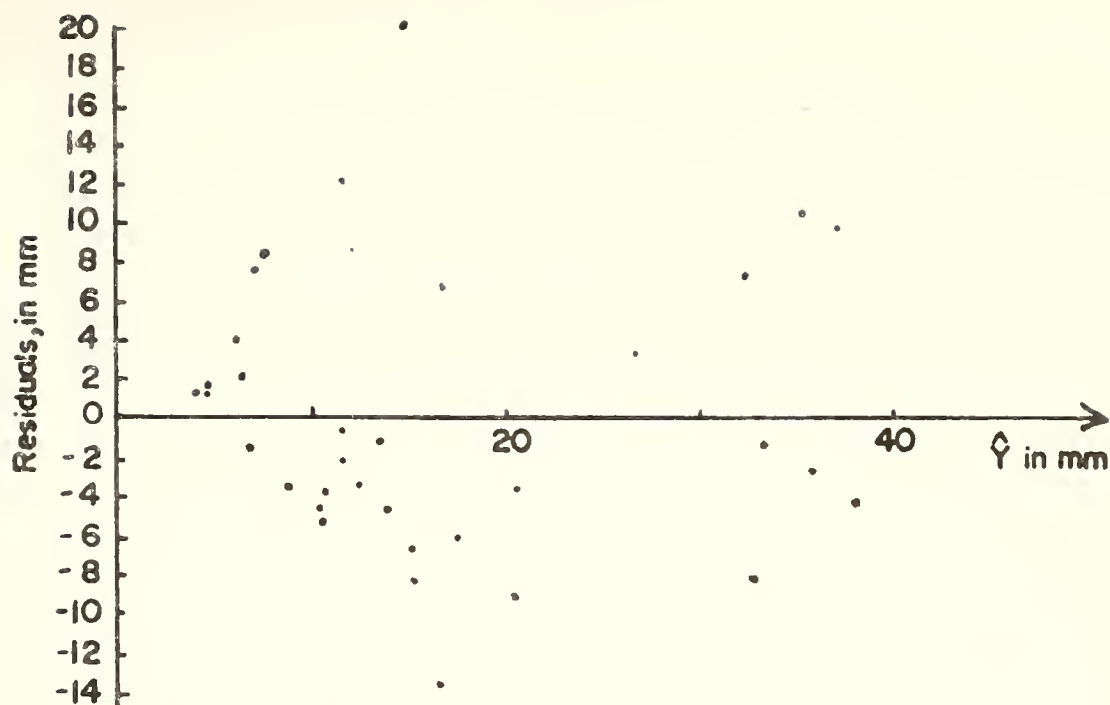
FIGURE 35 RESIDUALS VS FROST HEAVE FOR PREDICTION EQUATION $\hat{Y} = -0.3805 + 1.6940 \left(\dfrac{D_{40}}{D_{80}} \right)$
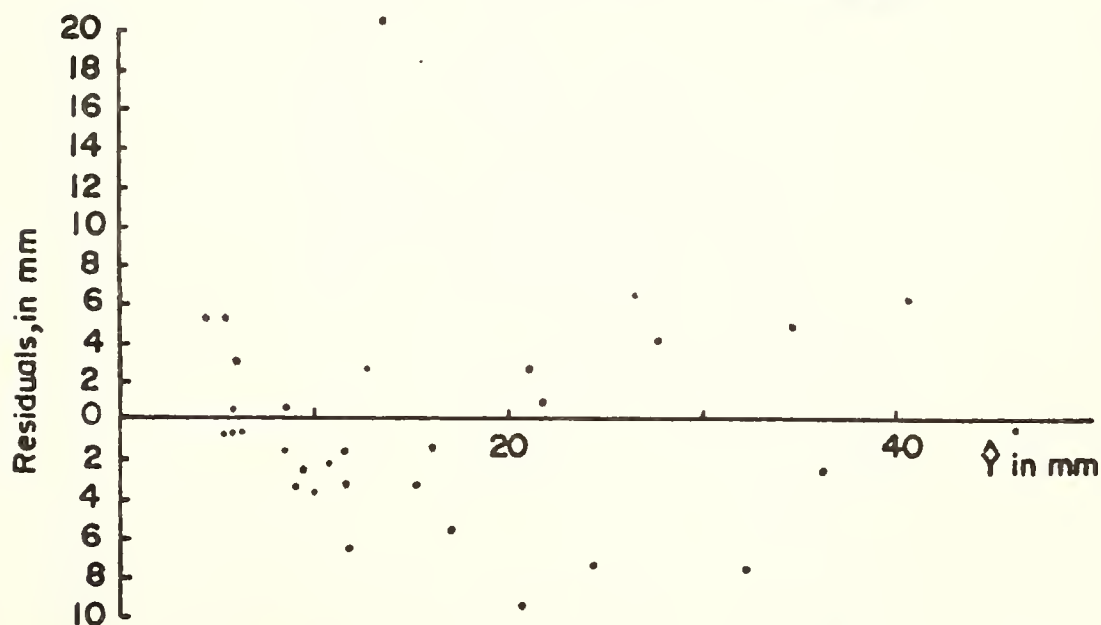
FIGURE 36 RESIDUALS VS FROST HEAVE FOR PREDICTION EQUATION $\hat{Y} = -4.81 - 8.445 \left(\dfrac{X_{2.0}}{X_0 - X_{0.1}} \right) + 393.5 (X_{2.0})$

Table 11. Frost Heave Prediction Equations with High Coefficients of Determination for Each Soil

Soils Considered	Frost Heave Rate Prediction Equation	R^2 in %	Significance Level for F Test
90% Silt - 10% Kaolin	$\hat{Y} = -18.41 + 237.9 \ (X_{2.0})$	80.8	.000
90% Silt - 10% Kaolin	$\hat{Y} = -8.35 + 211.4 \ (X_{3.0})$	89.0	.000
90% Silt - 10% Kaolin	$\hat{Y} = -1.79 + 198.0 \ (X_{4.0})$	93.7	.000
70% Silt - 30% Kaolin	$\hat{Y} = -0.56 + 255.2 \ (X_{2.0})$	73.6	.000
70% Silt - 30% Kaolin	$\hat{Y} = -2.07 + 363.0 \ (X_{3.0})$	72.4	.000
50% Silt - 50% Kaolin	$\hat{Y} = -13.72 + 394.8 \ (X_{1.5})$	89.3	.000
50% Silt - 50% Kaolin	$\hat{Y} = -14.17 + 474.6 \ (X_{2.0})$	86.3	.000
50% Silt - 50% Kaolin	$\hat{Y} = -12.87 + 572.5 \ (X_{3.0})$	67.3	.007

$\hat{Y}$ = Predicted Frost Heave Rate in mm
$X_{1.5}$ = Cumulative Porosity for Pores > 1.5 μm but < 300 mμ
$X_{2.0}$ = Cumulative Porosity for Pores > 2.0 μm but < 300 mμ
$X_{3.0}$ = Cumulative Porosity for Pores > 3.0 μm but < 300 mμ
$X_{4.0}$ = Cumulative Porosity for Pores > 4.0 μm but < 300 mμ

Table 12. Frost Heave Prediction Equations with High Coefficients of Determination for All Soils Tested

Frost Heave Rate Prediction Equation	R^2 in %	Significance Level for Partial F Test
$\hat{Y} = -4.81 - 8.44 \left(\dfrac{X_{2.0}}{X_0 - X_{0.1}} \right) + 393.5\ (X_{2.0})$	80.5	$X_{2.0}$: .000 $X_{0.1}$: .000
$\hat{Y} = -4.76 - 20.52 \left(\dfrac{X_{3.0}}{X_0 - X_{0.2}} \right) + 537.6\ (X_{3.0})$	81.0	$X_{3.0}$: .000 $X_{0.2}$: .000
$\hat{Y} = -5.46 - 29.46 \left(\dfrac{X_{3.0}}{X_0 - X_{0.4}} \right) + 581.1\ (X_{3.0})$	82.0	$X_{3.0}$: .000 $X_{0.4}$: .000

$\hat{Y}$ = Predicted Frost Heave Rate in mm
X_0 = Total Cumulative Porosity
$X_{0.1}$ = Cumulative Porosity for Pores > 0.1 µm
$X_{0.2}$ = Cumulative Porosity for Pores > 0.2 µm
$X_{0.4}$ = Cumulative Porosity for Pores > 0.4 µm
$X_{2.0}$ = Cumulative Porosity for Pores > 2.0 µm but < 300 µm
$X_{3.0}$ = Cumulative Porosity for Pores > 3.0 µm but < 300 µm
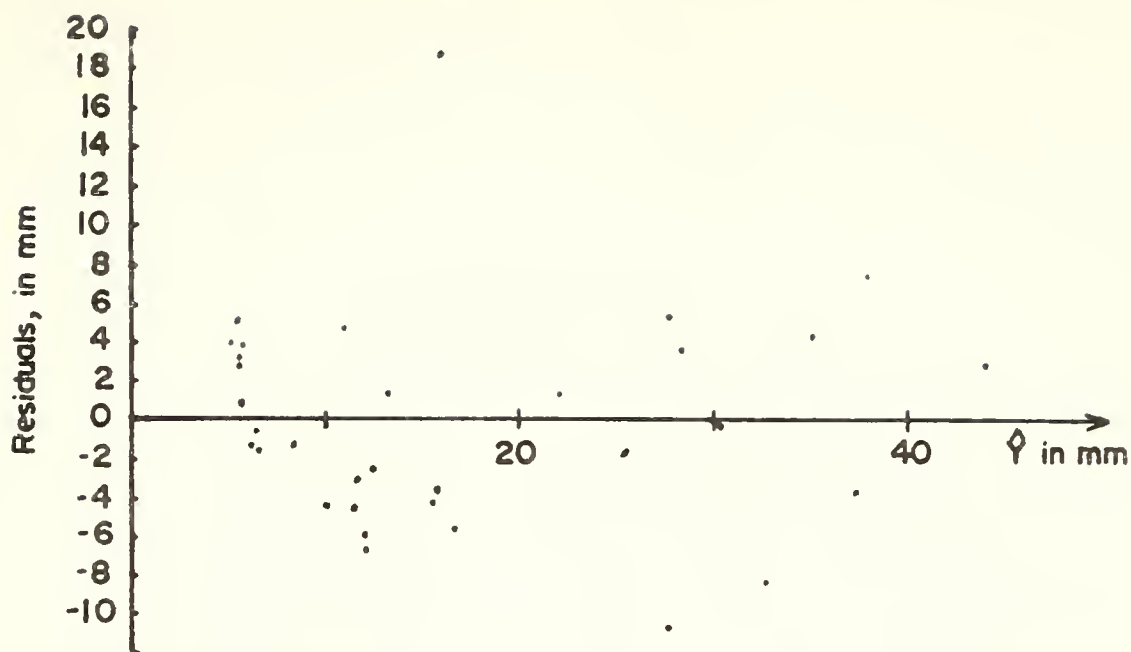
FIGURE 37 RESIDUALS VS FROST HEAVE FOR PREDICTION EQUATION $\hat{Y} = -4.76 - 20.52\left(\frac{x_{3.0}}{x_0 - x_{0.2}}\right) + 537.6(x_{3.0})$
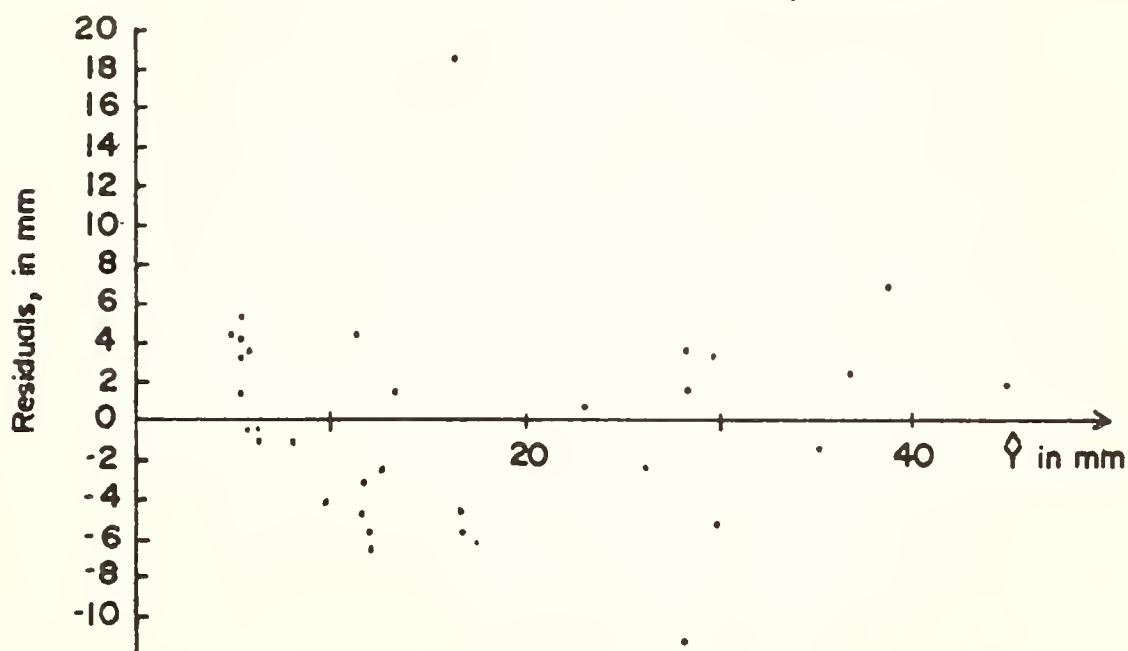
FIGURE 38 RESIDUALS VS FROST HEAVE FOR PREDICTION EQUATION $\hat{Y} = -5.46 - 29.46\left(\frac{x_{3.0}}{x_0 - x_{0.4}}\right) + 581.1(x_{3.0})$

where $\hat{Y}$ = frost heave rate, in mm/day,
 $X_{3.0}$ = cumulative porosity for pores > 3.0 μm but < 300 μm ,
  $\dot{X}_0$ = total cumulative porosity,
  $X_{0.4}$ = cumulative porosity for pores > 0.4 μm but < 300 μm,

is recommended for predicting frost heave from pore size distribution.
Possibly a more "precise" model can be found by using more parameters
however much can be said for simple models.

In physical explanation of the above equation, it is believed that
the large pores, quantified by the value $X_{3.0}$, offer the least resistance
for water to move to the freezing front, whereas the smaller pores rep-
resent the amount of available energy to do the work of frost heave.
For soils of the same type, the fine pores are essentially independent
of compaction and water contents and thus the larger pores will control
the frost heave. However, when evaluating different soils, heave will
be controlled by both fine and large pores.

With regards to the predicted heave value, the greater the heave,
the greater the frost susceptibility. Although there is no specific
correlation with field performance for the freezing test used, an indi-
cation of the degree of frost susceptibility can be found from the
prior mentioned author's criterion, shown in Table 8. The UNH classi-
fication, listed in Table 3, is also somewhat applicable to the test
results, although probably quite conservative.

If the soils studied had been evaluated solely by Casagrande's
(1932) criteria, they would have all been classified as frost susceptible.
When the soils are assigned "F-ratings" in the U. S. Army Corps of
Engineers' System (Table 4), they are classified as F-3 or F-4.

However, by varying clay content, water content, and compactive effort,
frost heave ranged from "very low" to "very high". This range of
heave can be predicted by using the proposed frost heave prediction
equation. The pore size based equation is valuable in that it allows
one to predict the degree of frost heave (and relative frost suscept-
ibility) as it is affected by compaction and soil variables.

CONCLUSIONS

For the silty soils studied, the following conclusions are drawn
with respect to frost heave, pore size distribution and the major
compactive variables.

1) Samples compacted dry of optimum displayed greater

    heave than those compacted at optimum or wet of

    optimum.

2) Increasing the compactive effort reduced heave

    for samples compacted dry of optimum.

3) It was not possible to predict whether a soil will

    have the higher frost heave compacted at optimum

    or compacted wet of optimum.

4) The rapid frost heave test, as used in these studies,

    gives reliable results with relatively inexpensive

    test equipment.

5) As long as the sample to be dried is no larger than

    about 8 mm square, the freeze drying process produces

    little volume change ($\pm$ 3%) of the sample.

6) For a particular soil type, the distribution of pores

    below 0.1 µm, and in most cases below 0.4 µm, is

    essentially the same regardless of the compaction

    water content or effort.

7) The degree of frost heave can be predicted by the equation

$$\hat{Y} = - 5.46 - 29.46 \left(\frac{X_{3.0}}{X_0 - X_{0.4}} \right) + 581.1 \ (X_{3.0}) \quad (15)$$

where $\hat{Y}$ = frost heave rate, in mm/day,
$X_{3.0}$ = cumulative porosity for pores > 3.0 μm but < 300 μm,
X_0 = total cumulative porosity,
$X_{0.4}$ = cumulative porosity for pores > 0.4 μm but < 300 μm.

8) Frost susceptibility criteria based upon textural

or grain size distribution measures have a more

limited prediction capability than pore size ones,

since the former do not take compaction variables

like moisture content and density into account.

Such compaction variables do influence the

distribution of porosity.

RECOMMENDATIONS FOR FURTHER RESEARCH

The evidence of this research supports the hypothesis that the distribution of porosity may be a superior predictor of frost heave rate and frost susceptibility of fine grained soils. This type of work should be extended in the following categories.

1) Dehydration Studies. Both critical region drying and freeze drying should be experimentally examined over a wide range of soil types and conditions in order to determine where each can be used with confidence.

2) Porosimeter Apparatus. The versatility of the porosimeter would be extended if the equipment were modified to accommodate larger samples of more coarse material.

3) Freezing Tests. A standard, universal, rapid freezing test should be established. This test should be correlated to appropriate field measures of frost susceptibility. When this is accomplished, practical predictions of field frost susceptibility can be determined from simple laboratory tests, including pore size distribution.

4) Control of Frost Susceptibility. An ultimate short range objective of experimental research of this type would be the control of frost susceptibility of a given soil type through control of the compaction variables. This will require extensive laboratory and field testing, but the potential benefits in improvement of the state-of-the-art justify the effort.

BIBLIOGRAPHY

BIBLIOGRAPHY

Ahmed, S. (1971), "Pore Size and its Effects on the Behavior of a Compacted Clay," MSCE Thesis, Purdue University, West Lafayette, Indiana, June, 200 pp.

Ahmed, S., Lovell, C. W., Jr. and Diamond, S. (1974), "Pore Sizes and Strength of Compacted Clay," Journal of the Geotechnical Division, ASCE, Vol. 100, No. GT4, April, pp. 407-425.

American Association of State Highway Officials (1970), "Standard Method of Test for the Moisture Relations of Soils Using a 5.5 lb. Rammer and a 12 in. Drop," Standard Specifications for Highway Materials and Methods of Sampling and Testing, Part II, AASHO Designation T99-70, pp. 301-307.

Anderson, D. M., Tice, A. R. and Banin, A. (1974), "The Water-Ice Phase Composition of Clay/Water Systems, I. The Kaolinite/Water System," CRREL Research Report 322, June, 13 pp.

Bailey, M. J. (1976), "Shale Degradation and Other Parameters Related to the Construction of Compacted Embankments," MSCE Thesis, Purdue University, West Lafayette, Indiana, August, 230 pp.

Beskow, G. (1935), "Soil Freezing and Frost Heaving with Special Application to Roads and Railroads," Swedish Geotechnical Society Series C, No. 375, 145 pp.

Bhasin, R. N. (1975), "Pore Size Distribution of Compacted Soils After Critical Region Drying," Ph.D. Thesis, Purdue University, West Lafayette, Indiana, May, 222 pp.

Casagrande, A. (1932), "Discussion on A New Theory of Frost Heaving by Benkelman and Olmstead," Highway Research Board Proceedings, Vol. II, Pt. 1, pp. 168-172.

Cass, L. A. and Miller, R. D. (1959), "Role of the Double Layer in the Mechanism of Frost Heaving," U. S. Army Snow, Ice and Permafrost Research Establishment Research Report 49, August, 15 pp.

Corte, A. E. (1963), "Vertical Migration of Particles in Front of a Moving Freezing Plane," CRREL Research Report 105, January, 8 pp.

Csathy, T. I. and Townsend, D. L. (1962), "Pore Size and Field Frost Performance of Soils," Highway Research Board Bulletin 331, pp. 67-80.

Diamond, S. (1970), "Pore Size Distributions in Clays," Clays and Clay Minerals, Vol. 18, pp. 7-23.

Diamond, S. (1971), "Microstructure and Pore Structure of Impact-Compacted Clays," Clays and Clay Minerals, Vol. 19, pp. 239-249.

Draper, N. R. and Smith, H. (1966), "Applied Regression Analysis," Wiley, New York, 407 pp.

Drake, L. C. and Ritter, H. L. (1945), "Macropore-Size Distributions in Some Typical Porous Substances," Industrial and Engineering Chemistry, Analytical Edition, Vol. 17, No. 12, December, pp. 787-791.

Everett, D. H. and Haynes, J. M. (1965), "Capillary Properties of Some Model Pore Systems with Reference to Frost Damage," RILEM Bulletin, New Series, No. 27, pp. 31-38.

Gaskin, P. N. and Raymond, G. P. (1973), "Pore Size Distribution as a Frost Susceptibility Criterion," Proceedings of the Symposium on Frost Action on Roads, Norwegian Road Research Laboratory, Oslo, Vol. 1, pp. 295-309.

Hoekstra, P., Chamberlain, E. and Frate, A. (1965), "Frost Heaving Pressures," CRREL Research Report 176, October, 12 pp.

Jacobs, J. C. (1965), "The Road Research Laboratory Frost Heave Test," Great Britain Department Science Industrial Research, Road Research Lab Note LN/766/JCJ.

Johnson, T. C., Berg, R. L., Corey, K. L. and Kaplar, C. W. (1975), "Roadway Design in Seasonal Frost Areas," CRREL Technical Report 259, March, 104 pp.

Jumikis, A. R. (1957), "Soil Moisture Transfer in the Vapor Phase Upon Freezing," Highway Research Board Bulletin 168, pp. 96-116.

Kaplar, C. W. (1968), "New Experiments to Simplify Frost Susceptibility Testing of Soils," Highway Research Record, No. 215, pp. 48-59.

Kaplar, C. W. (1970), "Phenomenon and Mechanism of Frost Heaving," Highway Research Record, No. 304, pp. 1-13.

Kaplar, C. W. (1971), "Experiments to Simplify Frost Susceptibility Testing of Soil," CRREL Technical Report 223, January, 21 pp.

Kaplar, C. W. (1974), "A Laboratory Freezing Test to Determine the Frost Susceptibility of Soils," CRREL Technical Report 250, June, 40 pp.

Keionen, L. (1973), "The Physical Basis of the Growth of Ice Lenses in Soils," Proceedings of the Symposium on Frost Action on Roads, Norwegian Road Research Laboratory, Oslo, Vol. 1, pp. 311-315.

Kemball, C. (1946), "On the Surface Tension of Mercury," Transactions, Faraday Society, Vol. 42, pp. 526-537.

Kolaian, J. H. and Low, P. F. (1963), "Calorimetric Determination of Unfrozen Water in Montmorillonite Pastes," Soil Science, Vol. 95, No. 6, June, pp. 376-384.

Lovell, C. W., Jr. (1957), "Certain Characteristics of Partially Frozen Soil," Ph.D. Thesis, Purdue University, West Lafayette, Indiana, January, 166 pp.

Lovell, C. W., Jr. (1957a), "Temperature Effects on Phase Composition and Strength of Partially Frozen Soil," Highway Research Board Bulletin 168, pp. 74-95.

Low, P. F., Anderson, D. M. and Hoekstra, P. (1968), "Some Thermodynamic Relations for Soil at or Below the Freezing Point 1. Freezing Point Depression and Heat Capacity," Water Resouces Research, Vol. 4, No. 2, April, pp. 379-394.

Low, P. F., Anderson, D. M. and Hoekstra, P. (1968a), "Some Thermodynamic Relations for Soil at or Below the Freezing Point 2. Effects of Temperature and Pressure on Unfrozen Soil Water," Water Resources Research, Vol. 4, No. 3, June, pp. 541-544.

Martin, R. T. and Wissa, A. E. Z. (1973), "Frost Susceptibility of Massachusetts Soils - Evaluation of Rapid Frost Susceptibility Tests," Massachusetts Institute of Technology Soils Publication 224, October.

Nie, N. C., Hull, C. H., Jenkins, J., Steinbrenner, K., and Bent, D. (1975), Statistical Package for the Social Sciences, 2nd ed., Mcgraw-Hill, New York, 670 pp.

Orr, C. Jr. (1970), "Application of Mercury Penetration to Materials Analysis," Powder Technology, Vol. 3, No. 3, pp. 117-123.

Osler, J. C. (1967), "The Influence of Depth of Frost Penetration on the Frost Susceptibility of Soils," Canadian Geotechnical Journal, Vol. 4, No. 3, September, pp. 334-346.

Penner, E. (1967), "Heaving Pressure in Soils During Unidirectional Freezing," Canadian Geotechnical Journal, Vol. IV, No. 4, November, pp. 398-408.

Penner, E. (1972), "Influence of Freezing Rate to Frost Heaving," Highway Research Record, No. 393, pp. 56-64.

Penner, E. (1973), "Frost Heaving Pressures in Particulate Materials," Proceedings of the Symposium on Frost Action on Roads, Norwegian Road Research Laboratory, Oslo, Vol. 1., pp. 311-315.

Schofield, R. K. (1935), "The pF of Water in Soil," International Congress of Soil Science, 3, Oxford, Transactions, Vol. II, pp. 37-48.

Scott, R. F. (1969), "The Freezing Process and Mechanics of Frozen Ground," CRREL Monograph II-DI, October, 67 pp.

Sridharan, A., Altschaeffl, A. G. and Diamond, S. (1971), "Pore Size Distribution Studies," Journal of Soil Mechanics and Foundation Division, ASCE, Vol. 97, No. SM5, pp. 771-787.

Sutherland, H. B. and Gaskin, P. N. (1970), "Factors Affecting the Frost Susceptibility Characteristics of Pulverized Fuel Ash," Canadian Geotechnical Journal, Vol. 7, No. 1, February, pp. 69-78.

Sutherland, H. B. and Gaskin, P. N. (1973), "A Comparison of the TRRL and CRREL Tests for the Frost susceptibility of Soils," Canadian Geotechnical Journal, Vol. 10, No. 3, August, pp. 553-557.

Taber, S., (1929), "Frost Heaving," Journal of Geology, Vol. 37, No. 1, pp. 428-461.

Takagi, S. (1965), "Principles of Frost Heaving," CRREL Research Report 140, September, 24 pp.

Tsytovich, N. A., edited by Swinzow, G. K. (1975), The Mechanics of Frozen Ground, McGraw-Hill, New York, 426 pp.

Washburn, E. W. (1921), "Note on a Method of Determining the Distribution of Pore Sizes in a Porous Material," Proceedings, National Academy of Sciences, Vol. 7, pp. 115-116.

Williams, P. J. (1968), "Properties and Behaviour of Freezing Soils," Norwegian Geotechnical Institute, Publication NR, 72, 119 pp.

Williams, P. J. (1972), "Use of the Ice Water Surface Tension Concept in Engineering Practice," Highway Research Record, No. 393, pp. 19-29.

Winn, H. F. and Rutledge, R. C. (1940), "Frost Action in Highway Bases and Subgrades," Engineering Bulletin, Purdue University, Vol. XXIV, No. 3, May, 104 pp.

Zimmie, T. F. and Almaleh, L. J. (1976), Shrinkage of Soil Specimens During Preparation for Porosimetry Tests, Soil Specimen Preparation for Laboratory Testing, ASTM STP 599, pp. 202-215.

Zoller, H. (1973), "Frost Heave and the Rapid Frost Heave Test,"
    Public Roads, Vol. 37, No. 6, pp. 211-220.

APPENDICES

Appendix A

```
C        THIS PROGRAM CALCULATES AND TABULATES PORE SIZE DISTRIBUTION
C        PARAMETERS, ALONG WITH PLOTTING PORE DIAMETER VERSUS CUMULATIVE
C        INTRUSION/GRAM, CUMULATIVE INTRUSION/VOLUME AND INCREMENTAL
C        INTRUSION /VOLUME.   THE MEAN AND VARIANCE ARE ALSO CALCULATED
         PROGRAM PORE (INPUT,OUTPUT,TAPE5=INPUT,TAPE6=OUTPUT)
         DIMENSION S(50),P(50),D(50),CU(50),SP(50),CUSP(50),GRAPH(451),
         CPGRD(451),HISTO(451),C(50)
         READ, NDATA
         DO 400 J=1,NDATA
C        THE PURPOSE OF THIS DO LOOP IS TO BE ABLE TO CALCULATE RESULTS FOR
C        MORE THAN ONE SET OF DATA IN A SINGLE RUN.   NDATA IS THE NUMBER
C        OF SETS OF DATA TO BE CALCULATED.   NDATA IS AN INTEGER VALUE, AND
C        IS THE FIRST DATA CARD FOR THE SET OF DATA.
C        DETERMINATION OF PORE SIZE DISTRIBUTION
         READ,DATE,SN
C        DATE AND SAMPLE NUMBER (SN) ARE TYPED ON THE FIRST DATA CARD FOR
C        EACH CURVE.
         WRITE (6,14)
14       FORMAT (1H1)
         PRINT, DATE, SN
         READ,WS,DS,DM,VP,WSP,WSPM,PE,PF,SR
C        WS=WEIGHT OF SAMPLE, DS=SPECIFIC GRAVITY OF SOLIDS, DM=DENSITY OF
C        MERCURY, VP=VOLUME OF PENETROMETER, WSP=WEIGHT OF SAMPLE AND PEN-
C        ETROMETER, WSPM=WEIGHT OF SAMPLE , PENETROMETER AND MERCURY,
C        PE =EVACUATING PRESSURE, PF=FILLING PRESSURE,IN MM OF MERCURY,
C        SR =STEM READING AT FILLING PRESSURE.  THE ABOVE VALUES ARE ALL ON
C        THE SAME DATA CARD
         PRINT,WS,DS,DM,VP,WSP,WSPM,PE,PF,SR
         VS=WS/DS
         WM=WSPM - WSP
         VM=WM/DM
         VSA=VP-VM*(1.+PE/PF)-SR
         VVD=VSA-VS
         VOIDR=VVD/VS
         POROS=VVD/VSA
         PV=PE*VM
         VAI=PV/PF
         PRINT,≠VOLUME SOLIDS IS≠,VS,/,≠VOLUME VOIDS IS≠,VVD
         PRINT,≠VOID RATIO IS≠,VOIDR,/,≠POROSITY IS≠,POROS
         READ,N,M,SI
C        N=INTEGER VALUE FOR THE NUMBER OF LOW PRESSURE READINGS MADE, NOT
C        COUNTING THE FILLING PRESSURE READING.  M=INTEGER VALUE FOR THE
C        NUMBER OF HIGH PRESSURE READINGS MADE, NOT COUNTING THE INITIAL
C        POROSIMETER READING.  SI=INTRUSION READING AT INITIATION PRESSURE
C        IN ML.  THE THREE VALUES ARE ALL ON ONE DATA CARD.
C        LOW PRESSURE CALCULATIONS
         WRITE (6,5)
5        FORMAT (//,37X,≠LOW PRESSURE CALCULATIONS≠)
         WRITE (6,6)
6        FORMAT (//,3X,≠MM OF HG  PRESSURE  VOL AIR   STEM RDG  INTRUS  . I
         ANTRU/GM  CUMUL IN  INTR/VSA  CU IN/VS  DIAMETER  ≠)
         CU(1) = 0.
         CUSP(1) = 0.
         DO 100 I=2,N+1
         READ,P(I),S(I)
C        P(I) AND S(I) ARE THE PRESSURE AND INTRUSION VALUES FOR EACH
C        READING.  P(I) IS GIVEN IN MM OF MERCURY FOR THE LOW PRESSURE
C        INTRUSION AND PSI FOR THE HIGH PRESSURE.   S(I) IS IN ML.   THE TWO
C        VALUES ARE TYPED ON ONE DATA CARD, WITH A CARD FOR EACH READING.
         PS=P(I)*.01934
         VA=PV/P(I)
         CVA=VAI-VA
         CSR=S(I)-SR
         SN=CSR-CVA
         IF (SN.LT.0.) GO TO 10
         SG =SN/WS
         GO TO 11
10       SG=0.
         SN =0.
11       CU(I) = CU(I-1) + SG
```

```
          SP(I) = TH/VSA
          CUSP(I) = CUSP(I-1) +SP(I)
          D(I)=((-4.)*484.*COS(2.5656)*.145)/PS
          PRINT 1,P(I),PS,VA,S(I),SN,SG,CU(I),SP(I),CUSP(I),D(I)
C         P(I)=INTRUSION PRESSURE IN MN OF MERCURY, PS=INTRUSION PRESSURE IN
C         PSI, VA=VOLUME OF AIR IN ML, S(I)= TEM READING, SN=CORRECTED
C         INTRUSION FOR EACH INCREMENT IN ML, SG=CORRECTED INTRUSION /GRAM
C         FOR EACH INCREMENT, CU(I)=CUMULATIVE CORRECTED INTRUSION/GRAM,
C         SP(I)=INCREMENTAL POROSITY, CUSP(I)=CUMULATIVE POROSITY,
C         D(I)=LIMITING PORE SIZE DIAMETER
1         FORMAT(X,10F10.4)
          VAI=VA
100       SP=S(I)
C         HIGH PRESSURE CALCULATIONS
          WRITE (6,7)
7         FORMAT (//,36X,*HIGH PRESSURE CALCULATIONS*)
          WRITE (6,8)
8         FORMAT (//,3X,*PRESSURE   STEM RDG   HG COR    CHG HGC    INTRUS     I
         BNTRU/GM  CUMUL IN  INTR/VSA  CU IN/VS  DIAMETER  *)
          HCI=11.*.0011*VM/15000.
          DO 200 I=N+2,M+N+1
          READ,P(I),S(I)
          P(I)=P(I)+11.
          HC=P(I)*.0011*VM/15000.
          CHC=HC-HCI
          CSR=S(I)-SI
          SN=CSR-CHC
          SP(I) = SN/VSA
          CUSP(I) = CUSP(I-1) + SP(I)
          SGH=SN/WS
          CU(I)=CU(I-1)+SGH
          D(I)=((-4.)*484.*COS(2.5656)*.145)/P(I)
          PRINT 2,P(I),S(I),HC,CHC,SN,SGH,CU(I),SP(I),CUSP(I),D(I)
C         P(I)=INTRUSION PRESSURE IN PSI, S(I)=STEM READING, HC=MERCURY
C         CORRECTION, CHC=CHANGE IN MERCURY CORRECTION IN ML, SN=CORRECTED
C         INTRUSION IN ML, SGH=CORRECTED INTRUSION /GRAM, CU(I)=CUMULATIVE
C         CORRECTED INTRUSION/GRAM,  SP(I)=INCREMENTAL POROSITY, CUSP(I)=
C         CUMULATIVE POROSITY)
2         FORMAT (X,10F10.4)
          HCI=HC
200       SI=S(I)
          DO 300 I=2,N+M+1
300       C(I)=ALOG10(D(I))
C         THE PURPOSE OF THIS DO LOOP IS TO CONVERT THE PORE SIZE DIAMETER
C         TO THE LOG OF THE DIAMETER
          CALL PLOT1 (0,4,10,5,20)
          CALL PLOT2 (GRAPH,451,3.,-2.,.4,0.)
          CALL PLOT3 (1H*,C,CU,N+M)
3         FORMAT (1H1,35X,54HPLOT OF LIMITING PORE DIAMETER VS CUMULATIVE IN
         9TRUSION//)
          WRITE(6,3)
          CALL PLOT4 (5,INTRU)
          WRITE (6,20)
          WRITE(6,4)
20        FORMAT (10X,*0.01*,17X,*0.1*,18X,*1.0*,17X,*10.*,17X,*100.*,16X
         C*10000.*)
4         FORMAT (1H0,45X,33HLIMITING PORE DIAMETER IN MICRONS)
          CALL PLOT1 (0,4,10,5,20)
          CALL PLOT2 (PORO,451,3.,-2.,.4,0.)
          CALL PLOT3 (1H*,C,CUSP,N+M)
12        FORMAT (1H1,26X,72HPLOT OF LIMITING PORE DIAMETER VS CUMULATIVE IN
         DTRUSION/VOLUME OF SAMPLE//)
          WRITE (6,12)
          CALL PLOT4 (5,INTRU)
          WRITE (6,20)
          WRITE(6,4)
          CALL PLOT1 (0,4,10,5,20)
          CALL PLOT2 (HISTO,451,3.,-2.,.2,0.)
          CALL PLOT3 (1H*,C,SP,N+M)
          WRITE (6,13)
```

```
13      FORMAT (1H1,35X,55HPLOT OF LIMITING DIAMETER VS INTRUSION/VOLUME O
       EF SAMPLE//)
        CALL PLOT4 (5,INTPU)
        WRITE (6,20)
        WRITE(6,4)
        D(1)=((-4.)*484.*COS(2.5656)*.145)/(PF*.01934)
        PRINT,*PORE DIAMETER AT FILLING PRESSURE IS*,D(1)
C       THE FOLLOWING COMPUTES THE MEAN, SECOND MOMENT ABOUT THE ORIGIN,
C       AND VARIANCE, BOTH WITH RESPECT TO PORE DIAMETER AND LOG OF PORE
C       DIAMETER.  THIS SECTION MAY BE LEFT OUT, HOWEVER, THE NUMBER 400
C       MUST BE IN COLUMNS 1 TO 3 OF THE LAST CARD OF THE PROGRAM
        SUM1 = 0.0
        SUM2 = 0.0
        DO 500 I = 2,N+M+1
        DM =  (D(I) + D(I-1))/2.
        SUM1 = SUM1 + SP(I)*DM
500     SUM2 = SUM2 + SP(I)*DM*DM
        DMEA1 = SUM1/POROS
        DMEA2 = SUM2 / POROS
        VAR = DMEA2 - DMEA1*DMEA1
        AMEA1 = SUM1 / CUSP(N+M+1)
        AMEA2 = SUM2 / CUSP(N+M+1)
        AVAR = AMEA2 - AMEA1*AMEA1
        PRINT,*MEAN PORE SIZE IS*,DMEA1,/,*SECOND MOMENT ABOUT THE ORIGIN
       GIS*,DMEA2
        PRINT,*VARIANCE IS *,VAR
        PRINT,*ADJUSTED MEAN PORE SIZE IS*,AMEA1,/,*ADJUSTED SECOND MOMENT
       H ABOUT THE ORIGIN IS*,AMEA2
        PRINT,*ADJUSTED VARIANCE IS*,AVAR
        SUM1 = 0.0
        SUM2 = 0.0
        DO 600 I = 2,N+M+1
        DM = (ALOG10(D(I))-ALOG10(D(I-1)))/2.
        SUM1 = SUM1 + SP(I)*DM
600     SUM2 = SUM2 + SP(I)*DM*DM
        DMEA1 = SUM1/POROS
        DMEA2 = SUM2 / POROS
        VAR = DMEA2 - DMEA1*DMEA1
        AMEA1 = SUM1 / CUSP(N+M+1)
        AMEA2 = SUM2 / CUSP(N+M+1)
        AVAR = AMEA2 - AMEA1*AMEA1
        PRINT,*MEAN LOG PORE SIZE IS*,DMEA1,/,*SECOND MOMENT ABOUT THE ORI
       AGIN IS*,DMEA2
        PRINT,*VARIANCE IS *,VAR
        PRINT,*ADJUSTED MEAN LOG PORE SIZE IS*,AMEA1,/,*ADJUSTED SECOND MO
       BMENT ABOUT THE ORIGIN IS*,AMEA2
400     PRINT,*ADJUSTED VARIANCE IS*,AVAR
        STOP
        END
C       DATA FOLLOWS THE 7/8/9 CARD
```

```
C       THIS PROGRAM IS ESSENTIALLY THE SAME AS THE PRECEEDING PROGRAM,
C       EXCEPT IT ONLY PLOTS A SET OF PORE SIZE CURVES USING THE GOULD OR
C       CALCOMP PLOTTER.  FOR EXPLANATION OF THESE PLOTTERS, SEE PURDUE
C       DOCUMENT J5 CALCOMP
        PROGRAM PORE (INPUT,OUTPUT,TAPE5=INPUT,TAPE6=OUTPUT,PLOT)
        INTEGER TITL
        INTEGER TITLE
        DIMENSION S(50),P(50),D(100),CU(100),SP(50),CUSP(100)
        CALL PLOTS
        A = 0.0
        READ, NSET
        DO 500 K=1,NSET
C       THE PURPOSE OF THIS DO LOOP IS TO PLOT MORE THAN ONE SET
C       OF CURVES.  NSET IS THE NUMBER OF SETS OF CURVES TO BE PLOTTED AND
C       IS AN INTEGER VALUE THAT IS TYPED ON THE FIRST DATA CARD.
        B = 0.0
        CALL FACTOR (2.538)
C       CALCOMP USE CALL FACTOR (1.6)
        CALL SYMBOL(A+1.85,.5,.7/6., 33HLIMITING PORE DIAMETER IN MICRONS,
       G0.0,33)
        CALL SYMBOL(A+1.,0.75,0.7/6.,
       F52H.01      0.1      1.0      10.0      100.0     1000.0,0.0,52)
C       THE ABOVE PLOTS AND LABELS THE X AXIS
        CALL SYMBOL (A+2.0,1.0,0.1,3,0.0,-1)
        CALL SYMBOL (A+3.0,1.0,0.1,3,0.0,-1)
        CALL SYMBOL (A+4.0,1.0,0.1,3,0.0,-1)
        CALL SYMBOL (A+5.0,1.0,0.1,3,0.0,-1)
C       THE ABOVE PLACES TICK MARKS ALONG THE X AXIS
        CALL SYMBOL (A+0.5,1.5,.7/6., 19HCUMULATIVE POROSITY,90.0,19)
        CALL SYMBOL (A+0.6,1.0,.7/6.0,3H.00,0.0,3)
        CALL SYMBOL (A+0.6,2.0,.7/6.0,3H.15,0.0,3)
        CALL SYMBOL (A+0.6,3.0,.7/6.0,3H.30,0.0,3)
        CALL SYMBOL (A+0.6,3.9,.7/6.0,3H.45,0.0,3)
C       THE ABOVE PLOTS AND LABELS THE Y AXIS
        CALL SYMBOL (A+1.0,2.0,0.1,3,0.0,-1)
        CALL SYMBOL (A+1.0,3.0,0.1,3,0.0,-1)
        CALL SYMBOL (A+1.0,4.0,0.1,3,0.0,-1)
C       THE ABOVE PLACES TICK MARKS ALONG THE Y AXIS
        CALL SYMBOL (A+4.0,3.9,.07,6HLEGEND,0.0,6)
C       THE ABOVE WRITES LEGEND ON THE PLOT
        CALL PLOT (A+1.0,4.0,3)
        CALL PLOT (A+6.0,4.0,2)
        CALL PLOT (A+6.0,1.0,2)
        CALL PLOT (A+1.0,1.0,2)
        CALL PLOT (A+1.0,4.0,2)
C       THE ABOVE 5 CARDS DRAW THE OUTLINE OF THE GRAPH
        READ, NDATA
C       NDATA IS THE NUMBER OF CURVES THAT WILL BE PLOTTED FOR EACH SET OF
C       CURVES.  NDATA IS AN INTEGER VALUE, AND IS TYPED ON THE FIRST DATA
C       CARD FOR THE SET OF CURVES.
        DO 400 J=1,NDATA
C       DETERMINATION OF PORE SIZE DISTRIBUTION
        READ,DATE,SN
C       DATE AND SAMPLE NUMBER (SN) ARE TYPED ON THE FIRST DATA CARD FOR
C       EACH CURVE.
        READ,WS,DS,DM,VP,WSP,WSPM,PE,PF,SR
C       WS=WEIGHT OF SAMPLE, DS=SPECIFIC GRAVITY OF SOLIDS, DM=DENSITY OF
C       MERCURY, VP=VOLUME OF PENETROMETER, WSP=WEIGHT OF SAMPLE AND PEN-
C       ETROMETER, WSPM=WEIGHT OF SAMPLE , PENETROMETER AND MERCURY,
C       PE =EVACUATING PRESSURE, PF=FILLING PRESSURE,IN MM OF MERCURY,
C       SR =STEM READING AT FILLING PRESSURE.  THE ABOVE VALUES ARE ALL ON
C       THE SAME DATA CARD
        VS=WS/DS
        WM=WSPM - WSP
        VM=WM/DM
        VSA=VP -VM*(1.+PE/PF)-SR
        VVO=VSA-VS
        VOIDR=VVO/VS
        POROS=VVO/VSA
        PV=PE*VM
```

```
        VAI=PV/PF
        READ,N,M,SI
C       N=INTEGER VALUE FOR THE NUMBER OF LOW PRESSURE READINGS MADE, NOT
C       COUNTING THE FILLING PRESSURE READING.  M=INTEGER VALUE FOR THE
C       NUMBER OF HIGH PRESSURE READINGS MADE, NOT COUNTING THE INITIAL
C       POROSIMETER READING.  SI=INTRUSION READING AT INITIATION PRESSURE
C       IN ML.  THE THREE VALUES ARE ALL ON ONE DATA CARD.
C       LOW PRESSURE CALCULATIONS
        CU(1) = 0.
        CUSP(1) = 0.
        DO 100 I=2,N+1
        READ,P(I),S(I)
C       P(I) AND S(I) ARE THE PRESSURE AND INTRUSION VALUES FOR EACH
C       READING.  P(I) IS GIVEN IN MM OF MERCURY FOR THE LOW PRESSURE
C       INTRUSION AND PSI FOR THE HIGH PRESSURE.  S(I) IS IN ML.  THE TWO
C       VALUES ARE TYPED ON ONE DATA CARD, WITH A CARD FOR EACH READING.
        PS=P(I)*.01934
        VA=PV/P(I)
        CVA=VAI-VA
        CSR=S(I)-SR
        SN=CSR-CVA
        IF (SN.LT.0.) GO TO 10
        SG =SN/WS
        GO TO 11
10      SG=0.
        SN =0.
11      CU(I) = CU(I-1) + SG
        SP(I) = SN/VSA
        CUSP(I) = CUSP(I-1) +SP(I)
        D(I)=((-4.)*484.*COS(2.5656)*.145)/PS
        VAI=VA
100     SR=S(I)
C       HIGH PRESSURE CALCULSTIONS
        HCI=11.*.0011*VM/15000.
        DO 200 I=N+2,M+N+1
        READ,P(I),S(I)
        P(I)=P(I)+11.
        HC=P(I)*.0011*VM/15000.
        CHC=HC-HCI
        CSR=S(I)-SI
        SN=CSR-CHC
        SP(I) = SN/VSA
        CUSP(I) = CUSP(I-1) + SP(I)
        SGH=SN/WS
        CU(I)=CU(I-1)+SGH
        D(I)=((-4.)*484.*COS(2.5656)*.145)/P(I)
        HCI=HC
200     SI=S(I)
        READ, NL,W,H
C       NL IS AN INTEGER VALUE WHICH DESIGNATES WHAT SYMBOL WILL BE
C       PLOTTED ON THE CURVE.  W IS THE WATER CONTENT.  H IS THE FROST
C       HEAVE.
        DO 300 I=2,N+M+1
        D(I-1) =ALOG10(D(I))
C       THE PURPOSE OF THIS DO LOOP IS TO CONVERT THE PORE SIZE DIAMETER
C       TO THE LOG OF THE DIAMETER
300     CUSP(I-1) = CUSP(I)
        D(M+N+1) =-3.0 -A
C       D(M+N+1) IS THE X AXIS VALUE RELATIVE TO THE ORDINATE OF THE PLOT
        D(M+N+2) =1.0
C       D(M+N+2) IS THE X INCREMENT FOR EACH INCH OF PLOT
        CUSP(M+N+1) =-0.15
C       CUSP(M+N+1) IS THE Y AXIS VALUE RELATIVE TO THE ORDINATE OF THE
C       PLOT.
        CUSP(M+N+2) =0.15
C       CUSP(M+N+2) IS THE Y INCREMENT FOR EACH INCH OF PLOT
        CALL SYMBOL (A+3.82,3.7-B,.07,NL,0.0,-1)
        CALL SYMBOL (A+4.0,3.7-B,0.07,15HWATER CONTENT =,0.0,15)
        CALL SYMBOL (A+4.0,3.6-B,0.07,19HHEAVE AT 24 HOURS =,0.0,19)
        CALL NUMBER (A+4.96,3.7-B,0.07,W,0.0,1)
```

```
       CALL NUMBER (A+5.20,3.6-B,0.07,H,0.0,1)
C      THE ABOVE LISTS THE WATER CONTENT AND FROST HEAVE FOR THE PORE
C      SIZE CURVE
       CALL LINE (D,CUSP,N+M,1,1,NL)
C      THE ABOVE PLOTS THE ACTUAL PORE SIZE CURVE
C      B IS FOR THE PLACEMENT OF THE FROST HEAVE AND WATER CONTENT VALUES
400    B = B + 0.3
500    A = A + 8.0
C      H IS USED FOR THE LOCATION OF THE PORE SIZE PLOT
       CALL PLOT (0.0,0.0,999)
       STOP
       END
```

Appendix B

As mentioned in the body of the report, critical region drying was tried, but was unsuccessful for the silt-kaolin test soils. The purpose of Appendix B is to explain the setup of apparatus and testing procedure that was used. Explanation of the soil structural damage that was encountered with this procedure will be given in a future report by Ignacio Garcia-Bengochea.

Assembly of Apparatus

The apparatus for critical region drying was the same as that used by Bhasin (1975), however it had been disassembled and moved. Due to reassembly, some leaks were encountered with the stainless steel fittings. In some cases they could be eliminated by using a vise to hold the assembly and then applying a large tightening force with a 12 in. Cresent wrench. The stainless steel fittings are quite strong, and thus it is almost impossible to overtighten. If this did not work, the fitting was disassembled, the ferrule was cut off the tube, a new ferrule was inserted, and the fitting was tightened. Once all leaks had been corrected, the system was able to maintain a pressure of 4000 psi, with pressure changes due solely to temperature fluctuations.

Along with reassembly of the critical region device, a shield was constructed to protect against any leaking superheated steam. The shield was constructed of 0.125 in. mild steel plates bolted to a angle iron framework. The shield was designed so that a cover plate could be removed to insert the critical region drying vessel into the furnace. The cover plate was left off the shield during the early part of the

critical region run in order to check for leaks. Once the pressure had risen to about 500 psi, the cover plate was bolted to the rest of the shield.

Procedure

The procedure used during a critical region run was essentially the same as that used by Bhasin (1975). However, the following points are listed in order to clarify the method.

1) The 0.5 in. diameter samples were trimmed using a push tube similar to that used by Bhasin, however, it was constructed so that the sharpened tube could be replaced. Also, the sampler was designed so that the sample container fitted into it, and thus the sample could be intruded directly into the container. Once the sample was trimmed, the container and sample were removed from the sampler. The sample ends were then trimmed flush to the 0.5 in. high sample container using a razor blade.

2) The carborundum porous stones that were placed on each end of the sample container are not commercially available for the small diameter needed. Therefore, they were broken from large diameter 0.25 in. thick porous stones with a cold chisel and pliars to a size to cover the sample container. It was not necessary that the stones be round, only that they fit between the stainless steel end plates and the sample container.

3) Following assembly of the sample containers, they were soaked in water till the critical region run was initiated. Since the samples were trimmed from soil that was saturated, it was not necessary to saturate the small samples as Bhasin did.

4) The samples were placed in the critical region vessel, and water was added while the vessel sat in the steel holder attached to the wall. The vessel top was lubricated using Never Seez, and then screwed onto the body of the vessel. The top was secured by tightening the six screws in a staggered order. The screws were tightened to 70 ft lbs with a torque wrench.

5) The vessel was placed inside the furnace and the thermocouple wire was attached. Two asbestos cover plates were placed on top of the furnace for insulation and the pressure line was attached to the main pressure system.

6) Following connection of the vessel, the pressure was raised to 200 psi with the hydraulic jack. To use the jack, the valve from the jack to the system was closed, after which the valve to the plastic water vessel was opened. To allow water to enter the jack, it was jacked outward, following which the valve to the water vessel was closed. The pressure was then raised to the system pressure, and the valve leading to the system was opened.

7) The temperature and pressure during the critical region run were raised using the time relationship shown in Figure 39. The heater temperature was controlled using a Research Incorporated Thermac Temperature Controller on the "set point" mode. The controller was calibrated using an ice bath, boiling water, and the melting point of lead.

8) To raise the temperature, the temperature selector on the Thermac Controller was set about $15^{o}F$ above the current temperature and the rate of heating was adjusted using the proportional band control so that about 200 to 800 watts were applied to the heater. The heater wattage was measured using a watt-amp meter connected to the temperature controller.

9) For the critical region run up to about 2000 psi, the pressure was controlled by using a nitrogen cylinder and regulator. Above 2000 psi, the nitrogen tank was shut off from the system and the pressure was controlled by the hydraulic jack. Because of the effects of rising temperature on pressure, the pressure usually had to be backed off. The jack could be emptied or filled during the run using the earlier mentioned procedure.

10) Once the critical region run was completed, and the pressure was back to zero, the vessel pressure tube was disconnected from the rest of the system at the first fitting.

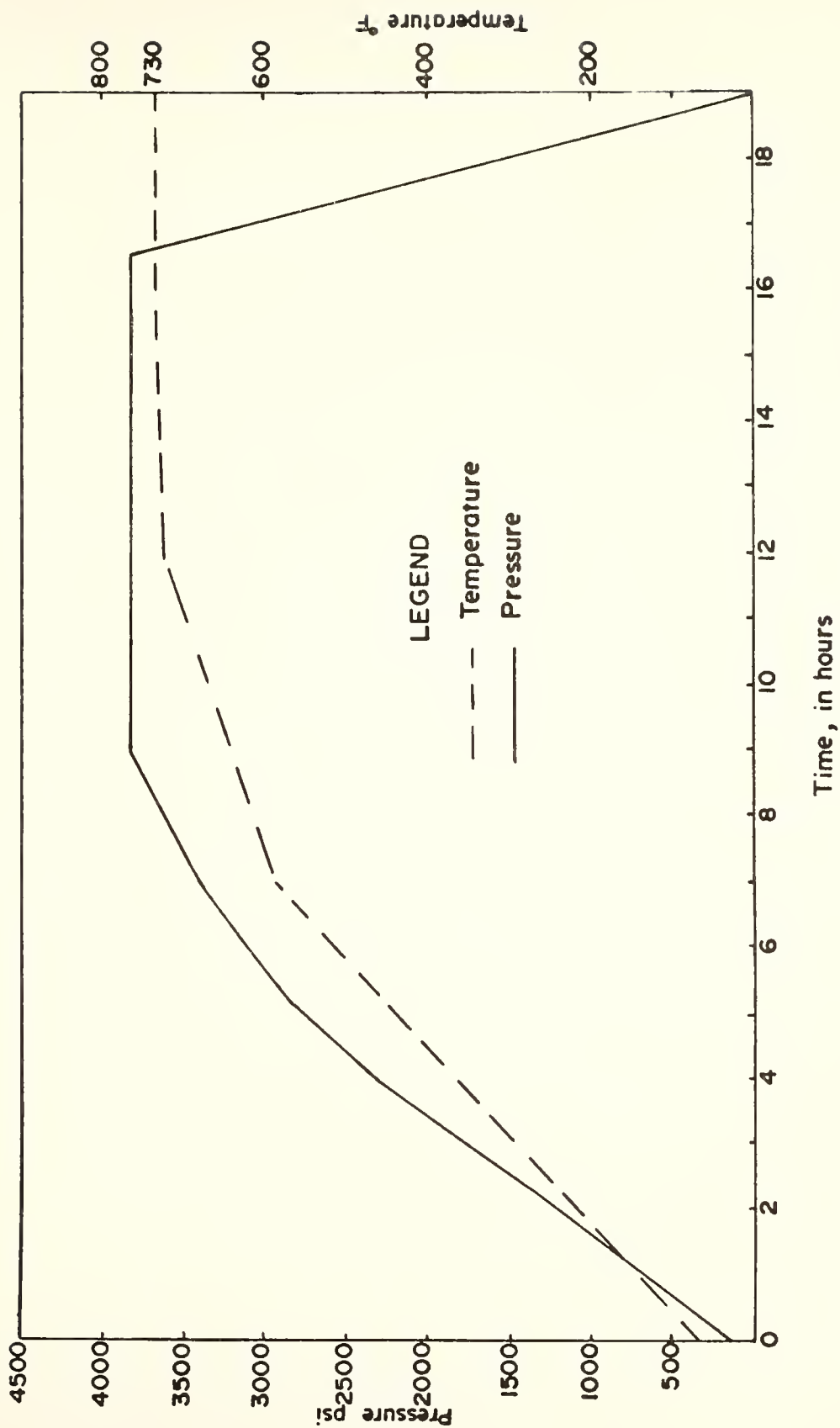11) Following disconnection, the vessel was cooled overnight and then disassembled.

FIGURE 39   TEMPERATURE AND PRESSURE VS TIME RELATIONSHIP FOR
CRITICAL REGION RUN

Appendix C

Purdue University Negative Numbers for Photographs

Figure Number		Negative Number
2		75529 24
3		75529 34
5		75529 32
6		75609 12
7		75529 30
8		75609 16
9		75609 19
10		75529 18
11		75529 25
12		75529 28
13		75609 14
14		75609 5
22	Dry of Optimum	75529 1
	Optimum	75529 4
	Wet of Optimum	75529 3
23	Dry of Optimum	75529 9
	Optimum	75529 10
	Wet of Optimum	75529 13